UNIVERSITÀ DEGLI STUDI DI MILANO

SCUOLA DI DOTTORATO DI RICERCA IN SCIENZE BIOCHIMICHE, NUTRIZIONALI E METABOLICHE

DOTTORATO DI RICERCA IN BIOCHIMICA

CICLO XXIII

SPHINGOLIPID METABOLISM ALTERATIONS CORRELATED WITH TUMOR CELL INVASIVITY AND FENRETINIDE RESISTANCE IN A HUMAN OVARIAN CARCINOMA CELL LINE

BIO 10

Tesi di Dottorato di:

Giuditta ILLUZZI

Matr. n. 821253

Docente Guida: Prof. Alessandro PRINETTI

Tutor: Prof. Sandro SONNINO

Coordinatore: Prof. Francesco BONOMI

Anno Accademico 2009-2010

INDEX

ABSTRACT

Glycosphingolipids (GSL) modulate several signal transduction processes controlling cell proliferation, survival, differentiation and transformation. Alterations in the expression of carbohydrate epitopes associated with GSL are frequent in tumors, and it has been hypothesized that GSL could play important roles in modulating some of the properties of tumor cells. The contribution of transformation-associated changes in GSL composition to the tumor phenotype are very complex and not fully elucidated, and likely implies heterogeneous molecular mechanisms. However, at least two well established paradigms support this role: 1) gangliosides have been described as modulators of growth factor receptor function, associated tyrosine kinase activities and cellular compartmentalization. 2) GM3 and/or GM2 inhibit integrin-dependent tumor cell motility *via* the formation of a ganglioside/tetraspanin/integrin receptor complex (the "*glycosynapse*") that is responsible for the negative regulation of c-Src tyrosine kinase activity [1].

In addition, several commonly used anticancer drugs exert their cytotoxic action at least in part by triggering the production of the sphingolipid ceramide, a mediator of apoptosis and an inhibitor of cell proliferation in a variety of tumor cell lines [2]. It has been demonstrated that chemoresistant tumor and tumor cell lines are frequently characterized by the increased glycosylation of ceramide with formation of glucosylceramide, due to an increased expression or activation of glucosylceramide synthase (GCS) [3]. Scavenging ceramide via its increased glycosylation would allow tumor cells to escape ceramide-induced apoptosis, thus contributing to the drug resistant phenotype [4-6]. However, it has been shown that GlcCer accumulation is not the only consequence of an altered sphingolipid metabolism in drug resistant cancer cells. In addition to its use as a precursor of complex sphingolipids, ceramide can be converted into sphingosine, which is then phosphorylated from sphingosine kinases to generate sphingosine 1-phosphate (S1P). Up-regulation of sphingosine kinase and concomitant decrease of the levels of sphingolipid mediators upstream to sphingosine kinase have been associated with resistance to camptothecin and docetaxel in prostate cancer cells [7, 8], to oxaliplatin in colon cancer cells [9] and to gemcitabine in pancreatic cancer cells [10].

During my PhD period, I have studied the alterations in sphingolipid metabolism and their functional relevance in different phenotypic variants of a human ovarian carcinoma cell line, A2780. A2780 cells are sensitive to a variety of antitumor drugs, including the synthetic retinoid *N*-(4-hydroxyphenyl)retinamide (fenretinide or HPR), that is currently it is under clinical trials as preventive chemotherapeutic drug for prostatic and ovarian cancer, neuroblastoma, lymphoma and leukemia. A2780/HPR is a HPR-resistant cell line obtained from the parental A2780 cell line by in

vitro exposure to increasing sublethal HPR concentrations. The A2780/HPR cell line presents a multiple phenotypic differences compared to A2780 cells. Previous work from this lab showed that A2780/HPR cells express higher ganglioside levels respect to the parental cell line, due to the overexpression of GM3 synthase, a key enzyme in ganglioside biosynthetic pathway, and a higher sphingolipid degradation rate [11].

In addition to HPR resistance, A2780/HPR cells are characterized by a reduced in vitro motility respect to the parental cell line. Subsequent experiments were aimed at elucidating a possible link between alterations in sphingolipid metabolism and modulation of cell motility and/or the acquisition of resistance to HPR. At first, we examined the effect of the overexpression of sialyltransferase-1 (SAT-1, GM3 synthase) on A2780 cells. Our results indicate that 1) GM3 synthase overexpression led to a marked increase in the ganglioside; 2) this was associated with a strong reduction of *in vitro* cell motility without affecting the growth rate, nor the sensitivity to HPR; 3) the expression of the membrane adaptor protein caveolin-1 was markedly upregulated in SAT-1 transfected cells and in A2780/HPR cells, naturally expressing high GM3 synthase levels. 4) in SAT-1 overexpressing cells, GM3 directly interacts with caveolin-1, as demonstrated by photolabelling experiments, with the use of radioactive and photoactivable GM3; 4) caveolin-1 formed a multimolecular complex with gangliosides, integrin receptor subunits and c-Src, as demonstrated by differential solubilization and co-immunoprecipitation experiments; 5) *In vitro* motility of A2780 cells was strongly reduced in the presence of a selective Src inhibitor, and SAT-1 transfected A2780 cells were characterized by higher levels of the inactive c-Src p-Tyr-527 form, that was concentrated in a detergent-resistant membrane fraction, co-localizing with the caveolin-1/ganglioside complex. These data suggest that motility of A2780 cell can be negatively influenced by a caveolin-1/ganglioside complex controlling Src activity. Supporting this hypothesis, we observed that exogenous administration of gangliosides or a pharmacological treatment able to increase cellular ganglioside levels in A2780 cells were able to effectively reduce their *in vitro* motility of these cells, with a concomitant increased phosphorylation of caveolin-1.

As mentioned above, GM3 synthase overexpression did not affect the sensitivity of A2780 cells to HPR. On the other hand, degradation of sphingolipids occurs at higher extent in drug-resistant A2780/HPR cells. Sphingolipid degradation pathway implies the conversion of ceramide in sphingosine, which afterwards can be phosphorylated to S1P by the action of sphingosine kinase (SK). We showed that the production of S1P is significantly higher in A2780/HPR vs. A2780 cells due to an increased SK activity and SK-1 mRNA and protein levels. Treatment of A2780 and

A2780/HPR cells with a potent and highly selective pharmacological sphingosine kinase inhibitor effectively reduced S1P production and resulted in a marked reduction of cell proliferation. Moreover, A2780/HPR cells treated with a SK inhibitor were sensitized to the cytotoxic effect of HPR, due to an increased dihydroceramide production. On the other hand, the ectopic expression of SK-1 in A2780 cells was sufficient to induce HPR resistance in these cells. Challenge of A2780 and A2780/HPR cells with agonists and antagonists of S1P receptors had no effects on their sensitivity to the drug, suggesting that the role of SK in HPR resistance in these cells is not mediated by the S1P receptors.

These data clearly demonstrate a role for SK in determining resistance to HPR in ovarian carcinoma cells, due to its effect in the regulation of intracellular ceramide/S1P ratio which is critical in the control of cell death and proliferation.

INTRODUCTION

SPHINGOLIPIDS

In the last years several studies discovered new aspects of lipid function: they are not only structural components of cell membranes but also fundamental members of signalling and regulatory pathways. In fact their role in several biological processes, such as cell growth and proliferation, apoptosis, ageing, adhesion, migration, angiogenesis and immune response has been discovered; alterations in the lipid regulated signalling pathways contribute to the pathogenesis of several diseases, like cancer and various metabolic disorders [12].

Lipids act in a cell-specific way: the same lipid molecule can cause different effects in different cell types, depending on which signalling pathway is activated in the target cell.

Bioactive lipids include, besides the well characterized eicosanoids and phosphoinositides, the sphingolipids. This lipid class, produced both in unicellular and multicellular eukaryotes [13], in addition to their role as ubiquitous constituents of cell membranes, appears to have a significant role as mediator of fundamental cell processes, like proliferation, survival, differentiation and motility.

Some of the best studied sphingolipids are ceramide, which controls the cell response to various stresses through the apoptosis induction [14] and cell ageing, sphingosine, involved in the endocytosis, cell cycle and apoptosis regulation [15], sphingosine-1-phosphate (S1P), and gangliosides as GM3 and GM2 whose functions will be explained in the next paragraphs.

Other sphingolipids with important bioactive role are ceramide-1-phosphate, involved in the regulation of inflammation [16, 17], apoptosis [18, 19] and cell proliferation [20, 21], glucosylceramide, with a role in the protein transport from Golgi to the cell membrane and in anticancer drug resistance [22], lyso-sphingomyelin and dihydroceramide.

Structure and physical-chemical properties

Sphingolipids constitute a family of amphipathic lipids involved in numerous and important biological functions. Ceramide is the simplest sphingolipid: it is formed by a long chain sphingoid base linked to a fatty acid through an amide bond. The prevalent sphingoid base in mammal tissues is *D-erythro-(2S,3R)-sphingosine* (trans-D-erythro-2-amino-4-octadecen-1,3-diol), a 18 carbon atoms primary amine with a double bond in position 4, 5 and two hydroxyl groups in position 1 and 3. Homologous lipids with a different length of the carbon chain or with a saturated chain (4-dihydrosphingosine or sphinganine) are present in cells in minor amount. The fatty acid linked to

the amine group in position 2 of the sphingoid base has a length between 16 and 24 carbon atoms and it is generally linear, saturated or rarely unsaturated; less frequently it is possible to find branched- or hydroxylated-chains fatty acids. In general, stearic acid is prevalent in the nervous system, while fatty acids are more heterogeneous in extra nervous tissues and a very long chain is frequently present.

Ceramide is the fundamental structural unit common to all complex sphingolipids, which are characterized by the presence of a charged group linked to the hydroxylated group in position 1 of the sphingoid base [23]. The polar group, that defines the specific sphingolipid class, is a phosphate group in ceramide-1-phosphate, phosphorylcholine in sphingomyelin, monosaccharides in cerebrosides, one or more sugar residues linked with a β-glycosidic bond in complex glycosphingolipids.

Gangliosides constitute a particular class of acid glycosphingolipids, discovered by Ernest Klenk in 1936 in the central nervous system. Their peculiarity is to contain 1-7 residues of a particular acid sugar, the sialyc acid. The acid oligosaccharide chain is bound to ceramide through a β-glycosidic bond between the C1 of the sugar and C1 of the sphingosine. The sialyc acid residues are bound with *α*-glycosidic bonds to an oligosaccharide core constituted by neutral hexoses (*D*-glucose, *D*-galactose, *D*-fructose more rare) and by hexosamine *N*-acetylated (*N*-acetylglucosamine, *N*-acetylgalactosamine, this is prevalent in nervous tissues). Because of the complexity of the oligosaccharide chain, that can be formed by 2 to 10 carbohydrates, and of the heterogeneity of the hydrophobic portion, until today about 50 ganglioside structures are characterized. The classification used for gangliosides is based on the number and on the position of the sialyc acid residue. The most common nomenclature is the one proposed by Svennerholm [24]. There are monosialo, disialo, trisialo, tetrasialo and pentasialo gangliosides depending on the number of residues of sialyc acid. The type of neutral oligosaccharide chain present, considering the basal composition more frequently used in the ganglio series: Gal(β1---3)GalNac(β1---4)Gal(β1---4)Glc β1, 1 = Gal(β1---3)GalNac(β1---4)Gal(β1---4)Glcβ1, 2 = GalNac(β1---4)Gal(β1---4)Glc β1, 3 = Gal(β1---4)Glc β1. Finally the position of the sialyc acid bond to the internal galactose is indicated with a minor letter (a=1, b=2, c=3).

The different composition of the hydrophobic chain, together with the chemical and geometrical features of the polar group, can cause a lateral lipid separation with the consequent isolation of these lipids from the remaining membrane, promoting the formation of “microdomains” or

sphingolipid "clusters". This phenomenon has been studied in both artificial and cell membranes [25].

Sphingolipids are a family of membrane lipids characterized by particular physical-chemical properties. These molecules are strongly amphiphilic: they are characterized by a hydrophobic portion (ceramide), embedded in the lipidic core of biological membranes, and by a hydrophilic portion protruding in the extracellular milieu. The ceramide backbone confers some physical-chemical properties to the sphingolipids that differs from those of other membrane lipids. In fact, the amidic linkage, with the contemporary presence in the same molecule of a hydrogen bond donor and an acceptor group (the carbonyl oxygen and the amidic hydrogen), allows the formation of a thick network of hydrogen bonds among different sphingolipid molecules in the lipid bilayer. The presence of hydrogen linkages considerably stabilizes the sphingolipid segregation in specific membrane areas, which appear enriched with this lipid family and for this reason they have been defined "sphingolipid-rich membrane domains". In addition, the numerous hydrogen bonds in these domains confer rigidity and resistance to the membrane allowing their differentiation by physical-chemical properties from the remaining membrane.

Sphingolipid metabolism

The sphingolipid metabolism mostly takes place in intracellular compartments with the participation of several subcellular organelles and it implies the presence of an efficient sphingolipids transport mechanism among the cell membrane, the sphingolipid-rich domains and the biosynthesis and degradation sites. This process consists of several events, including *de novo* biosynthesis, degradation, internalization-dependent glycosylation and recycling. In addition, a recent study has analyzed the role of enzymatic activities localized on the cell surface in the sphingolipid metabolism [26].

Ceramide is the central molecule in both sphingolipid synthesis and catabolism. The ceramide production in mammal cells is performed through three main metabolic pathways: *de novo* biosynthesis, complex sphingolipid degradation and sphingosine recycle.

The enzymes involved in the sphingolipid biosynthesis and degradation are finely tuned since several intermediates of these metabolic pathways regulate different biological processes [27].

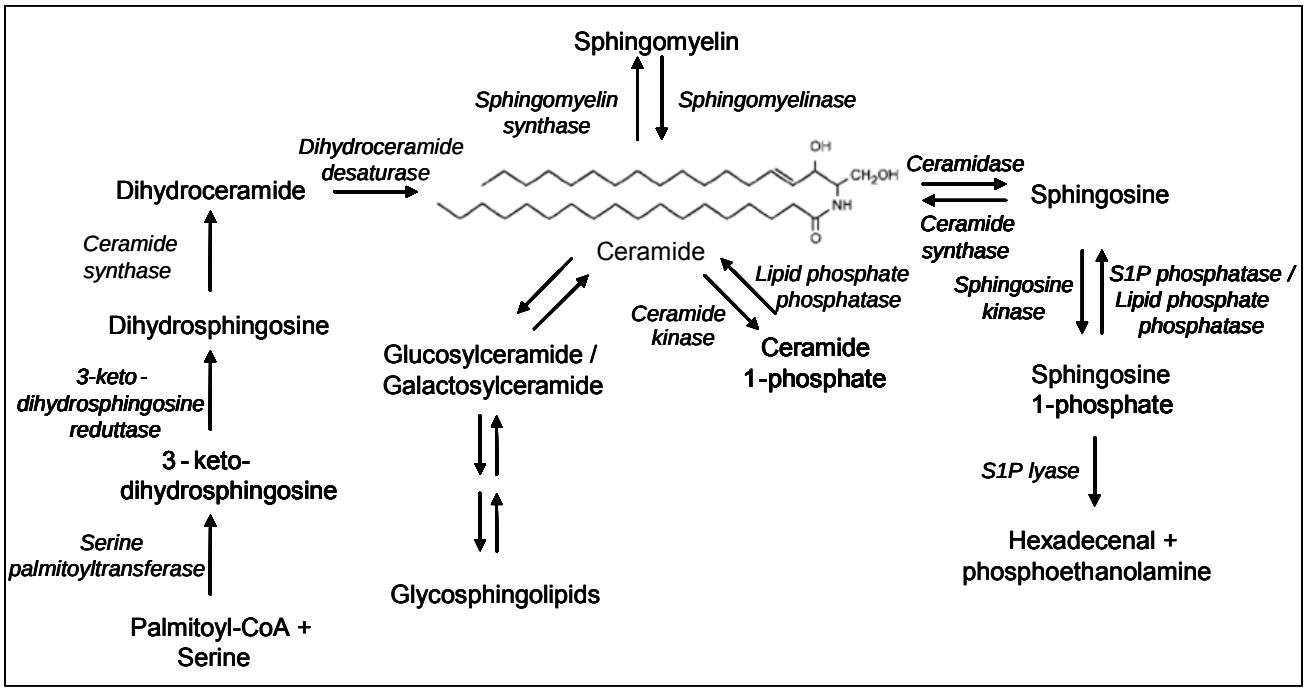

Figure 2. Sphingolipid metabolism

Sphingolipid *de novo* biosynthesis

The *de novo* sphingolipid synthesis takes place in the endoplasmic reticulum and in the Golgi apparatus [28] and it is a multistep process. The first step is a condensation between serine and palmitoyl-CoA to form 3-keto-dihydrosphingosine (3-keto-sphinganine), a 18 carbon atom long-chain base; this reaction is catalyzed by the pyridoxal-phosphate-dependent enzyme serine palmitoyltranferase [29, 30]. The 3-keto-dihydrosphingosine synthesis limits the speed of the entire biosynthetic process [31] and it is probably a main regulation point: in fact, the serine palmitoyl tranferase activity is downregulated by the sphingoid bases [32]. The 3-keto-dihydrosphingosine is reduced to dihydrosphingosine (sphinganine) by a NADPH-dependent reduttase [33], called 3-keto-dihydrosphingosine reduttase. The following step is the fatty acid incorporation in position 2 of the sphingoid base with the dihydroceramide formation. The catalyzing enzyme of this reaction is the acyl-CoA:sphingosine N-acyltranferase [34], or ceramide synthase, that preferentially uses stearoyl-CoA as substrate. This enzyme acylates both sphinganine and sphingosine with the same efficiency. The enzymes for the biosynthetic dihydroceramide formation are localized on the cytosolic surface of the endoplasmic reticulum [35, 36]. The dihydroceramide is subsequently desaturated through introduction of a double bond in position 4,5 [37] by the dihydroceramide desaturase enzyme, localized in the endoplasmic reticulum with a cytosolic active site.

Ceramide is an important intermediate both from the structural point of view, as starting point of the sphingolipid synthesis, and from the functional one, regulating the activity of several intracellular effectors [38-40].

Ceramide can be phosphorylated to ceramide-1-phosphate [41, 42] by a specific membrane bound Ca^{2+}-dependent ceramide kinase [43]. Ceramide-1-phosphate can be reconverted to ceramide by a ceramide-1-phosphate phosphatase, which presence has been demonstrated in rat liver and brain, probably localized on the cell membrane [44]. The metabolic significance of these reactions is not yet clear but the cellular regulation of ceramide-1-phosphate could be of great relevance for its regulatory role [45].

Ceramide can be used for sphingomyelin synthesis through phosphocholine transfer from phosphatidylcholine to ceramide by a phosphatidylcholine:ceramide choline phosphotransferase [23], or sphingomyelin synthase, localized in the Golgi apparatus; during this reaction diacylglycerol, an important second messenger, is also produced.

The hydroxyl group in the C1 of ceramide can be glycosylated by specific glycosyltransferases that mediate the regulated addition of saccharidic units, with the formation of glycosphingolipids. Since the sphingomyelin and glucosylceramide production (precursor of other glycosphingolipids) takes place on the luminal side of the *cis* or medial Golgi [46, 47] and on the cytosolic side of a pre-Golgi compartment [48] respectively, ceramide produced in the endoplasmic reticulum must be transported to those sites. Glycosphingolipids are then moved through vesicles to the cell membrane where they regulate cell-cell recognition, adhesion and differentiation. The ceramide transport from the endoplasmic reticulum, where it is produced, to the Golgi apparatus, where it can undergo further synthetic reactions, is performed by a specific transfer protein (CERT) or by vesicular transport, depending if the sphingolipid is used to synthesise sphingomyelin or glucosylceramide, respectively [49].

Sphingomyelin is transferred, probably through vesicular transport, from the Golgi apparatus to the cell membrane where it can act as a structural component or it can be further metabolized to bioactive sphingoid molecules.

Sphingolipid degradation

Ceramide is produced during the catabolism of every complex sphingolipid, either glycosphingolipids [50] and phosphosphingolipids (sphingomyelin) [51]. Glycosphingolipid catabolism takes place in the lysosomal vesicles by the action of glycohydrolases, which catalyze

the detachment of single saccharidic units from the non-reducing oligosaccharide end. Cell membrane sphingolipids reach the lysosomes through the endocytic pathway. An alternative pathway for ganglioside degradation, and in general for sphingolipids, involves the breakage of the β-glycosidic linkage between glucose and ceramide with the release of ceramide and oligosaccharides [52-54]. The enzymes involved in this reaction are substrate-specific endoglycoceramidases (ceramide glycanase) [55]. The role of these enzymes, potentially relevant for the sphingolipid-mediated signal transduction, has not been so far completely understood.

Ceramide produced by this mechanism is then converted into sphingosine through deacylation by the acid ceramidase present in lysosomes. Sphingolipid lysosomal catabolism intermediates, as saccharidic groups, fatty acids and sphingosine, can be further degraded or recycled.

The sphingomyelin hydrolysis to form ceramide and phosphorylcholine is catalyzed by sphingomyelinases (sphingomyelin phosphodiesterases) [51, 56], differing each other for optimal pH, subcellular localization and cation dependence.

Since ceramide synthase is able to use both sphingosine and sphinganine with similar efficiency, ceramide can also be produced by *N*-acylation of sphingosine derived by the catabolism of complex sphingolipids. In fact several studies demonstrated [57, 58] that a fraction of the sphingosine produced by the ganglioside lysosomal catabolism does not undergo complete degradation but is used for biosynthetic purposes through a pathway known as "salvage pathway" [59]. The sphingosine recycled during the ganglioside GM1 catabolism significantly contributes to the free sphingosine cell amount.

The obtained ceramide can enter multiple biosynthetic pathways for the production of sphingolipids or it can be further catabolized. Sphingosine formed by ceramide deacylation through ceramidase activity can either be recycled in the sphingolipid biosynthetic pathway, through its conversion to ceramide by the ceramide synthase, or be phosphorylated by sphingosine kinase to S1P. This molecule, representing the sphingolipid metabolism end product, can be degraded by two different reactions: through dephosphorylation, a reversible process catalyzed by the S1P phosphatase, or through C2,C3 linkage hydrolysis, an irreversible process catalyzed by the S1P lyase, which produces phosphoethanolamine and hexadecenal used for the phosphatidylethanolamine biosynthesis (PE). Hexadecenal can also be oxidized to palmitate and enter in this way in the lipid metabolism. The S1P dephosphorylation can also be catalysed by non-specific phosphatases belonging to the lipid phosphate phosphatases family [60].

Sphingolipid-ernriched membrane domains

Thoroughly studies demonstrated that altered expression of ganglioside GM3 plays various roles in the control of tumor cell motility, invasiveness and survival. GM3 is highly expressed in non invasive respect to more invasive bladder cancers [61, 62]. The increased expression of GM3 obtained pharmacologically [62, 63] or by exogenous administration [61] reduces the invasive potential of colon and bladder cancer human cells, while the stable overexpression of GM3 synthase reduces the cell proliferation, motility and invasiveness with increase in apoptotic cell number [64]. High expression level of GM3 and the concomitant expression of tetraspannin CD9 in the same cell type [65, 66] inhibit laminin-V dependent cell motility on Matrigel, in mutants for CHO the coexpression of CD9 and GM3 is essencial for downregulation of cell motility. The mechanism that undergoes this fenomenon at cellular and molecular level already needs to be clarified.

The lipid bilayer is characterized by several basic properties that are relevant to its biological functions. The bilayer as a whole is a very stable structure, however it allows its components a certain degree of lateral motility. As a consequence of this fluidity components of biological membrane can be arranged following a non-homogenous lateral distribution, leading to the creation of membrane areas, “domains”, with a highly differentiated molecular composition and supermolecular architecture. Membrane macrodomains are in general characterized by the presence of specific subsets of proteins, and differential sorting and trafficking of proteins has been understood as one of the mechanisms responsible for the creation of polarized domains. In membrane regions lacking a morphologically distinguishable architecture, certain proteins cannot undergo a free and continuous lateral diffusion, but rather are transiently confined to small domains, “microdomains”.

Sphingolipids have a unique feature among complex membrane lipids, they act as donor and acceptors for the formation of hydrogen bonds, and the consequent network at the water/lipid interface strongly stabilizes the segregation of a rigid segregated phase enriched in sphingolipids.

Moreover in the case of glycosphingolipids, another factor favouring their segregation within biological membrane is represented by the presence of the bulky oligosaccharide hydrophilic headgroup. Earlier studies suggested that membrane glycosphingolipids or glycoproteins must be clustered, providing a basis for interaction with other membrane components. Interactions of clustered glycosphingolipids or gangliosides with signal transducers, key membrane receptors, or tetraspanins [67, 68] plays an essential role in defining the organizational framework of membrane components in microdomains, through which cellular phenotype is manifested. Among the various

types of microdomains, those controlling glycosphingolipid-dependent or -modulated cell adhesion and signal transduction were termed "glycosynapse." They usually consist of glycosphingolipid, tetraspanin (proteolipid proteins), Src family kinases, small G-proteins (RhoA, Ras, and Cas), growth factor receptor, and integrins [1, 69].

A large number of studies on molecular interactions of various components in microdomains were developed during the late 1980s to early 1990s, indicating the presence of sphingolipid/cholesterol-enriched domains which are resistant to non-ionic detergents. Such microdomains were variously termed as ''DRM" (detergent resistant membrane).

Gangliosides, particularly GM3 and GM2, are known to interact with growth factor receptors (GFRs), and to inhibit the enhanced tyrosine kinase activity of the receptor induced by growth factor. Typical examples are GM3-dependent inhibition of tyrosine kinases associated with epidermal GFR ([22][70], with fibroblast GFR (FGFR) [23,24][71, 72], and with insulin receptor [25,26][73]. GM3 also interacts with and activates cSrc, Src family kinases, and G-proteins [10][74]. The relationship of this process with integrin-dependent signalling was subsequently clarified by studies using ldlD cells and their CD9 transfectant, GM3 level regulate snot only the association between CD9 and integrin α3 but also the activation state of c-Src through Csk translocation [18,19][75, 76].

CAVEOLIN

Caveolin is an integral membrane protein of 22 to 24 KDa molecular weight and the main structural components of non-chlatrin, flask-shaped invaginations called *caveolae*, originally described by Palade et al. and Yamada in the 1950s [77]. Three distinct caveolin genes, caveolin-1, caveolin-2 and caveolin-3 have been identified [78]. Caveolin-1 is expressed in two isoforms, caveolin-1α and caveolin-1β; the α and β isoforms start from methionine at positions 1 and 32, respectively. The isoforms have in common a hydrophobic stretch of aminoacids, the scaffolding domain and the acylated C-terminal region, whereas the N-terminal 31 aminoacids are only found in the α isoform. The two isoforms were reported to show an overlapping but slightly different distribution in mammals [79]. While caveolin-3 is found mainly in skeletal muscle fibres and cardiac miocytes, caveolin-1 and caveolin-2 are co-expressed in most cells (they are highly expressed in adipocytes, endothelial cells and fibroblasts) and share many physical properties, although the latter seems to lack full functional capacity to form *caveolae*. These specialized microdomains are enriched in

specific lipids (glycosphingolipid, sphingomyelin and cholesterol) and important signalling molecules.

Caveolins form oligomerized complexes (200 to 350 KDa) that act concentrating certain caveolin interacting signalling molecules within *caveolae*. These interactions occur through a defined modular protein domain, known as the caveolin-1 scaffolding domain. Caveolin-1 can modulate the function of many signal transducers integrated in *caveolae*, including epidermal growth factor receptor (EGFR) [80], platelet-derived growth factor receptor (PDGFR), insuline receptor, H-Ras, Raf, c-Src [81] and G proteins.

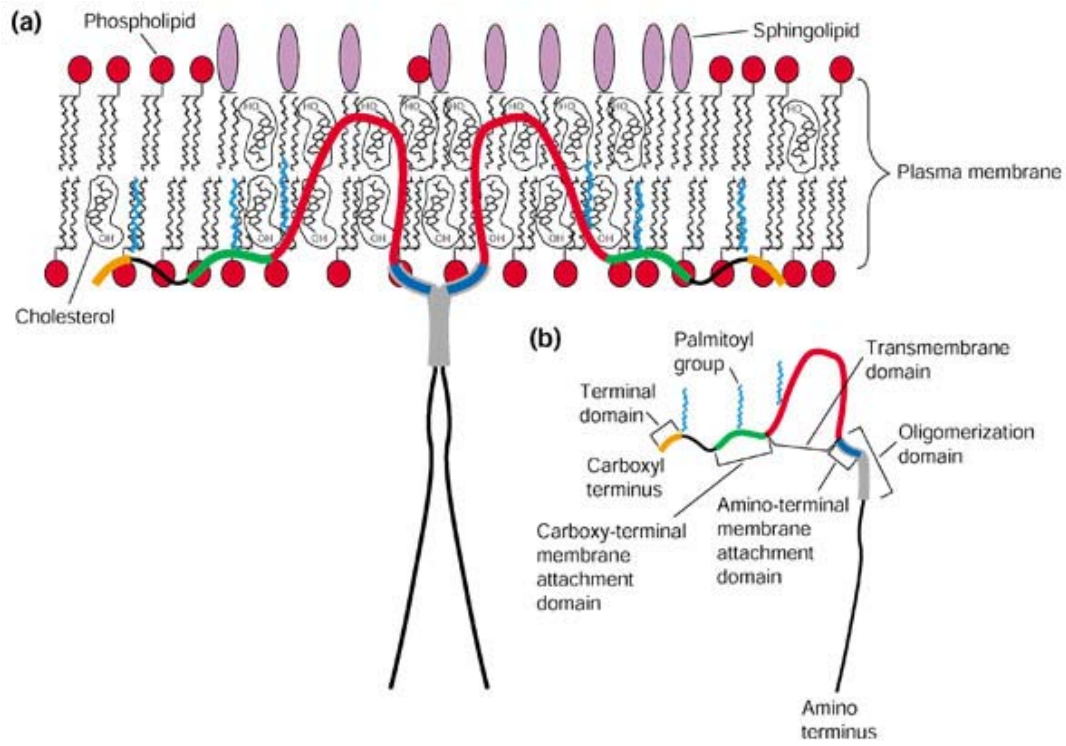

Caveolin molecular model Primary structure and topology of Cav-1. **(a)** The predicted membrane topology of Cav-1. Two caveolin-1 monomers are shown forming a dimer for simplicity, but about 14-16 monomers normally self-associate to form a single caveolin homo-oligomer (the caveolar assembly unit, aktin to the clathrin triskelion). Note that both the amino- and carboxy-terminal domains are oriented towards the cytosolic face of the plasma membrane, with a hairpin loop structure inserted within the membrane bilayer. Modified from Razani *et al.* [82]. **(b)** The domains present in Cav-1. Note that the amino-terminal membrane-attachment domain is also called the caveolin scaffolding domain.

Signal transduction mediated by caveolin

Caveolae may work as specialized structures in cell membranes regulating the functions of protein complexes involved in signal transduction, in which caveolin may have a key role as organizing molecule [83, 84]. In particular caveolin-1 acts as a membrane adaptor protein coupling the intracellular region of integrin receptors to cytosolic Src tyrosine kinase family. In fact it was reported that tyrosine kinases, such as Fyn, Yes, Lck and Lyn, belonging to the Src family, are localized in cholesterol-enriched domains (known as lipid rafts) and in *caveolae* thanks to their double acylation [85, 86].

Caveolin-1 is phosphorylated on tyrosine 14 in response to a number of growth factors such as VEGF, EGF and PDGF [87, 88] and in response to integrin activation [89]. The phosphorylation and recruitment of caveolin-1 to integrin and growth factor receptors sites may serve multiple roles in regulating functions of these proteins: for example caveolin-1 clustering has been hypothesized to promote integrin clustering, permitting increased avidity for ligand binding. Many lines of evidence indicate that Src family kinases play an essential role in these processes [90]. Src and caveolin-1 appear to be strongly interconnected: the Src kinase activity is important for stimulation of the caveolar endocytosis and a Src specific siRNA is able to reduce the caveolin-mediated endocytosis and it increases the amount of *caveolae* on the cell surface. To date, only two molecules, Csk and Grb7, have been demonstrated to associate with the PY14 site of caveolin-1 [91]. Grb7 contains two functional phosphotyrosine binding domains and forms large hetero-oligomeric complexes; it seems to be critical for growth factor induced migration responses [92] and this association may serve to link phosphocaveolin-1 to the focal adhesion machinery involved in cell motility. In support of this notion, phosphocaveolin-1 is localized within a subpopulation of caveolar membranes that are proximal to focal adhesions [91].

It was demonstrated that the phosphocaveolin-Csk interaction may involve the activation of Csk to act as a negative feedback regulator of Src kinases family signalling. Oxidative and osmotic stress-induced phosphorylation of caveolin-1 requires the activation of Fyn, which was then negatively regulated by the recruitment of Csk to the caveolin-1 phosphorylation site [93]. In aortic endothelial cells it was shown that the Csk association to caveolin-1 is constitutive but Csk and pY14 caveolin-1 association is significantly increased after laminar shear stress [94]. Csk contains a conserved sequence that has been shown to mediate Src family kinase association to the caveolin-1 scaffolding

domain. Once activate, Csk might then bind to the phosphorylation domain of caveolin-1 and inhibit c-Src activity through Tyr527 phosphorylation.

In normal cells, transmission of growth factor signals from their membrane receptors to the nucleus is a highly organized process that involves controlled *spatio*temporal activation of signalling molecules. This is in part accomplished by *caveolae*: caveolin-1, principal component of the caveolar coat, plays a role in caveolar-dependent signalling, transcytosis and lipid metabolism. In addition, caveolin-1 has the ability to interact with and modulate multiple signalling pathways, suggesting that its expression profoundly affects cell function and fate. Indeed, the expression of caveolin-1 is tightly regulated: it is upregulated in terminally differentiated cells, like adipocytes, endothelial and muscle cells. Conversely, caveolin-1 expression is lost or reduced during the oncogenic transformation.

Effect of caveolin-1 expression in tumor cells

A growing number of experimental evidences indicates that caveolin-1 profoundly influences the tumor development, and in particular in microdomains caveolin, among various components, has received great attention as major adapter molecule affecting cellular phenotype. However, the precise functional role of this molecule is not yet known.

Caveolin-1 is highly expressed in the normal ovary but it is strongly down-regulated in human ovarian carcinoma and generally also in human tumors deriving from breast and colon[95, 96], while it is up-regulated in tumor samples from kidney, prostate and stomach.

Caveolin-1 is highly expressed in immortalized human ovarian epithelial cells, in benign serous adenome and in SKOV-3 and ES-2 ovarian cell lines, but it is not in four highly aggressive ovarian carcinoma cell lines [97]. Caveolin-1 is likely acting as a tumor-suppressor gene in human ovarian epithelia, potentially pulling down tumor growth and metastasizing efficacy. Caveolin-1 re-expression in human breast cancer and in colon carcinoma cell lines inhibits the tumor cell growth [98] and the tumorigenicity [99], also in vivo studies on mammary tumor demonstrated that it negatively influences tumor growth, the metastatic invasivity and the metastasis production, in fact caveolin-1 promotes cell-cell adhesion in ovarian carcinoma cells through a Src inhibition mechanism [100]. The inhibitory effect of caveolin-1 on tumor progression may be based on its interaction with integrin which causes activation of Fyn, in turn activating Shc tyrosine phosphorylation. This sequential process is necessary to open up the Ras/Erk pathway, to control tumor cell motility [15][101] . In some cell lines the siRNA inhibition of caveolin-1 is sufficient to

induce the oncogenic transformation. The down-regulation of caveolin-1 in NIH-3T3 cells activates MAPK and stimulates the anchorage-independent growth [102]. The caveolin-1 loss accelerates the tumorigenesis and the metastatisation: PyMT/Cav1 (-/-) mice are characterized by a fast development of mammary tumors and lung metastasis [103]. In OVCAR-3 human ovarian carcinoma cells the induced expression of caveolin-1 reduces by 90% the colony formation and it significantly increases the apoptotic cell number. The caveolin-1 induced apoptosis may be consequent to the increased amount of membrane *caveolae* and their enrichment in sphingomyelin and sphingomyelinase, with a consequent ceramide production.

The caveolin-1 function may be completely different, or even opposite, in different tissues: it can promote the tumor progression rather than its inhibition. As previously reported, transformed cells usually produce low caveolin-1 levels but the caveolin-1 expression is increased in kidney, prostate and stomach deriving tumors comparing to the corresponding normal tissues [97]. A high caveolin-1 expression is associated to progression in prostate, colon, breast and lung carcinomas. In addition, the re-expression of caveolin-1 in poor invasive or caveolin-negative lung cancer cell lines increases their invasive ability [104]. In conclusion, the involvement of caveolin-1 as promoter or suppressor of tumor metastasis is strongly influenced by the cell types and, from the molecular point of view, by the interaction between signalling pathways and caveolin-1.

However, an important question whether gangliosides and GSLs affect caveolin function in microdomain was not considered before.

TUMOR CELL MOTILITY AND INVASION

Defining cell migration and invasion is challenging, since these entities overlap in many ways. To invade means *to go into*, and migration means *to move*.

Cell invasion is often associated with cancer and destruction of normal surrounding tissue by cancer cells, however it represent much more than just an element in the development of cancer. It is also a crucial step in several physiological events such as embryo implantation, placentation, embryogenesis, wound healing and inflammation and in deseases such as atherosclerosis, cancer and pre-eclampsia. The steps involved in tumor cell invasion are: 1. attachment of tumor cell to the basement membrane, 2. proteolysis or breakdown of basal membrane, 3. cell migration through the destroyed basal membrane. So, in fact, cell migration is a characteristic feature of invasive cells.

Cell migration/motility is also important in physiological and pathological processes cited before. Cell migration is a multistep process that involves the integration and coordination of complex

biochemical and biomechanical signals, it includes: 1. the protrusion of the leading edge, 2. the formation of new adhesions at the front, 3. the contraction of the cell, and the 4. release of adhesions at the rear [105, 106].

The migration of cells can be initiated by chemical and physical factors in their microenvironment. These extracellular signals can be sensed by receptors or mechanosensors on the cell surface or in the cell interior to initiate the migratory response. A key event in the response is the actin polymerization in the direction of migration to provide the protrusion force for the extension of the leading edge, where new focal adhesions are formed to anchor the actin filaments and the cell to the substratum. Subsequently, the actin cytoskeleton and focal adhesions exert traction force on the substratum, which results in a counter-force on the cell to promote cell migration. The contraction of actomyosin filaments pulls the cell body toward the leading edge, with a consequent release of focal adhesions at the rear to allow the tail to retract and the cell to move forward.

Extra cellular matrix provides the mechanical support and chemical cues for cell adhesion and motility. The dynamic cell- extra cellular matrix adhesion at the leading edge and detachment at the rear are critical steps in cell migration. Integrins are the major receptors for extra cellular matrix proteins. The integrin family includes more than 20 transmembrane heterodimers composed of α and β subunits with non-covalent association [107]. The extracellular domain of integrin binds to specific ligands, e.g., extracellular matrix proteins such as fibronectin, vitronectin, collagen, and laminin. The cytoplasmic domain interacts with cytoskeletal proteins (e.g., paxillin, talin, vinculin, and actin) and signalling molecules in the focal adhesion sites [108, 109]. Cell-extra cellular matrix adhesion not only serves as an anchorage for cell adhesion and migration, but also initiates signalling events to modulate cell motility. Integrins, the major cell- extra cellular matrix adhesion receptors, function as transducers for inside-out as well as outside-in signalling, and regulate cell motility through multiple signalling molecules. In addition, integrin-mediated signalling can crosstalk with other signalling pathways to coordinate cell motility.

Elucidating the mechanisms of cell motility is critical to the understanding of a multitude of physiological and pathological processes and to develop effective strategies to treat and prevent diseases.

INTEGRIN-MEDIATED SIGNALING IN CELL MOTILITY

The effects of the extra cellular matrix on cells are mainly mediated by the integrins, a large family of cell-surface receptors that bind, and therefore mediate adhesion to, extra cellular matrix

components, organise the cytoskeleton, and activate intracellular signalling pathways. Each integrin receptor consists of two transmembrane subunits: α and β. In mammals, 18 α and 8 β subunits associate in various combinations to form 24 integrins that can bind to distinct, although partially overlapping, subsets of extra cellular matrix ligand [110, 111]. The integrins transmit both mechanical and chemical signals. As well as imparting polarity to the cell and organizing and remodelling its cytoskeleton during adhesion and migration, these signals exert a stringent control on cell survival and cell proliferation. Most integrins activate focal adhesion kinase (FAK) and thereby also Src-family kinases (SFKs), which causes the phosphorylation of, p130CAS and paxillin. A subset of integrins, including α1β1,α5β1, and α5β3, also activates a pathway that is mediated through the adaptor protein SHC, which associate with α subunits, and ILK, which is a serine/threonine protein kinase that interacts with the cytoplasmic domains of β1 and β3 integrins, are localized at focal adhesions and regulate cell motility, in parallel with the FAK pathway ,through a palmitoylated SFK, such as Fyn or Yes. Mitogen-activated protein kinases (MAPKs), including ERK, p38MAPK, and JNK, can be activated by integrin-mediated signalling [112, 113]. There is evidence that MAPKs can promote cell migration by regulating actin dynamics. P38MAPK can be activated by α2 integrin, which is required for cell migration on collagen [114], and p38MAPK may regulate actin polymerization through HSP27 phosphorylation [115].

Despite this complexity and specificity, the essence of integrin signalling, that is what integrins do, is simple: they promote cell survival and impart positional control to the action of receptor tyrosine kinases, and therefore determine whether cells proliferate and migrate in response to soluble growth factors and cytokines.

It is increasingly clear that neoplastic cells enhance the expression of integrins that favour their proliferation, survival and migration, whereas they tend to lose expression of the integrins that exert the opposite effect.

Shc regulates random cell motility through ERK, and Shc can be downregulated by the tyrosine phosphatase PTEN [116].

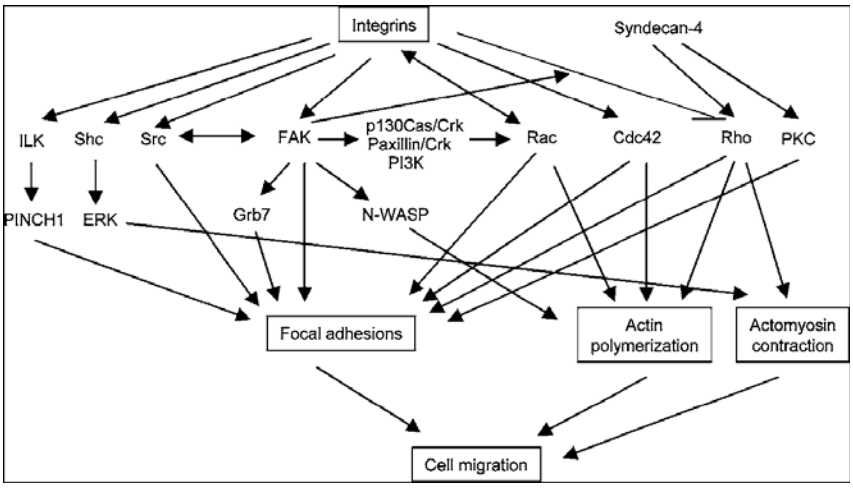

Figure. Schematic diagram showing the cell-ECM adhesion-mediated signalling in cell migration. .

SPHINGOSINE-1-PHOSPHATE

S1P is a signalling molecule involved in the regulation of important biological processes, both physiological and pathological ones. S1P is present with high concentrations in plasma (0.1 μmol/L) and serum (0.4 μmol/L). However the amount of biological active molecule is low since S1P has a low half life in extracellular fluids; in blood it is mainly bound to plasma components, such as albumin, other proteins or lipoprotein particles [117].

Platelets, characterized by high level of sphingosine kinase and no expression of S1P lyase, represent an important source of bioactive lipid, which is released in the blood flow after the platelet activation by many stimuli [118]. Also other hemopoietic cells, like monocytes, mast cells and erythrocytes, release S1P in the blood [119]. Several other cell types have the required enzymes for the S1P synthesis and they produce it after extracellular stimulation mediated by growth factors and cytokines.

S1P cell levels are kept low and they are strongly regulated through the regulation of the biosynthetic and degradative pathways. Therefore S1P levels could be potentially altered by every stimulus that is able to influence the activity or expression of enzymes involved in S1P synthesis or degradation. In particular, the S1P metabolism modulation is primarily performed through the activation and expression regulation of sphingosine kinase.

Metabolism of S1P

As previously stated, S1P is produced by sphingosine kinase through transfer of a phosphate group from ATP to the hydroxyl group on sphingosine C1.

The S1P intracellular level modulation is obtained also by its elimination through multiple pathways; the enzymes responsible for the S1P degradation are S1P lyase, S1P phosphatase and enzymes of the lipid phosphate phosphatase family.

S1P lyase is a key enzyme in the S1P degradation process. The S1P lyase catalyzes the breakage of the C2 and C3 bond with the production of hexadecenal and phosphoethanolamine [120]; this reaction is irreversible.

The S1P lyase is present in every mammal cell with the exception of platelets, in which a high amount of S1P is released after activation [121].

Embryo cells of S1P lyase knock-out mice show an accelerated differentiation; this effect may be due to the S1P accumulation since the administration of *N*,*N*-dimethylsphingosine, a sphingosine kinase inhibitor, results in the inhibition of this process. This hypothesis is supported also by the observation that sphingosine kinase overexpressing cells are characterized by the same acceleration of the differentiation process [122]. *D. Melanogaster* mutants in which the S1P lyase gene has been deleted show serious alterations in muscle development and integrity, suggesting a role for S1P metabolism in the correct myogenic development [123].

S1P lyase is localized in the endoplasmic reticulum with the active site oriented toward the cytosol.

The other S1P degradation pathway is mediated by S1P phosphatase. This enzyme belongs to the lipid phosphate phosphatase family, a class of membrane proteins involved in the lipid dephosphorylation in both intracellular and extracellular sites [124]. S1P phosphatase produces sphingosine from S1P, allowing its recycle: the obtained sphingosine can be addressed to the sphingolipid biosynthesis or being phosphorylated by the sphingosine kinase to S1P. The regulation of the S1P phosphatase expression may be due to extracellular signals and this influences the intracellular S1P levels, modulating its biologic effects.

Two enzyme isoforms have been identified in *S. Cerevisiae* and in mammals and they are localized on the endoplasmic reticulum.

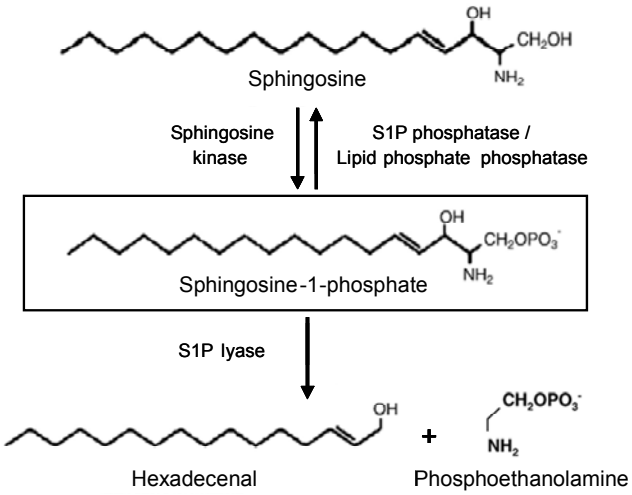

Structure, synthesis and degradation of S1P

Mechanism of action of S1P

S1P can act as a second messenger, modulating the activity of specific intracellular targets [125], or as extracellular agonist, through interaction with specific receptors (S1PR) located on the plasma membrane, through an autocrine or paracrine signalling [126]. Anyway it is not possible to separate the processes that S1P activates acting as a second messenger to those it activates through its receptor activation: in fact the regulation of some cell processes could involve both mechanisms of action.

In any case, some cell processes are activated by S1P in a receptor independent way, although the intracellular molecular targets are not yet known. The processes related to the S1P action as second messenger are the calcium mobilization from intracellular stores in an inositol triphosphate independent manner [127], cell proliferation and apoptosis inhibition [128]. Actually, the data referring to cell proliferation and survival regulation by S1P are contrasting: in fact indications support both the intracellular action and the involvement of S1P receptors.

S1P can activate cell processes also by the interaction with specific G-protein coupled receptors, known as $S1P_{1\text{-}5}$. Through the activation of these receptors, S1P regulates the cytoskeleton rearrangement [129], cell migration [130, 131], cell junction assembly [132], embryonic development [128], angiogenesis [133] and muscular regeneration [134]. Obviously, the S1P action as a receptor agonist requires its release in the extracellular milieu: because of the polarity of the S1P head, its translocation may be permitted by specific ABC family transporters (ATP-binding

cassette) [135]. As previously reported, S1P can be directly produced in the extracellular milieu: the secretion of active sphingosine kinase has been proved in some cells [136].

Biological functions

S1P principal effects in cells are the survival and growth promotion and the apoptosis inhibition, as it will be later described.

S1P is a potent regulator of cell migration in vitro, but its effect on this process is contradictory. In fact cell migration is dependent on the interaction between S1P and S1PR. Depending on the receptor subtypes expressed by cells, S1P can either act as a potent stimulator of cell migration or as a chemotaxis inhibitor. In one case however a receptor independent cell migration inhibition has been described [137].

S1P may act as a vasoactive and cardioactive mediator because of its presence in blood and its receptors are highly expressed on the cardiovascular system.

In endothelial cells S1P has multiple effects: it stimulates the production of nitric oxide (NO), an important muscle tone regulator [138], through activation of PI3K. This signalling pathway cause the activation of Akt, which then activates NO synthase by phosphorylation [139].

An increase amount of evidences supports a role of S1P as pro-angiogenic factor: this lipid promotes endothelial cell survival, chemotaxis, angiogenesis and vasculogenesis [140].

The S1P receptors are expressed also in immune system cells such as B and T cells [141]. Most of these cells release S1P when activated, suggesting an autocrine binding between the lipid and its receptors and modulating the immune system and the hypersensitivity.

In addition to the effects of S1P on the immune and cardiovascular system, S1P exerts important actions also on reproductive system, liver and nervous system cells.

An emerging concept in the S1P biology is the interaction between this lipid and tyrosine kinase receptors (cross-talk), in which this lipid has a double role: on the one hand as second messenger of growth factors, on the other hand as ligand for specific G-protein coupled receptors. In this context, it has been proved that the PDGF-induced cell migration depends on the $S1PR_1$ expression in mouse embryonic fibroblasts [142]. The molecular mechanism of cross-talk is quite controversial. One of the proposed models involves the sphingosine kinase activation by the PDGF receptor (PDGFR), the consequent S1P release in the extracellular milieu and finally its interaction with $S1PR_1$, while another model states that a physical interaction between PDGFR and $S1PR_1$ is sufficient [128].

From all these data is clear that S1P is an important bioactive lipid and that it plays a key role in several physiological and pathological processes in different cell types.

SPHINGOSINE KINASE

Sphingosine kinase is an evolutionary conserved lipid kinase that catalyzes the phosphorylation of the hydroxyl group present on the sphingosine C1 through a reaction that requires ATP and a bivalent cation. This reaction catalyzes the S1P production with a contemporary reduction in ceramide intracellular level.

In mammal cells two sphingosine kinase isoforms have been characterized, sphingosine kinase-1 (SK1) and sphingosine kinase-2 (SK2) [143], different by structure, kinetic properties, regulation mechanisms, sub-cellular and tissue localization and temporal expression pattern during embryogenesis [144]. Because of these differences between the two isoforms, an involvement in different cell functions has been hypothesized. In fact the two isoforms activate opposite cell response, even if the same reaction is catalyzed: while SK1 promotes cell survival and proliferation [145, 146], SK2 (at least when overexpressed) activates apoptosis and cell cycle arrest [147, 148]. A reason for the two isoform different function might be their different sub-cellular localization, with, as consequence, S1P production in different cell districts [144, 149]. In fact while SK1 localization is mainly cytoplasmic and, after stimulation, it migrates to the cell membrane producing an outer-released S1P, SK2 is mainly associated to cell organelles, in particular to the nucleus and to the endoplasmic reticulum [147, 148]. The SK2 endoplasmic reticulum localization may explain its pro-apoptotic action: there S1P phosphatase and ceramide synthase enzymes are confined and they may be responsible for the conversion of S1P to sphingosine and then to ceramide, a pro-apoptotic metabolite. Actually, it was not well understood if the SK2 anti-mitogenic and pro-apoptotic effect are due either to S1P production or to the enzyme activity, which could be directly involved in DNA synthesis inhibition and in mitochondrial apoptosis pathway activation. This presumption is supported by the discovery that SK2 nuclear localization is linked to the cell cycle arrest in G1/S phases [147] and that this isoform contains a 9 aminoacid sequence homolog to the *Bcl2-homology domain 3-only* of pro-apoptotic proteins [148].

Four membrane-spanning domains in SK2 and none in SK1 have been predicted by hydrophobicity analyses [128]. Splicing variants of the two isoforms were recently reported [150], differing by the N-terminal portion: three SK1 protein variants are 384, 398, 470 aminoacid long, while two SK2

protein variants are 618 and 654 aminoacid long. The SK1 and SK2 coding genes are localized on chromosome 17 and 19, respectively.

The two sphingosine kinase isoforms possess five homology domains known as C1-C5. The C1-C3 domains are localized in the catalytic domain, which shares the structure with diacylglycerol kinase and ceramide kinase [151]. The ATP binding domain resides in the C2 domain within the SGDGx17-21K consensus sequence [152], while the sphingosine binding site involves an aspartic acid conserved residue located in the C4 domain [153].

The sphingosine kinase regulation is a vital event for the modulation of S1P intracellular levels and biological effects. SK1 undergo a complex regulation mechanism through several molecular mechanisms, most of which are not yet completely understood.

Many extracellular molecules are able to activate the enzyme and to stimulate the S1P production [154]: ligands of G-protein coupled receptors such as acetylcholine, lysophosphatidic acid and S1P; ligands of tyrosine kinase receptors such as PDGF, VEGF, EGF; several cytokines such as TNFα and TGFβ; hormones such as estrogens and glucocorticoids. The SK1 inhibition has proved to block some of the signalling pathways downstream to these agonists, interrupting, at least partially, the biological effects [128]. Therefore S1P represents an important modulator for the action of several growth factors, cytokines and hormones [155].

Recently, the molecular mechanisms underlying the SK1 regulation by these agonists have started to be clarified. Most of these stimuli increase the enzyme activity through post-transductional mechanisms, such as localization, degree of phosphorylation and interaction with proteins or phospholipids. In addition other extracellular agents are able to modulate the enzyme activity acting on a transcriptional level.

The regulation of SK1 localization represents an important factor for the enzyme activation and the S1P production [128]. In fact, the enzyme activation often comes along with its translocation from the cytosol to the plasma membrane [144]. SK1, in absence of stimulation, can be mainly located in the cytosol, while sphingosine is found in plasma and inner membranes. This translocation, in addition to the substrate recruitment, is important because SK1 can interact in membrane with anionic lipids, mainly phosphatidylserine, that stimulates its activity [156].

The molecular mechanisms for the SK1 translocation from the cytosol to the membranes are not completely understood. The involvement of anionic membrane lipids has been hypothesized, which could act as docking sites for the enzyme, leading it to the cell membrane [144, 157, 158]. In

addition the SK1 translocation appears to be involved in its association with other proteins, such as calmodulin [159].

SK1 is regulated also through its export from the cell, with a consequent S1P production in the extracellular milieu [136].

Depending on whether SK1 is translocated to the plasma membrane, to the inner membranes or it is secreted, the S1P is produced close to its surface receptors or to intracellular molecular targets. The enzyme localization regulation could therefore have important consequences in the determination of the S1P effects.

Sphingosine kinase and the sphingolipid rheostat

Ceramide, sphingosine and S1P have an important role in the regulation of survival and cell death. In fact, it has been shown that they can behave as second messengers, conserved from yeast to human. Resting cells are characterized by low levels of these three sphingolipids. The metabolism and the signalling pathways are stimulated by different forms of sphingomyelinases that convert sphingomyelin to ceramide and phosphocholine. In several cell types, high ceramide levels promote cell growth arrest and apoptosis induction [160]. UV radiation, antitumor drugs and cytokines activate sphingomyelinases, increasing the ceramide level and inducing apoptosis [39, 161, 162]. The increased ceramide production is often fundamental for the apoptosis induction, since sphingomyelinase activity-lacking cells result protected from apoptosis and the exogenous ceramide administration is able to reactivate it [154, 163]. Strong evidences support the fact that few antitumor drugs activate apoptosis through the increased *de novo* ceramide production [164].

The only pathway for sphingosine formation is the ceramide deacylation. Sphingosine acts as a protein kinase C (PKC) inhibitor [165] and increased sphingosine levels are able to block the cell growth and to activate apoptosis. For example in Jurkat T cells the Fas mediated apoptosis is due to an increased ceramidase activity with a consequent increased sphingosine production [166]. The activation of caspase-3-like proteases has been recently proved during sphingosine induced apoptosis in hepatoma cells [167]. Anyway, it is not clear yet if an increased production of sphingosine is sufficient for the induction of apoptosis.

S1P has opposite effects compared to its precursors, ceramide and sphingosine, in the regulation of cell survival: in fact this molecule promotes survival and inhibits cell death [168, 169]. Many extracellular stimuli, mainly growth and survival factors, activate sphingosine kinase causing an increase in S1P levels and a contemporary decrease in ceramide levels. This evidence, together with

the notion that these are interconvertible molecules, suggests that the cell fate may not depend on the absolute intracellular concentration of each of these sphingolipids, but on their relative levels. This model, known as "sphingolipid rheostat", states that the activity modulation of the enzymes involved in the interconversion of these molecules (ceramidase, sphingosine kinase and S1P phosphatase) has a fundamental role in the choice between survival and cell death [170]; this happens through the ratio regulation of the intracellular levels of ceramide and S1P. In fact, the conversion of ceramide and sphingosine to S1P not only causes the formation of an anti-apoptotic molecule, but also removes pro-apoptotic molecules.

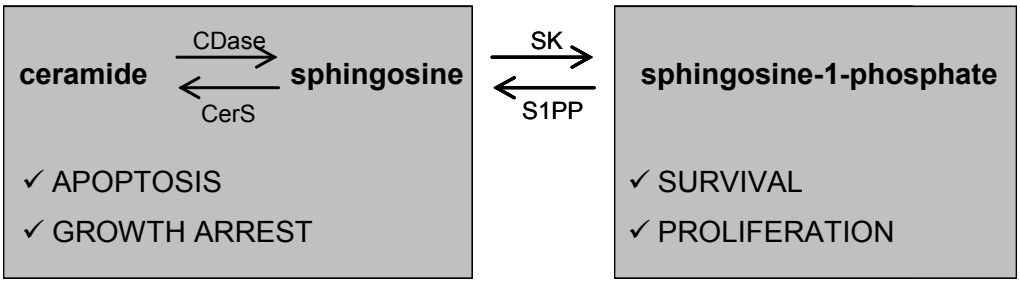

Sphingolipid rheostat

DRUG RESISTANCE IN TUMOR CELLS

Chemotherapy is the first approach for cancer metastases treatment. The majority of the currently used anticancer drugs, in particular the cytotoxic ones, interferes with the cell division mechanisms. The anti-proliferative action of cytotoxic drugs could be caused not only by a direct effect on G1 and S cell cycle phases, but also by the action on the cellular events that activate apoptosis.

One of the greater problems of chemotherapy is the presence or the onset of drug resistance. Some tumor types, like liver and colon cancer, present a primary resistance, which is an absence of response to the first administration of some therapeutic drugs. The acquired resistance on the other hand develops in normally sensible tumors. Drug resistance can be highly specific for a single drug and it is usually based on a genetic change in tumor cells caused by genetic amplification or increased expression of one or more genes. In other instances the resistance to anticancer drugs characterized by different chemical structure can develop after repeated exposition to a single drug.

This phenomenon is called MDR (multidrug resistance) [51, 171]. Several mechanisms appear to be involved in the MDR phenotype and they can be classified in two groups:

1. reduction in the intracellular drug accumulation
2. reduction in the consequences derived by the intracellular drug accumulation

The first group includes drug resistance mechanisms that involve both the reduction of drug internalization, for example by reduction of cell membrane permeability [172], and the greater drug efflux toward the extracellular milieu. In this case, the diminished drug accumulation in cells is due to an increased expression of a transport protein on the cell membrane, known as P-glycoprotein (Pgp). Pgp is a 170 KDa membrane protein produced by the MDR1 gene [173, 174] and it belongs to the ABC transporter protein family. One model of the P-glycoprotein structure predicts the presence of six membrane spanning domains, which form a porous on the cell membrane, and an ATP binding site on the intracellular portion.

Pgp expression studies in normal tissues show high expression levels in kidney, liver, pancreas, small intestine, colon and adrenal glands, while very low expression levels are found in the other tissues. P-glycoprotein is localized in the apical or luminal portion of the cell membrane. This localization suggests that P-glycoprotein could have a physiological role in the secretion processes. In fact, its high presence in liver, kidney and intestine is an evidence for its role in the drug and xenobiotic elimination from the body. The MDR phenotype in tumor cells could reflect the increased expression or the amplification of genes normally involved in drug elimination.

Besides the Pgp, other ABC transporter proteins have been identified as drug excreting pumps. For example MRP (multidrug resistance-associated protein) is a 190 KDa protein that plays a role in drug resistance. Although it has just a 15% homology with Pgp, the two protein confer resistance to similar cytostatic agents [175].

The second group of MDR mechanisms does not reduce the intracellular drug amount but it induces a reduction in the drug effect. For example, a drug conversion to a less toxic metabolite can happen or, on the contrary, a pro-drug conversion to the active form can be prevented. Another possible mechanism of drug resistance is based on the altered enzyme or receptor expression: if a drug inhibits an enzyme that is important for cell growth, for example topoisomerase II [176], cells that produce a higher enzyme amount can still produce enough product metabolite to survive when treated with drug pharmacological concentrations. Finally some MDR mechanisms increase the cell survival through inhibition of the apoptotic process; this could happen through regulation of p53 and proteins belonging to the Bcl-2 family.

Sphingolipids and drug resistance

Ceramide and complex sphingolipids are involved in the apoptotic process [177]. Ceramide production results from several stimuli, such as growth factor privation, cytokines, ionizing radiations, thermal shock, chemotherapy and other cytotoxic agents and environmental factors, such as stress or diet [178]. These stimuli activate the ceramide pathways. In addition, the exposition of cells to some ligand, such as vitamin D3 [179], TNF-α, CD28 or CD95/APO-1/Fas ligand [180], stimulates the signalling pathways activated by ceramide. The ceramide-activated cell signals contribute to cell cycle arrest, terminal differentiation and apoptosis. Ceramide can directly or indirectly activates specific proteins: those that are directly activated by ceramide are ceramide-activated protein kinase [181], ceramide-activated protein phosphatases, atypical protein kinase Cξ and protein kinase Raf-1; ceramide can also activate signalling pathways in which MAPK and SAPK are involved. Besides ceramide, other sphingolipids, such as S1P and glucosylceramide, are involved in the cell growth and differentiation. It has been shown that the levels of glucosylceramide, a ceramide direct metabolite, are significantly higher in several Pgp overexpressing cell lines [182]. High levels of glucosylceramide in tumor cells could represent a marker for the drug resistant phenotype identification [183].

In MDR ovarian carcinoma cells glucosylceramide, sphingomyelin and galactosylceramide levels have been proved to increase, while, on the contrary, lactosylceramide and other complex sphingolipids have a lower concentration than the drug sensible cells [177]. The increased glucosylceramide levels could be due to an increased activity of glucosylceramide synthase. This mechanism prevents the ceramide accumulation and therefore the apoptotic process. In addition, a decreased glucosylceramide transporter activity in the Golgi apparatus could explain the reduced ceramide production. This finding can provide an explanation to the decreased lactosylceramide and complex sphingolipid levels.

The ABC transport proteins allow the movement of amphiphilic molecules through cell membranes, including sphingomyelin and glucosylceramide. Several studies have in fact provided indications about a different ABC protein role in sphingolipid localization.

Although the greater portion of cellular sphingomyelin is localized in the plasma membrane outer layer, the sphingomyelin that is involved in the sphingomyelin-ceramide signalling pathway is localized in the inner layer. The overexpression of the Pgp transporter protein can cause the depletion of the sphingomyelin inner portion with a consequent fall of ceramide production.

Pgp protein is localized in the plasma membrane as well as in the Golgi complex. It has been hypothesized that in the Golgi complex Pgp can have a role in the glucosylceramide translocation from the cytosol to the Golgi lumen, where it is used as substrate for the lactosylceramide and complex sphingolipid production. In this way the ceramide is used for the glucosylceramide synthesis and it cannot activate the ceramide-dependent apoptosis pathway.

A2780AD cells (adriamycin resistant) overexpress Pgp, which is localized both in the plasma membrane and in intracellular vesicles (but not in the Golgi complex). As previously stated, Pgp removes glucosylceramide from the cytosol reducing its concentration in the Golgi complex, thus reducing the production of lactosylceramide and decreasing the ceramide intracellular concentration.

Sphingosine kinase and drug resistance

Several commonly used anticancer drugs, such as daunorubicin, vincristine and retinoids, exert their cytotoxic action through the induction of ceramide production, which is able to induce apoptosis and inhibit proliferation in several cell lines. It has been proved that drug resistant tumors and cell lines are often characterized by an increased ceramide glycosylation to form glucosylceramide due to an increased glucosylceramide synthase expression or activation [3]. The ceramide elimination allows the tumor cells to prevent the ceramide-induced apoptosis and to display drug resistance [4, 5]. The glucosylceramide accumulation has been proved to not be the only result of an altered sphingolipid metabolism. In MDR ovarian carcinoma cells sphingomyelin and galactosylceramide levels are also increased, while lactosylceramide and complex sphingolipids levels are reduced compared to the drug sensible cell line [22]. In addition, retinoids-resistant ovarian carcinoma cells are characterized by a similar glucosylceramide level but an increased production of GM3 compared to the drug sensible cells [184].

Besides the ceramide functions as complex sphingolipid precursor, it can be converted to sphingosine and then phosphorylated to S1P by the sphingosine kinase. The S1P production is important for the complete ceramide and other sphingolipid elimination. S1P is also an important intracellular signalling molecule that takes role in signal transduction. In particular, S1P represents an apoptosis inhibitor and a positive regulator of cell survival and proliferation.

Ceramide and S1P exert opposite effects on the cell fate and the enzymes that regulate their concentration, like sphingosine kinase, represent an important checkpoint for the activation of cell proliferation or apoptosis [38, 170].

Recently a role for sphingosine kinase in tumor cell drug resistance has been suggested. For example, possible roles of the ceramide/S1P pathway in the Imatinib resistance in K562 chronic myeloid leukemia cells have been investigated. Continuous exposition of K562 cells to increasing Imatinib concentrations has caused the selection of Imatinib resistant cells (K562/IMA-1 cells). The Imatinib treatment causes an increased ceramide production in the sensible parental cells but not in the resistant clones. In the latter, the ratio between ceramide and S1P levels was altered by the SK1 overexpression. In fact, in these cells the SK1 expression was 2.5 times higher than in the parental cells with a consequent higher S1P production. In addition, the partial SK1 silencing through siRNA reduces the S1P level and increases the resistant cell sensitivity to Imatinib [185].

In solid tumors, hypoxia and HIF-1 (hypoxia-inducible factor-1) signaling are correlated with tumor progression and therapeutic failure. In a study performed on etoposide-resistant A549 lung cancer cells an increased SK2 expression and activity has been observed in hypoxic conditions. This increase in SK2 activity correlates with the S1P increased production and release in colture medium and it protects A549 cells from the etoposide cytotoxic effect. The SK2 inhibition through siRNA has restored the drug resistance in A549 cells in hypoxic conditions [186].

The cell ratio between ceramide and S1P is crucial for gemcitabine sensitivity in pancreatic cancer cells; a low ceramide/S1P ratio, together with a high SK1 activity, is indicative of high chemoresistance. The increase of the ceramide/S1P ratio through pharmacological SK1 inhibitors or siRNA has allowed the sensitization of pancreas carcinoma cells to gemcitabine. On the opposite, drug resistance has been promoted in these cells lowering the ceramide/S1P ratio through upregulation of SK1 activity [10].

MATERIALS AND METHODS

Lipids and radioactive lipids

GM1, GM2, GD1a [187] and lactosylceramide [188] were prepared from the bovine brain ganglioside mixture. GM3 was prepared from GM1 [189]. [1-^{3}H]sphingosine (radiochemical purity over 98%; specific radioactivity 2.2 Ci/mmol), GM3 tritium labeled at the position 3 of sphingosine, [3-^{3}H(*sphingosine*)]GM3 (radiochemical purity 98%, specific radioactivity 1.2 Ci/mmol), [3-^{3}H(*sphingosine*)]LacCer (radiochemical purity over 99%, specific radioactivity 1.2 Ci/mmol) and [^{3}H]lipids used as chromatographic standards were prepared as described [11]. Radioactive and photoactivable ganglioside [11-^{3}H(*Neu5Ac*)]GM3-N_3 was prepared as previously reported [190].

Chemicals

HPR was from Sigma. VPC23019, JTE013, CAY10444, W146, SW2871, VPC24191, S1P, sphingosine kinase inhibitor 2-(*p*-hydroxyanilino)-4-(*p*-chlorophenyl) thiazole were obtained from Calbiochem. [1-^{3}H]sphingosine (radiochemical purity over 98%; specific radioactivity 2.2 Ci/mmol), and [^{3}H]lipids used as chromatographic standards were prepared as described in [11].

Cell Culture and Transfection

A2780 and A2780/HPR cells, were cultured in RPMI 1640 (Sigma) supplemented with 10% of heat-inactivated FBS (GIBCO), 2 mM glutamine, 100 units/ml penicillin and 100 μg/ml streptomycin. A2780/HPR were cultured in presence of 5 μM HPR [191]. The GM3 synthase expression vector (pSAT1-Rc/CMV) (a generous gift of Dr. I. Colombo, University of Milano, Italy) was constructed by subcloning SAT-1 cDNA into an expression vector pRc/CMV [192]. A2780 cells were transfected by cationic polymers (Open Biosystems, Huntsville, AL) with the pSAT1-Rc/CMV or with the empty vector, following the manufacturer's protocol. Stable transfectants were isolated after selection with 750 μg/ml of geneticin (G418, Sigma, St. Louis, MO). A2780 cells were transfected by FuGENE®(Roche) with the pcDNA3-hSK1^{WT}Flag [193] (a gift of Dr. Stuart M. Pitson, Hanson Institute human Immunology, Institute for Medical and Veterinary Science, Adelaide, Australia) or with the empty vector, following the manufacturer's protocol. Stable transfectants were isolated after selection with 500 μg/ml of geneticin (G418, Sigma).

siRNA transfection CAV-1 silencing

For the silencing of the CAV-1 gene in A2780/HPR and SAT-I A2780 cells a transient transfection was performed with CAV-1 specific siRNA (FlexiTube Validated siRNA, Qiagen). As negative

control a scrambled sequence was used that does not recognize any mRNA sequence (AllStars Negative Control siRNA, Qiagen). For the transfection of the siRNAs Lipofectamine™ 2000 (Invitrogen) was used.

For the assessment of the silencing efficiency the day before the transfection 5,000 A2780/HPR and SAT-I cells were plated in 0.3 cm^2 surface wells in 100 μl of antibiotic-free medium obtaining in this way the following day a confluence of about 40-50%. Three different reaction mixtures were prepared: the first one containing 4 ρmol of scrambled siRNA as negative control, another one with 4 ρmol of CAV1 siRNA and the third one without RNA.

For every well 0.25 μl of Lipofectamine™ 2000 were diluted in 25 μl of Opti-MEM Reduced Serum Medium and were incubated at room temperature for 5 minutes. The following day the medium was replaced with complete medium. The cells were then collected for protein or mRNA extraction after 24 hours of transfection or kept in culture until 72 hours of transfection.

For immunofluorescenceassay the day before the transfection 250,000 A2780/HPR cells were plated in 10 cm^2 surface wells containing 24 mm glass coverslips in 2ml of antibiotic-free medium. For every well 5 μl of Lipofectamine™ 2000 were diluted in 250 μl of Opti-MEM Reduced Serum Medium and were incubated at room temperature for 5 minutes. 8 ρmol of RNA were then diluted in other 250 μl of Opti-MEM Reduced Serum Medium and the two volumes were combined and incubated for 20 minutes at room temperature. The transfection complex was administrated to the cells and after 48 hours the transfection was repeated. Finally, after 48 hours the immunofluorescence analysis was performed.

Cell proliferation and viability: MTT reduction and Trypan Blue dye exclusion assay

For the MTT assay, A2780, A2780/HPR and A2780 transfectants were plated into 96-well tissue culture plates and kept in culture for up to 96 hours in normal cell culture medium or under different experimental conditions as described below. For the basal proliferation, the same amount of cells were plated (2,000 cells for well). After treatments, the cells were incubated at 37 °C for 1 h with 100 μl of cell culture medium containing 120 μM MTT and then lysed with 100 μl of lysis solution (10 % SDS in 10 mM HCl aqueous solution) and maintained for 12 h at 37 °C. The absorbance was measured at 570 nm with Victor plate reader instrument (Perkin Elmer).

The number of living and dead cells has been determined by counting after Trypan blue staining, as previously described [194]. Three thousand A2780, A2780/HPR and A2780 transfectants cells were plated in 60 mm tissue colture plates. Briefly, cells were detached with PBS containing 0.02 %

EDTA, incubated in 0.25 % Trypan blue solution for 2 min and counted using a Bürker chamber. The extent of cell death was calculated as the percent of trypan blue-positive cells in each cell population.

RNA extraction, RT-PCR and Quantitative Real-Time

Total RNA was isolated by single-step acid-guanidine-isothiocyanate- chloroform extraction methods and purified by PureLink™ Macro-to-Midi kits (Invitrogen, Carlsbad, CA), according to manufacturer's instructions. Five microgram of RNA was treated with 3 U of RNase-free DNase for 25 min at room temperature to remove possible DNA contamination. The total amount of extracted RNA was estimated by a quantitative fluorescent method using the Quant-iT™ RiboGreen RNA Reagent Kit (Invitrogen). Using random hexamers, 1 μg of RNA were reverse-transcribed using SuperScript™ III First-Strand Synthesis System for RT-PCR (Invitrogen) in a final 20 μl reaction volume. cDNA representing 50 ng of total RNA was used as a template for RT-PCR.

For multiplex RT-PCR, we used a mixture containing 0.2 μM primers, AccuPrime™ PCR Buffer, and 1 unit of AccuPrime™ *Taq* in a final volume of 50 μl. The amplification was performed using the following cycle conditions: initial denaturation at 94 °C for 2 min, followed by 35 cycles of 15 s at 94 °C (denaturation), 20 s at 58 °C (annealing) and 30 s at 68 °C (elongation). RT-PCR mixture included 0.5 μM primers, 200 μM Deoxynucleotides triphosphate, Fusion HF Buffer, 0.4 U of Phusion Hot Start DNA polymerase (Finnzymes, Espoo, Finnland) and 3 % of dimethyl sulfoxide in a final volume of 20 μl. The amplification was performed using the following cycle conditions: initial denaturation at 98 °C for 1 min, followed by 30 cycles of 10 s at 94 °C (denaturation), 45 s at 58 °C (annealing) and 30 s at 72 °C (elongation). As internal controls, human β-actin and G3PDH cDNA was amplified at the same time. The PCR products were subjected to agarose gel electrophoresis and visualized by UV after ethidium bromide staining. Images were acquired using a digital GelDoc2000 trans-illuminator (BioRad, Hercules, CA) and elaborated with Quantity One software. To detect the expression of SK1 and SK2, cDNA from A2780 and A2780/HPR cells were subjected to polymerase chain reaction (PCR) using specific primer listed in Table 1.

The following primer were used:

Gene	Forward primer	Reverse primer
SAT-1	5′-GGGAGTAATAGCATGGGCAACCAT-3′	5′-CAGCTCTCAGAGTTAGAGTTGCATT - 3′
CAV-1	5′ - GAGCTGAGCGAGAAGCAAGT- 3′	5′ - TCCCTTCTGGTTCTGCAATC - 3′
CAV-2	5′ - ACGACTCCTACAGCCACCAC- 3′	5′ - CGTCCTACGCTCGTACACAA - 3′
GalNacT	5′ - CCTCCGTTATGATCGGCTAC - 3′	5′ - CCGAAGGGCATGAGATAGTG - 3′
SAT-4	5′- ATGTGGACCCTATGCTGGAG -3′	5′- CTTGGTCCCAACATCAGCTT -3′
NEU1	5′- AGAAGGATGAGCACGCAGA -3′	5′- CATCGCTGAGGAGACAGAAG -3′
NEU3	5′- TTCCAGCTACCATGTAAAACC -3′	5′- CTGGCACCTATGTGGGATCTC -3′
ACTIN	5′- CGACAGGATGCAGAAGGAG -3′	5′- ACATCTGCTGGAAGGTGGA -3′
GAPDH	5′- CGAGATCCCTCCAAAATCAA -3′	5′- GGTGCTAAGCAGTTGGTGGT -3′
SPT	5′- CTTGTTCCTCCTGTCCCAAA -3′	5′-CCCCACGCCATACTTCTTTA -3'
GLCT	5′- CTGGAAACATTCTTTGAATTGGAT -3′	5′-CTCATTAAACAAGACATTCCTGTC-3′
SK1	5’-CCCCAGCAAACCGGACCGAC-3’	5’-CCCCAGCAAACCGGACCGAC-3’
SK2	5’-CCCCTCAGACTCAGCGGCCT-3’	5’-GTGGGCGAGGCAGGTTCCAC-3’

The quantification of S1PR mRNA was performed by Real-Time PCR employing TaqMan Gene Expression Assays, using the automated ABI Prism 7700 Sequence Detector System (Applied Biosystems, Foster City, CA) essentially as previously described [195]. Each measurement was carried out in triplicate in Micro-Amp optical 96-well plates (Applied Biosystems) with a TaqMan Universal PCR Master Mix (Applied Biosystems). Primers and probe for $S1P_1$, $S1P_2$, $S1P_3$, $S1P_4$ and $S1P_5$ were Assay-On-Demand gene expression products (Applied Biosystems). Simultaneous amplification of the target sequence together with the housekeeping gene, 18S rRNA, was carried out with the following universal profile: initial denaturation for 10 min at 95° C was followed by denaturation for 15 sec at 95° C, primers annealing and elongation at 60° C for 1 min for 40–50 cycles. Results were analysed by ABI Prism Sequence Detection System software (version 1.7) (Applied Biosystems, Foster City, CA). The $2^{-\Delta\Delta Ct}$ method was applied as a comparative method of quantification [196] and data were normalized to ribosomal 18S RNA expression.

Lipid analysis

Cell sphingolipids were steady-state metabolically labeled by 2 h *pulse*/48 h *chase* with 3.6 x 10^{-8} M [1-^{3}H]sphingosine as previously described [11]. Lipids from cells, sucrose gradient fractions and immunoprecipitation samples were extracted with chloroform/methanol/water (2:1:0.1 by volume)(in the case of gradient fractions, water was omitted), subjected to a two-phase partitioning, and radioactive lipids were analyzed by mono- or two-dimensional HPTLC as previously described [11] [197]. For the analysis of S1P production, cells were pulsed with [1-^{3}H]sphingosine for 45 minutes as previously described [198]. Cell lipids were extracted with chloroform/methanol, the total lipid extracts were partitioned with 0.15 volumes of 0.1 M NH_4OH. S1P in the upper alkaline phase was separated by HPTLC using the solvent system n-butanol/ acetic acid/water 3:1:1. The radioactivity with the samples was determined by liquid scintillation counting. Radioactive lipids on HPTLC plates were detected and quantified by radioactivity imaging performed with a Beta-Imager 2000 instrument (Biospace, Paris, France) using an acquisition time of about 48 h. The radioactivity associated with individual lipids was determined with the specific β-Vision software provided by Biospace. The total lipid extract from about 5 mg of cell proteins was used for the analysis of endogenous lipids. The phospholipid content was determined by the method of Bartlett [199]. The ganglioside content was determined as lipid-bound sialyc acid by the resorcinol method [200].

GM3 synthase, GD1a synthase and sialidase assay

GM3 synthase activity was assayed on cell homogenates using [3-^{3}H(*sphingosine*)]LacCer as substrate [11]. GD1a synthase activity was measured as previously described [201] using [3-^{3}H(*sphingosine*)]GM1 as substrate The enzymatic activity of Neu3 sialidase was determined using 6 μM [3–^{3}H(*sphingosine*)]GM3 as substrate [202]. Total sialidase activity was determined with 2′-(4-Methylumbelliferyl)-α-D-*N*-acetylneuraminic acid sodium salt hydrate as substrate [203]. Assays were performed in triplicate. Data were expressed as nmol of converted substrate/hour x mg of cell protein, and are the means ± SD of three independent experiments.

Determination of in vitro cell motility by wound healing assay

Cells grown in 100 mm culture dishes as confluent monolayers were mechanically scratched using a 200 μl pipette tip. Cells were washed with complete culture medium and then incubated in the presence of complete culture medium for different times allowing wound healing. Phase contrast

images of the wounds were taken in nine random fields immediately after wounding (time 0) and after 24 and 48 hours, and wound width was measured. Each experimental point was in duplicate, and data were expressed as the mean values ± SD of three independent experiments.

Determination of in vitro cell motility by Phagokinetic Gold Sol Assay

2,000-3,000 cells, pre-treated or not with D- or L-PDMP were plated on 24 mm glass coverslips coated with gold colloidal solution [204] placed in 6 well plate, allowed the cell attachment and then added medium in the presence or not of the treatments. Incubated at 37 °C for the indicated times and photographed with 4X and 10X objective at different times. Cell tracks areas of 30-50 cells were calculated by pixel counting on the images using Image J software.

Transwell migration assay

Transwell migration assay were perfomed using InnoCyte TM Cell Migration Assay, 24 well (Calbiochem, Germany) following manufacturer's instructions. Briefly, 350 μl of a suspension with 10^5 cell/ml in serum free cell culture medium were added to cell culture insert with an 8 μm pores size membrane that was used as migration chamber. Cell culture medium containing serum is applied to the wells of the 24-well cell culture plate and the cell culture insert containing cells are placed in the wells. Cell migration trough the membrane is assessed by staining the cells that attach to the lower side of the membrane with calcein-AM. After staining cells were lysed and transferred to the black module strip and fluorescence is measured at 485 nm (excitation) and 520 nm (emission). As background calcein-AM was incubated without cells.

Administration of exogenous sphingolipids

To evaluate the effect of exogenous sphingolipids on the *in vitro* cell motility of A2780 cells, confluent cell monolayers were wounded as described above. Cells were washed with serum-free culture medium and then incubated in the presence of 50 μM GM3, GM2, GM1 or GD1a in serum-free medium for up to 48 hours [205] and references herein). Wound width was measured as described above. Each experimental point was in duplicate, and data were expressed as the mean values ± SD of three independent experiments. To check the extent of incorporation and metabolism of the administered gangliosides, cells were washed with 10% FBS-containing culture medium and with 0.1% trypsin in PBS to remove gangliosides loosely bound to the cell surface [206, 207]. Cell lipids were extracted and analyzed as described above.

Brefeldin-A treatment

Brefeldin-A (BFA) was solubilized in ethanol at the concentration of 0.01 mg/ml. A2780 cells were treated with BFA at the final concentration of 0.01 mg/ml or with vehicle (control) in complete medium. After 8h, control and BFA-treated cell confluent monolayers were wounded as described above, and cells lipids were labeled with $3x10^{-8}$ M [1-^{3}H]sphingosine in culture medium. After different times, the wound width was evaluated as described above. Radioactive lipids were extracted and analyzed as described above. Each experimental point was in duplicate, and data were expressed as the mean values ± SD of three independent experiments.

c-Src inhibition

A2780 cells grown in 100 mm culture dishes as confluent monolayers were pretreated for 6h with 3 μM SU6656 Src inhibitor (Sigma, St. Louis, MO) or with DMSO (vehicle), then confluent cell monolayers were wounded and cell motility was assessed by wound healing assay as described above. Cells were maintained in the presence of vehicle or 3 μM SU6656 for the duration of the migration assay.

Cell Proliferation Assay

A2780, mock- or SAT-1 transfected A2780 cells were plated in 60 mm culture dishes (500,000 cells/dish) and cultured in complete medium for up to 96 hours. The number of cells at different times after plating has been determined by counting after Trypan blue dye staining, as previously described [194]. Briefly, cells were detached with PBS containing 0.02 % EDTA, incubated in 0.25 % Trypan blue solution for 2 min and counted using a Bürker chamber.

Preparation of DRM fractions by sucrose gradient centrifugation

Cells were subjected to homogenization and to ultracentrifugation on discontinuous sucrose gradient, as previously described [208]. Briefly, cells were harvested, lysed in 1 % Triton X-100 in TNEV (10 mM Tris-HCl buffer, pH 7.5, 150 mM NaCl, 5 mM EDTA) in presence of 1 mM Na_3VO_4, 1 mM PMSF, and 75 mU/ml aprotinin, and Dounce homogenized (10 strokes, tight). Cell lysate (1 mg of cell protein/ml) was centrifuged 5 min at 1,300 x *g* to remove nuclei and cellular debris. The postnuclear surnatant (PNS) was mixed with an equal volume of 85% sucrose (w/v) in TNEV,

placed at the bottom of a discontinuous sucrose gradient (30–5%), and centrifuged for 17 hours at 200,000 x *g* at 4 °C. After ultracentrifugation, eleven fractions were collected starting from the top of the tube. Equal amounts of the low-density fractions 5 and 6 were put together to obtain the DRM fraction, whereas equal amounts of the high-density fractions 10 and 11 were put together to obtain the HD fraction. The entire procedure was performed at 0 – 4 °C in ice immersion. For the sphingolipid and phosphatidylethanolamine cells were previously metabolically labeled with 1-[^{3}H]sphingosine.

Western blot analysis

The samples were before analyzed by SDS-PAGE. After separation, proteins were transferred to polyvinylidene difluoride membranes (PVDF) and immunoblotted using mouse polyclonal anti-caveolin-1 (BD Transduction Laboratories, Lexington, KY), rabbit monoclonal anti-c-Src (Cell Signaling Technology, Danvers, MA), rabbit polyclonal anti-Src-pY416, anti-Src-pY527 (Cell Signaling) and Akt 1/2 (Santa Cruz, CA) followed by reaction with secondary horseradish peroxidase-conjugated antibodies and enhanced chemiluminescence detection (Pierce Supersignal, Rockford, IL). The presence of transfected SK was assessed by immunoblotting using an anti-flagM2 mouse polyclonal antibody (Sigma), SK1 was detected with polyclonal anti-SK1 antibodies [209] (kindly provided by Dr. Y. Banno Gifu University School of Medicine, Japan), SK-2 was immunorevealed employing rabbit polyclonal anti-SK2 antibodies [147], a kind gift of Dr. S. Nakamura (Department of Molecular and Cellular Biology, Kobe University Graduate School of Medicine, Kobe, Japan), $S1P_1$ and $S1P_3$ receptors were detected using subtype-specific polyclonal antibodies (Abcam). β-actin or β-tubulin were used as loading control (anti-β-actin rabbit polyclonal from, Santa Cruz, CA, anti-β-tubulin monoclonal from Sigma). α-SMA was detected using mouse monoclonal anti-α-SMA (Sigma) antibody followed by reaction with secondary horseradish peroxidase-conjugated antibodies and detected by *o*-phenylenediamine (tablets from Sigma). The data acquisition was performed using a GS-700 Imaging Densitometer and acquired blots were elaborated using the Quantity One software (BioRad, Hercules, CA).

Treatment of cells with a radioactive photoactivable derivative of GM3 ganglioside

Mock and SAT-1-transfected A2780 cells were incubated with a mixture of 10^{-6} M GM3 and 10^{-6} M [11-^{3}H(*Neu5Ac*)]GM3-N_3 ([^{3}H]GM3N_3), for 6 h in serum-free medium. After incubation, cells were washed five times with culture medium containing 10% FBS, and further incubated for 1 hour in 10

% FBS-containing culture medium. The cells were washed five times with ice-cold PBS, and then 4 mL/dish of ice-cold PBS were added and the cells were illuminated for 45 min under UV light (λ= 360 nm) on ice [207, 210-212]. Cells were harvested, lysed in lysis buffer containing 1 % Triton X-100 and detergent-resistant membrane fractions (DRM), were prepared by sucrose gradient centrifugation as described before at 4°C [213]. Aliquots of the DRM were treated with 1% SDS in lysis buffer at 100°C for 5 min to allow complete antigen solubilization, diluted to a 0.1 % SDS final concentration, precleared for non-specific binding (non-specifically bound material was used as negative control) and immunoprecipitated with anti-caveolin-1 antibody [213]. Proteins in cell lysates, negative control and anti-caveolin-1 immunoprecipitate were separated by SDS-PAGE. Proteins cross-linked to radioactive GM3 were detected by radioactivity imaging performed with a Beta-Imager 2000 instrument (Biospace, Paris, France) using an acquisition time of about 96 hours. Caveolin-1 and β-tubulin were detected by western blot as described above. All procedures before exposure to UV light were performed under red safelight.

Sphingosine kinase activity assay

To measure SK activity, cell lysates (60 μg) were incubated [214] in the presence of 50 μM D-*erythro*-sphingosine dissolved in 4 mg/ml BSA and 1 mM ATP. Reaction was initiated by addition of [^{32}P] γ-ATP (0.5 μCi, 1 mM) and 10 mM $MgCl_2$ and terminated after 30 min incubation at 37 °C by addition of 20 μl 1 N HCl and 900 μl of chloroform/methanol/HCl (100:200:1 v/v). 240 μl of chloroform and 240 μl of 1 M KCl were added, and phases were separated by centrifugation. 500 μl of the lower phase were dried under a stream of nitrogen and dissolved in 100 μl of chloroform/methanol (2:1 by volume). [^{32}P]S1P was separated by TLC with 1-butanol/methanol/acetic acid/water (80:20:10:20, v/v) and visualized by autoradiography. The radioactive spots corresponding to [^{32}P]S1P were scraped and counted in a scintillation counter. SK specific activity was expressed in pmol/min*mg protein in experiments performed at least in duplicate.

Pharmacological inhibition of sphingosine kinase

Twelve hours after seeding, A2780/HPR cells were treated or not with 10 μM SK inhibitor solubilized in cell culture medium containing 0, 5 and 10 μM of HPR. Cell proliferation and viability were estimated at different times of treatment by the MTT reduction assay and the Trypan blue dye exclusion assay respectively, as described above.

Treatment of A2780 and A2780/HPR cells with agonists and antagonists of S1P receptors

1,000- 2,000 of A2780 or A2780/HPR cells were plated in 96-well culture plates. After 12 h, A2780 cells were treated with culture medium containing or not 1 μM agonists SEW2871 ($S1P_1$ agonist), or VPC24191 ($S1P_{1/3}$ agonist) or S1P for 96 h. A2780/HPR cells were treated or not with 1 μM VPC23019 ($S1P_{1/3}$ antagonist), or JTE013 ($S1P_2$ antagonist), or CAY10444 ($S1P_3$ antagonist) or 10 μM W146 ($S1P_1$ antagonist), for 95 h followed by 1 h treatment with or not 1 μM S1P. In both treatments the conditioned medium, with agonists or antagonists, were changed every 48 h.

DNA Fragmentation analysis

Analysis of genomic DNA: the analysis of genomic DNA, from A2780/HPR cells, treated or not with SK inhibitor in the presence of different HPR concentrations, was carried out using Mammalian Genomic DNA Kit (Invitrogen) according to manufacturer's instructions. The DNA extract was quantified by absorbance at 260 nm. Equal amounts of total DNA were analyzed by agarose gel electrophoresis and detected by ethidium bromide staining. Analysis of fragmented DNA: 1 ml aliquots of PBS suspension containing 3 x 10^6 A2780/HPR cells treated as described above were centrifuged at 200 *x g* for 10 minutes at 4°C. Cells were lysed by adding 0.5 ml of 0.2% Triton X-100 in TE buffer, pH 7.4 to the pellet. In order to separate fragmented DNA from intact chromatin, the cell lysates were centrifuged at 20,000 *x g* for 10 min at 4 °C. The supernatant was removed and the pellet was resuspended in 0.5 ml of 0.2% Triton X-100 in TE buffer, pH 7.4 and 0.1 ml of ice-cold 5 M NaCl and vigorously vortexed. Then 0.7 ml of ice-cold *iso*-propanol were added, vortexed vigorously and DNA was allowed to precipitate overnight at -20 °C. DNA was recovered by centrifugation for 10 minutes at 20,000 *x g* at 4 °C. The supernatants were carefully removed and the samples were dried. DNA was dissolved by adding to each tube 20 μL of TE solution and left at 37 °C for 12 hours. Then DNA was mixed with loading-buffer and heated at 65 °C for 10 minutes. Samples were loaded in 1 % agarose gel containing ethidium bromide.

Mass spectrometry

The total lipid extract derived from 4 x 10^7 A2780/HPR and SK1-overexpressing A2780 cells under basal conditions or treated with HPR, SK inhibitor or both were subjected to a two-phase partitioning with 0.15 volumes of 0.1 M NH_4OH, the organic phases were treated with alkali as described previously [215] and were subjected to mass spectrometry analysis MS analyses were

carried out using a Thermo Quest Finnigan LCQDeca ion trap mass spectrometer (FINNIGAN MAT, San Jose, CA) equipped with an ESI ion source and an Xcalibur data system and a TSP P4000 quaternary pump HPLC. Separations of LCBs and Cer molecular species were obtained on a 5 μm, 250 x 4 mm LiChrospher 100 RP8 column (Merck).

Elution of LCBs and Cer molecular species was carried out, at a flow rate of 0.5 ml/min, with a gradient formed by the solvent system A, consisting methanol/water (90:10 by volume), and solvent system B, consisting of methanol, both containing 5 mM ammonium acetate. The gradient elution program was as follows: 5 min with solvent A; 5 min with a linear gradient from 100% solvent A to 100% solvent B; 15 min with 100% solvent B; 5 min with a linear gradient from 100% solvent B to 100% methanol. Methanol was also used to wash the column for 10 min, followed by equilibration procedure with solvent A for 15 min.

Optimum conditions for Cer molecular species MS analyses included sheath gas flow of 50 arbitrary units, spray voltage of 4 kV, capillary voltage of -47 V, capillary temperature of 260 °C, fragmentation voltage (used for collision induced dissociation) of 40-60%. Mass spectra were acquired over a m/z range 200-1000 in negative mode.

Optimum conditions for LCBs MS analyses included sheath gas flow of 50 arbitrary units, auxiliary gas flow of 5 arbitrary units, spray voltage of 4 kV, capillary voltage of 34 V, capillary temperature of 250°C, fragmentation voltage (used for collision induced dissociation) of 60 %. Mass spectra were acquired over a range m/z 200-1000 in positive mode.

For all experiments, source ion optics were adjusted to accomplish desolvation of ions while minimizing fragmentation.

As internal standards were used uncommon *d*18:1/17:0 ceramide, *d*18:0/17:0 ceramide and *d*20:0 sphinganine. A stock solution of internal standards in ammonium acetate 5 mM in methanol was quantitatively prepared (50 μM) and stored at -20 °C. Serial dilutions were prepared from this stock solution and utilized for calibration curves.

Other experimental procedures

The protein content was determined according to Lowry [216], using bovine serum albumin as the reference standard. Radioactivity associated with cells, with medium, with gradient fractions, and with lipid extracts was determined by liquid scintillation counting.

RESULTS

Analysis of phenotypic differences between A2780 and A2870/HPR human ovarian carcinoma cells

A2780 human ovarian carcinoma cells are very sensitive to the cytotoxic effect of a wide range of antitumor drug, including fenretinide (HPR), a synthetic retinoid. The A2780/HPR cell line is resistant to fenretinide insofar as it was obtained from the A2780 cell line through incubation with increasing sublethal concentrations of HPR. In particular the A2780/HPR cell line is ten times more resistant to HPR (IC_{50} = 10μM) respect to A2780 cells (IC_{50} = 1 μM).

A previous work showed that A2780/HPR cells were characterized by a different glycosphingolipid composition, due to the overexpression of GM3 synthase, a key enzyme in ganglioside biosynthetic pathway. In particular A2780/HPR cells were characterized by lower levels of lactosylceramide and higher levels of gangliosides (in particular GM2 and GM3) compared to A2780 cell line [6].

In addition to the HPR resistance, the A2780/HPR cell line shows other phenotypic differences compared to the A2780 parental cell line: altered morphology, more rounded and smaller shape, reduced ability of colony formation, different expression of adhesion and differentiation molecules, and different expression of tumor progression markers (Fig. 1).

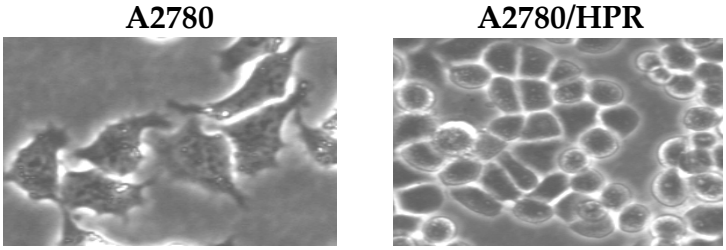

Figure 1. Morphologic differences between A2780 and A2780/HPR cell lines observed on optical microscopy.

We analyzed the in vitro cell motility, by wound healing assay and phagokinetic gold sol assay and, we noticed that the A2780/HPR represent also a less motile phenotype compared to A2780 cells. Wound healing assay shows that after 48 hours A2780 cells completely close the wound, while the A2780/HPR cells leave the wound virtually unchanged (Fig. 2). Moreover the phagokinetic gold sol assay shows that A2780 cells phagocyte an area six times larger than A2780/HPR, considering the different cell size (Fig. 3).

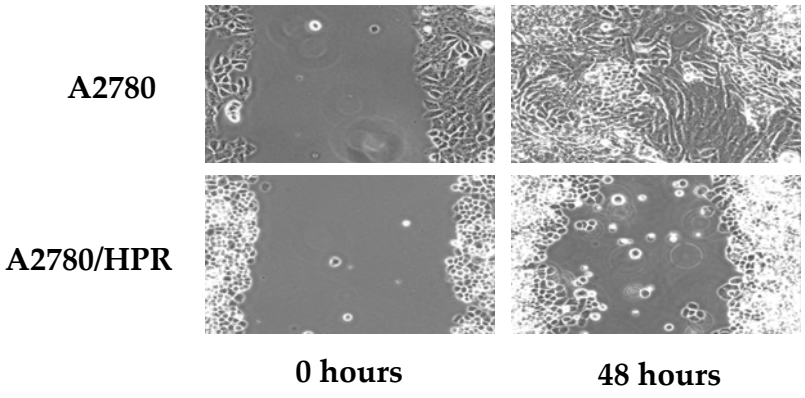

Figure 2. Wound healing assay of A2780 and A2780/HPR

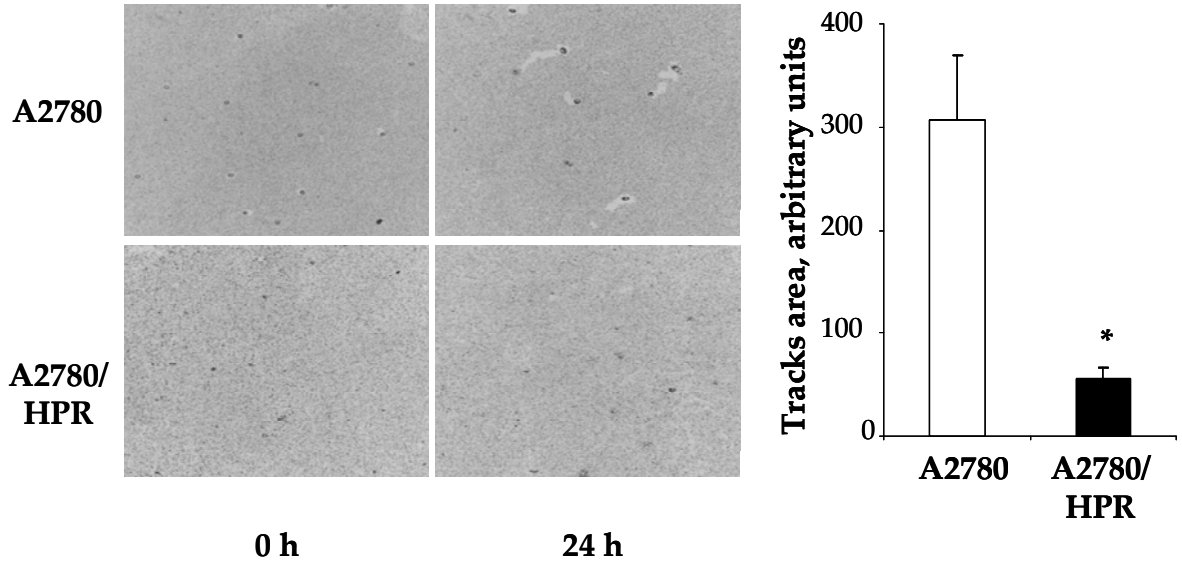

Figure 3. Phagokinetic gold sol assay for cell motility of A2780 and A2780/HPR cells.

Effects of artificially induced changes in glycospingolipid composition, by exogenous gangliosides administration or Brefeldin-A treatment, on the motility of A2780 cells.

As first way to understand the effect of a different ganglioside cell content on the motility of our cell model, an exogenous administration of different gangliosides has been performed on the A2780, high motile cells. GM3, GM2, GM1, GD1a and LacCer has been administered at a final concentration of 50 μM in serum free medium. It has been demonstrated that exogenous administration of GSLs induces modification on the cellular GSL composition. GSLs enter the plasma membrane becoming part of the endogenous lipid pool of the treated cells. Anyhow, also for this experiment after the 48 hours treatment, the trypsin stabile endogenous glicosphingolipid

content has been checked and it was increased from 3 to 20 fold increased respect to untreated cells. The effect of exogenous ganglioside administration on cell motility has been analyzed by wound healing assay up to 48 hours treatment, as described in Material and Methods section. The quantitative analysis shows that the gangliosides GM3 and GM2, both natural components of A2780 cells, and GM1, virtually absent in these cells, determine a strong reduction on cell motility, already visible at 24 hours, compared to control cells, treated with serum free medium only. GD1a, present as minor ganglioside in these cells, and LacCer had no effect on cell motility (Fig. 4).

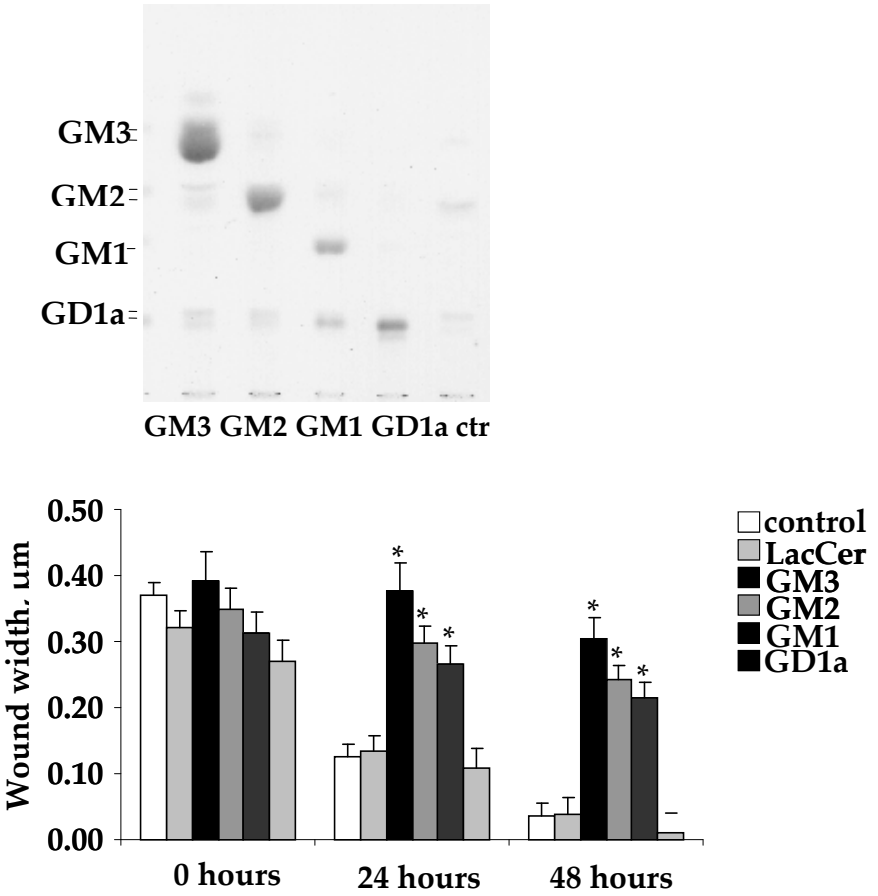

Figure 4. Wound healing assay of A2780 cells treated with different gangliosides. To check the extent of incorporation and metabolism of the administered gangliosides to A2780 cells compared to non treated cells (ctr), after 48 h incubation in serum free medium and in the presence of 50 μM GM3, GM2, GM1 or GD1a gangliosides or of the vehicle (control), cells were washed with medium containing 10% FBS and with 0.1% trypsin in PBS to remove gangliosides loosely bound to the cell surface. Cell lipids were extracted and partitioned as described in Material and Methods section, and the aqueous phase, was analysed by TLC (upper panel) using as solvent system chlorophorm/methanol/0.2% aqueous $CaCl_2$, 50:42:11 (spray reagent:

p-dimethylaminobenzaldehyde). In each lane the equivalent to 250 μg of proteins were loaded. Lower Panel: Results of wound healing assay. A2780 confluent monolayers were wounded and incubated in medium with or without gangliosides as previously described. Images of the wounds were collected at different times up to 48 hours and wound widths were measured at 0, 24 and 48 hours. Data are expressed in μm and are the means ± SD of three different experiments. * P < 0.001 vs time matched control.

Alternatively, the pharmacological treatment with Brefeldin-A (BFA) has been also used to manipulate the ganglioside content of A2780 cells and to examine the effect on cell motility. In agreement with the literature [61] BFA induce a marked increase in GM3 and GM2 cell content (Fig. 5, lowest panel). Moreover, as shown in figure 5 Brefeldin-A treatment significantly reduce the cell motility, evaluated by wound healing assay.

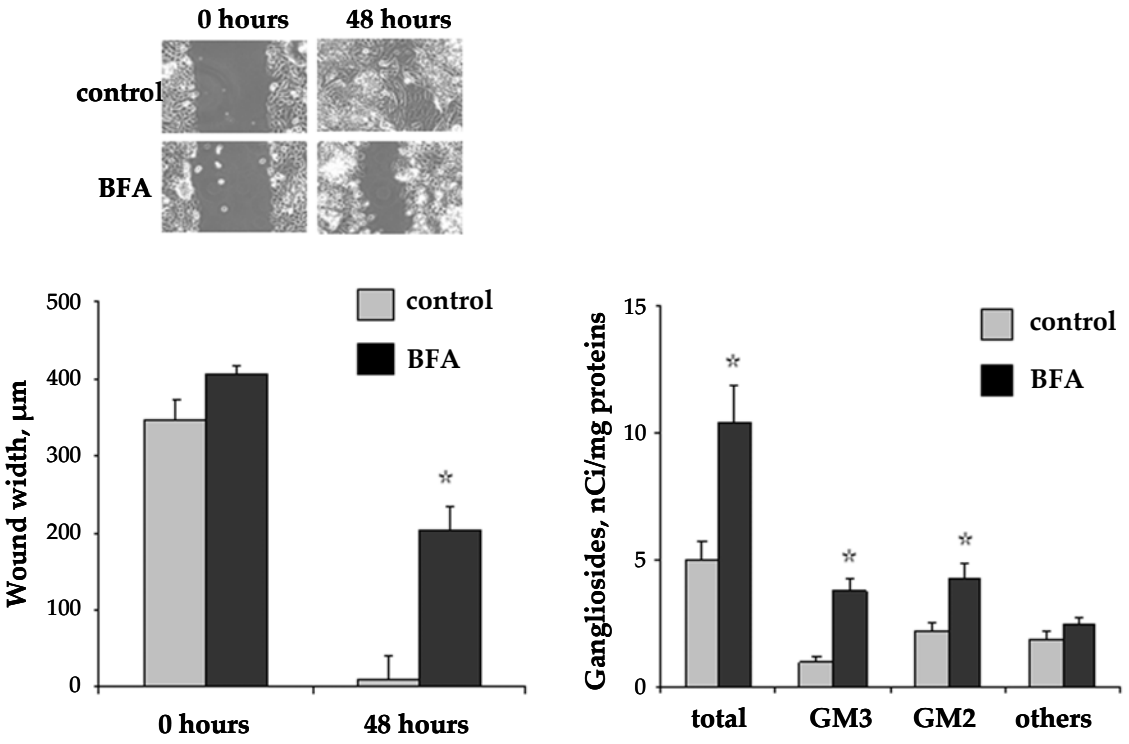

Figure 5. Brefeldin-A treatment and effects on in vitro cell motility of A2780 cells. A2780 cells incubated in medium with 10% FBS in the absence (control) or presence of 0.01 mg/mL Brefeldin-A. Monolayers were wounded; the upper panel show representative images of the wounds, the graph below reports the measurements of the wound widths at 0 and 48 hours expressed in μm and are the means ± SD of three different experiments. * P< 0.01 *vs.* time matched A2780. Lower Panel: to assess the effectiveness of BFA treatment, cell lipids were metabolically labelled with

[1-^{3}H]sphingosine, and the radioactivity associated o each lipid was determined by autoradiography. Data are expressed as nCi/mg of protein and are the means ± SD of three different experiments. * P< 0.01 *vs.* A2780.

GM3 synthase overexpression in A2780 cells

To better study if alterations of the sphingolipid metabolism, in particular of gangliosides, could be linked to a different motility in our cell model, we stably overexpressed the gene encoding for GM3-synthase (sialyltransferase I or SAT-I) in A2780 cells , using pRc/CMV 5.5 vector as described in Materials and Methods section. The sialyltransferase-I is a key enzyme controlling the sialylation levels of GSL.

The analysis on mRNA levels and in vitro activity of GM3-synthase show that the three selected clones present a marked upregulation compared to the control mock transfected and wild type A2780 cells, and similar to the enzyme activity in A2780/HPR cells (Fig. 6 upper left panel).

Next we evaluated the effects of GM3 synthase overexpression on the lipid composition. The phospholipids and cholesterol levels were not changed, while the ganglioside content markedly increased in the SAT-I overexpressing clones. For a more detailed analysis of glycosphingolipids, cells were metabolically labelled at the steady-state with [1-^{3}H]sphingosine. SAT-I clones present a 2-fold increase of the total ganglioside production, particularly of GM3, GM2 and GD1a, while the LacCer is markedly reduced because of its increased use as substrate compared to mock-transfected and A2780 cells (Fig. 6 lower panel).

The expression levels of the other important enzymes of the sphingolipid metabolism have been also analysed: serine palmitoyl transferase (SPT) , ceramide glucosyl transferase (GlcT), *N*-acetylgalactosaminyltransferase (GalNacT), lysosomal sialidase Neu1 and plasma membrane sialidase Neu3 were unchanged in SAT-1 transfected clones compared to mock transfected and A2780 cells (Fig. 7).

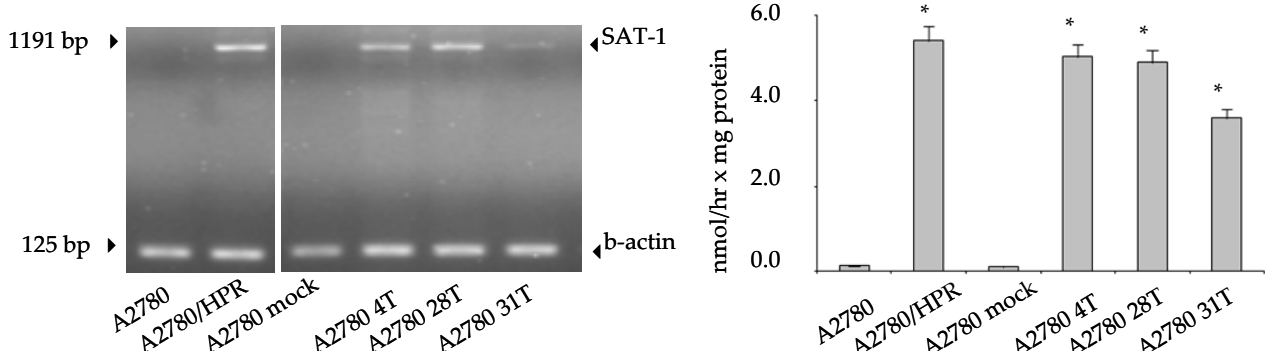

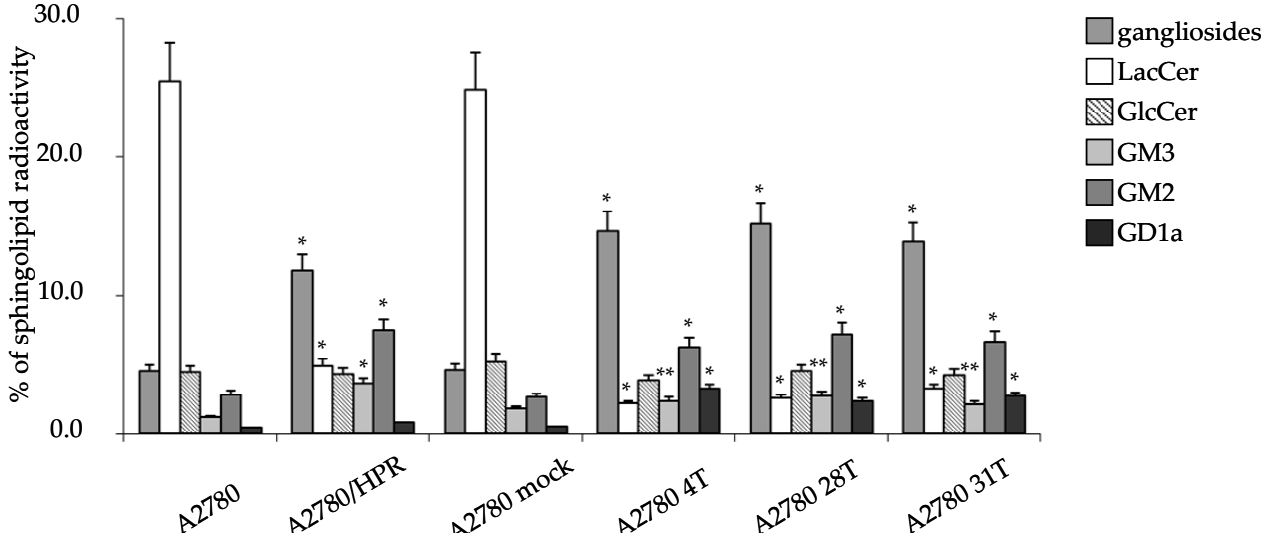

Figure 6. SAT-I overexpressing A2780 cells characterization. In the upper left panel the mRNA expression level of SAT-1, and β-actin as housekeeping gene, were analysed by RT-PCR and agarose gel electrophoresis. The right panel shows the results of in vitro enzyme activity assay of SAT-1, using tritiated LacCer as substrate. Data are expressed as nmoles LacCer converted in GM3/ hour x mg cell proteins, and are the means ± SD of three different experiments. * $P < 0.001$ *vs*. A2780. In the lower panel the glicosphingolipid patterns of all the A2780 cell types, obtained by metabolic labelling with [1-^{3}H] sphingosine at the steady state, 2 hours pulse and 48 hours chase, and analysed by HPTLC after aqueous and organic partitioning and visualised by digital autoradiography, as described in Material and Methods section. * $P < 0.01$ *vs*. A2780, ** $P < 0.05$ *vs*. A2780.

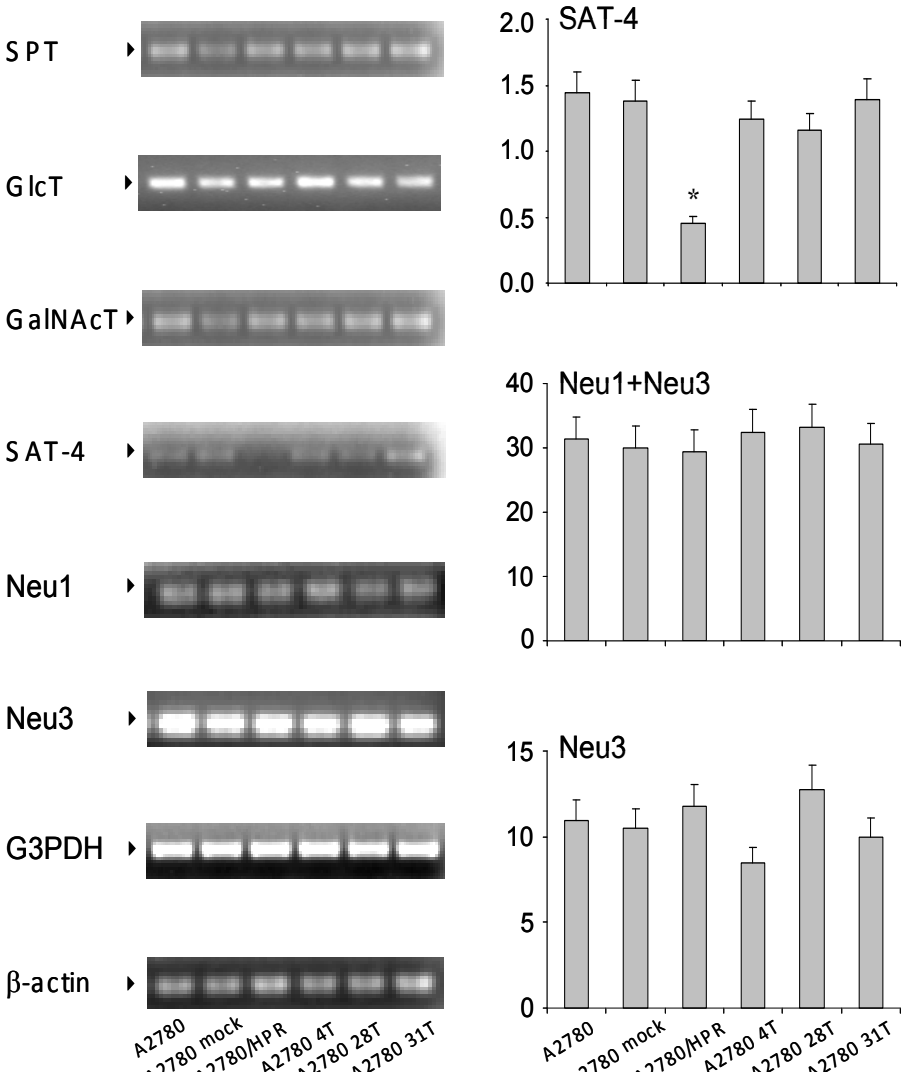

Figure 7. Expression of sphingolipid metabolism enzymes in A2780 variants and SAT-I transfected clones. In the left panel the mRNA expression level of all the enzymes were analysed by RT-PCR and agarose gel electrophoresis analysis using β-actin and G3PDH as internal control genes. In the right panel are shown the in vitro enzyme activity results for GD1a synthase (SAT-4) measured using tritiated GM1 as substrate, the total sialidase activity (Neu1 + Neu3) measured with the use of artificial substrate and Neu3 alone measured using tritiated GM3 as substrate. Data are expressed as nmol/h x mg of cell proteins and are the means of ± SD of three different experiments.

Effect of GM3 synthase overexpression on cell proliferation and in vitro cell motility

The overexpression of the GM3 synthase did not affect the cell growth rate, evaluated by cell counting (Fig. 8 upper panel). On the other hand cell migratory capability changed subsequently SAT-I overexpression in A2780 cells. In fact for the motility analysis the wound healing assay

shows that SAT-I clones are not able to close the wound after 48 hours as mock and A2780 cells do (Fig. 8 middle graph), furthermore also the transwell migration assay highlighted a reduced migratory potential of the GM3 synthase overexpressing cells compared to mock transfected and A2780 cells (Fig. 8 lower graph). So we evidenced again a correlation between higher ganglioside expression and reduced cell motility.

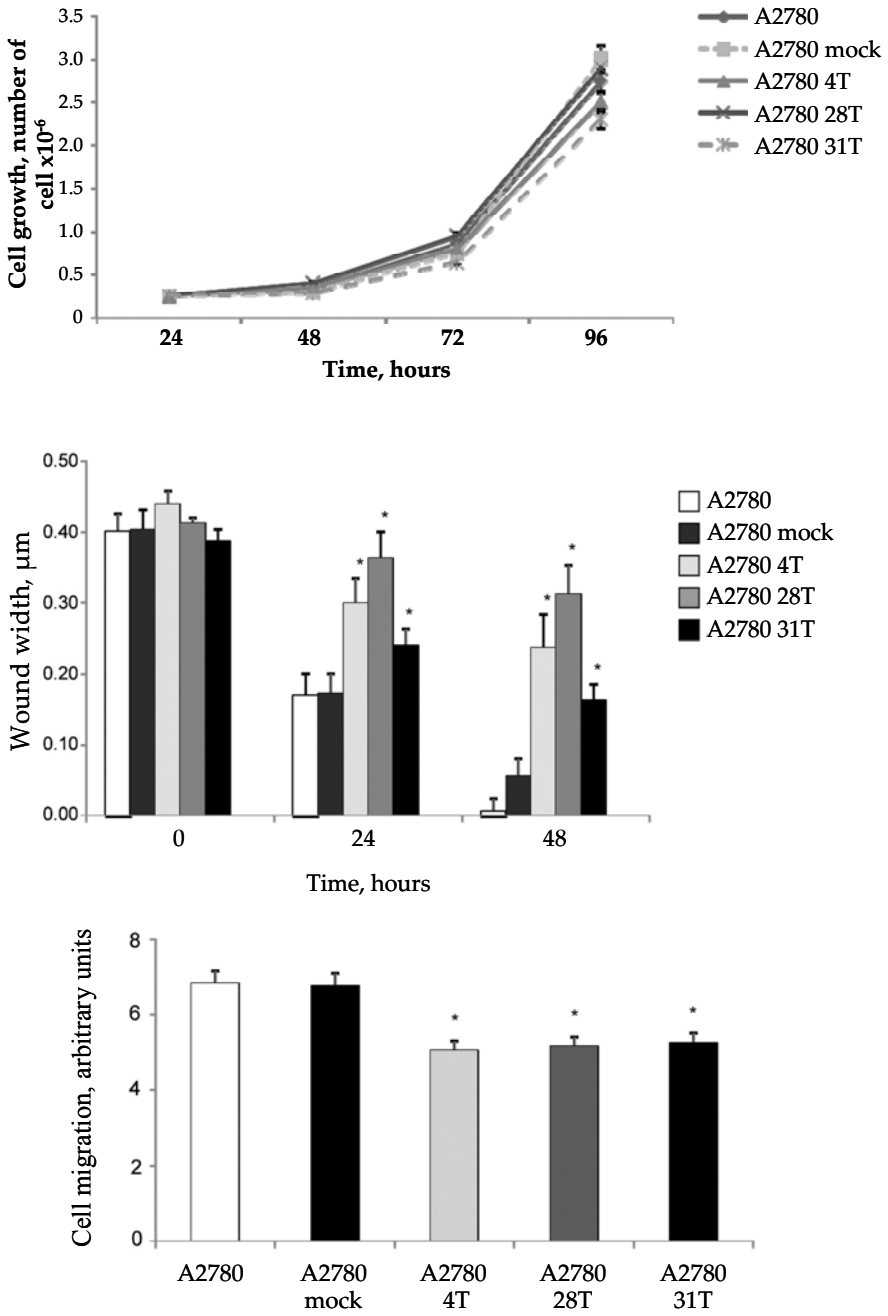

Figure 8. Proliferation and in vitro cell motility of A2780 SAT-I transfected clones. The growth rate (upper graph) of the indicated cells has been assessed at different time points by counting living cells using a Bürker counting chamber. The in vitro cell motility (middle graph) has been assessed by wound healing assay, the wound width has been measured at 0, 24 and 48

hours. Data are expressed in μm and are the mean ± SD of three different experiments. * P < 0.001 *vs.* time-matched A2780. In vitro motility analysed by transwell migration assays. The lower graph show the migrated cells 48 hours after seeding were stained with calcein-AM, detached and lysed. The lower graph shows the fluorescence associated with the lysed cells (ex. λ = 485 nm, em. λ = 520 nm) detected using Victor fluorimeter. Data are expressed in arbitrary units and are the mean ± SD of three different experiments. * P < 0.001 *vs.* A2780.

Caveolin-1 expression

A growing number of experimental evidences indicates that caveolin-1, an integral membrane protein, profoundly influences the tumor progression of many several types of tumors, including ovarian cancer. Caveolin-1 has received also great attention as an important membrane adapter molecule affecting cellular phenotype. However, the precise functional role of this molecule is not yet fully understood.

For this reasons, the expression levels of caveolin-1 in A2780 cell models have been analysed through RT-PCR, for the mRNA analysis (Figure 9 left panel), and through SDS-PAGE followed by western blot analysis, for the protein analysis (Figure 9 right panel). The results of both analysis were that caveolin-1 is markedly upregulated in A2780/HPR cells and in SAT-I overexpressing clones in respect to A2780 cells, in which the protein is expressed at very low levels, in agreement with previous published data [217]. The expression of other two isoforms of caveolin has been analysed but no differences resulted for caveolin-2 between the different cell types, while caveolin-3 was not detectable.

Since caveolin-1 is upregulated in all the cells characterized by a high expression of the enzyme GM3 synthase, we were prompted to study a possible connection between the two membrane components: ganglioside GM3 and caveolin-1.

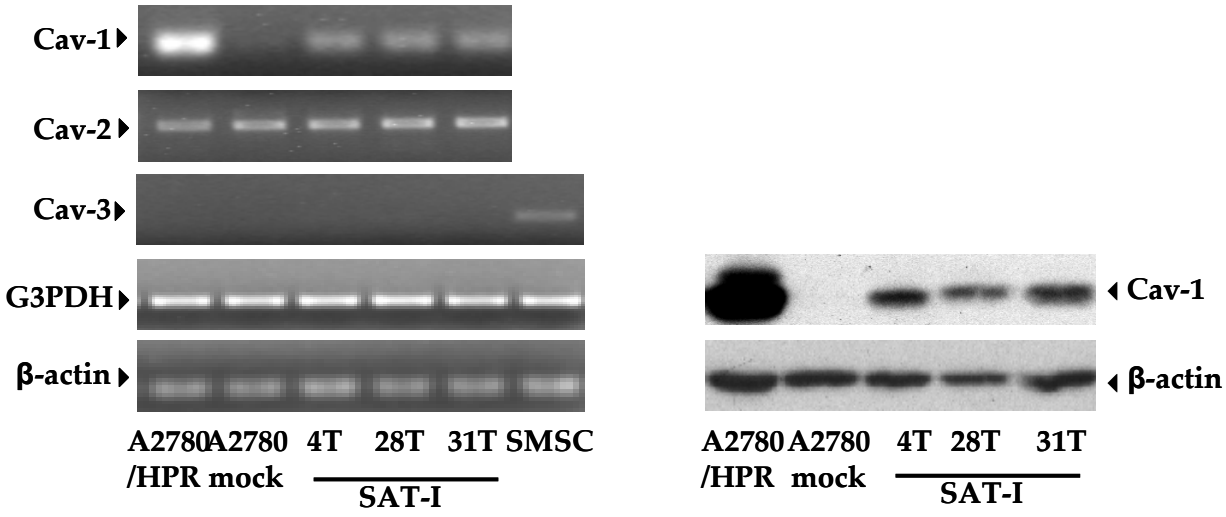

Figure 9. Expression of caveolin-1 in A2780/HPR and SAT-I transfected cells. Left Panel: mRNA expression levels of caveolin-1, -2 and -3 assessed by RT-PCR; G3PDH and β-actin measured as internal control. Human Scheletal Muscle Satellite Cells (SMSC) have been used as positive control for caveolin-3 expression. Right Panel: caveolin-1 protein level assessed by western blot. Equal amount of cell proteins (30 μg) were separated by SDS-PAGE, transferred to PVDF membrane, and probed using monoclonal antibodies for caveolin-1 and β-actin, used as loading control.

Study of caveolin-1-glycosphingolipid complex and interactions

Analysis of Detergent Resistant Membrane fractions

The first step toward the study of a possible complex composed of a glycosphingolipid, as gangliosides, and a protein component as caveolin-1, has been the analysis of detergent insoluble membrane fractions (DRM), which are low density fractions obtained after ultracentrifugation on sucrose density gradient of total cell lysates obtained in the presence of the detergent Triton X-100 as described in Materials and Methods section. Usually DRM prepared from a wide variety of cell types and tissues are highly enriched in sphingolipids and caveolin-1.

The A2780/HPR and the SAT-I transfected clones has been subjected to this experimental procedure after metabolic labelling of cell sphingolipid with [1-^{3}H]sphingosine. Around 50-60% of total radioactivity, associated with sphingolipids, has been found in DRM fractions (5 and 6) and the rest was distributed in the high density fractions (HD 9 - 11) (Fig. 10 upper panel).

Also the presence of caveolin-1 was analysed resulting more enriched in the DRM fractions, as attended. In particular 60% of total caveolin-1 was found associated with DRM in all the cell types expressing high level of GM3 synthase (Fig. 10 lower panel).

Glycosphingolipids and in particular gangliosides, are able to interact with several membrane proteins and to modulate their functions, as integrins, Src family kinases, G proteins and several signal transducers [218].

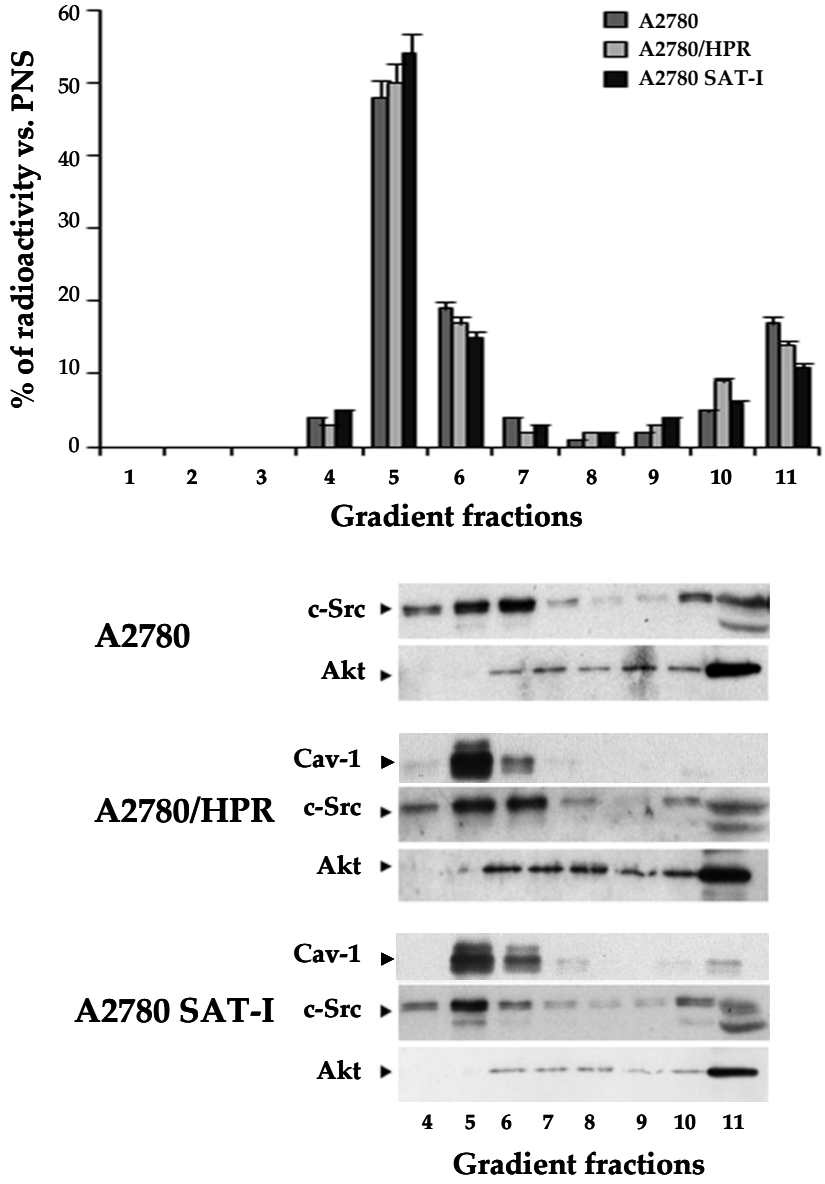

Figure 10. Preparation of detergent-resistant membrane fractions from A2780/HPR and SAT-I transfected cells. Cells were metabolically labelled with 1-[^{3}H]sphingosine and lysed in the presence of Triton X-100. Post-nuclear supernatants were loaded on discontinuous sucrose gradient and 11 fractions were collected after ultracentrifugation. Upper Panel: distribution of

radioactive sphingolipids within the gradient fractions from A2780, A2780/HPR and A2780 SAT-I cells. Lower Panel: Equal volumes of each gradient fraction from A2780, A2780/HPR and SAT-I cells were loaded in SDS-PAGE and immunoblotted for DRM-associated protein c-Src and caveolin-1 (present only in A2780/HPR and SAT-I cells) and for Akt as non-DRM marker.

Caveolin-1 immunoprecipitation and characterization of its environment

Caveolin-1 was immunoprecipitated from DRM fractions of A2780/HPR and SAT-1 transfected cells, using a specific monoclonal antibody against caveolin-1 in non-disruptive conditions, for the membrane integrity preservation. With this procedure about 20 % of DRM caveolin-1 and a part of sphingolipid-associated radioactivity, has been immunoprecipitated.

The immunoprecipitated complex was analysed by western blot for the detection of several proteins. Following proteins were found associated with caveolin-1 in DRM fractions: β1 and α5 integrins, c-Src and p130 CAS.

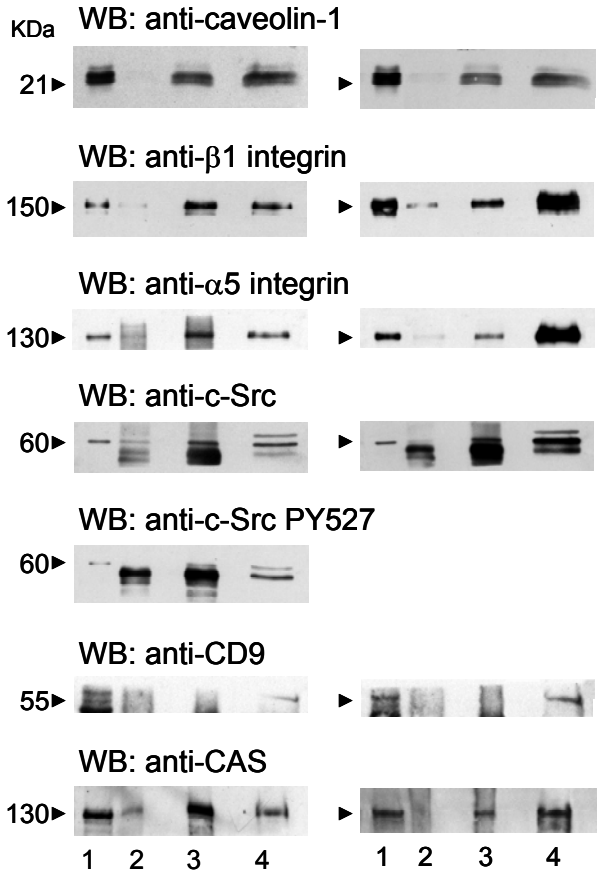

Figure 11. Proteins associated with the anti-caveolin-1 immunoprecipitates from DRM prepared from A2780/HPR and SAT-1

transfected cells. A2780/HPR and SAT-I transfected cells have been lysed in presence of Triton X-100 and from the obtained by fractionation on sucrose gradient, immunoprecipitation against caveolin-1 has been assessed in non-disruptive conditions, to preserve the complexes and its internal lipid-protein interactions. On SDS-PAGE DRM fraction (1), negative control (2) the immunoprecipitate (3), and the surnatant (4) of the immunoprecipitation experiment were loaded and western blot analysis were performed using specific antibodies against the indicated antigens.

Together with caveolin-1, 13 % of DRM-associated sphingolipid radioactivity has been co-immunoprecipitated (Fig. 12 left panel). The patterns of sphingolipids associated with anti-caveolin-1 immunoprecipitates were analysed by HPTLC and bidimentional-HPTLC separation (Fig 12 right panel). The radioactivity distribution associated with sphingolipids in the immunoprecipitate is qualitatively similar to that in DRM before immunoprecipitation.

This experiment of co-immunoprecipitation demonstrates the co-localization of the following molecules: caveolin-1, sphingolipids and integrin subunits α5 and β1, Src and p130-CAS, in specific membrane domains (DRM).

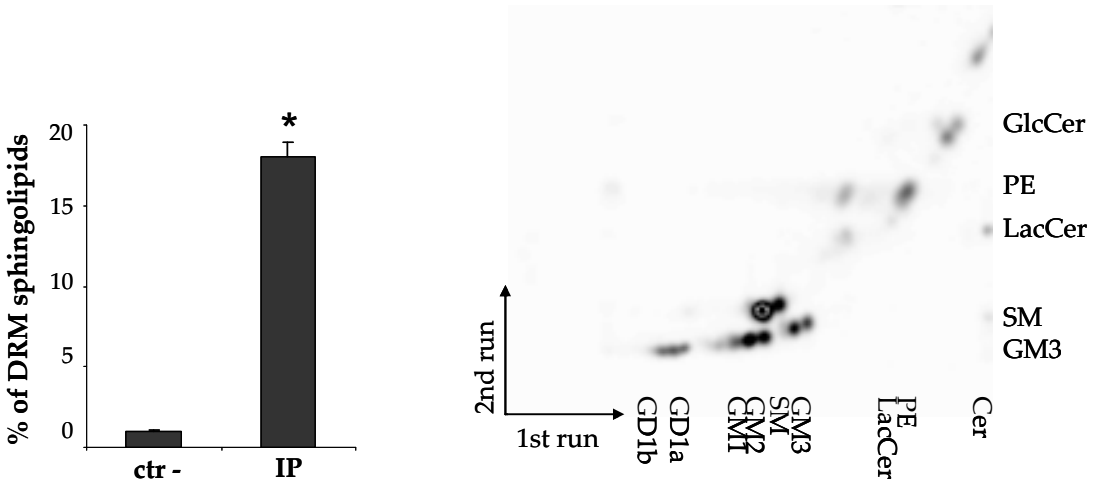

Figure 12. Caveolin-1 immunoprecipitation from DRM fractions of A2780/HPR cells and SAT-I cells. Left panel: the cell sphingolipids were metabolically labelled, on the obtained DRM fractions the immunoprecipitation using anti-caveolin-1 antibody has been assessed and on it the tritiated sphingolipids has been measured, as negative control the IP on the boied sample has been assed. Data are expressed as percentage respect to the total DRM radioactivity. * $P < 0.002$ vs DRM. Right panel: bidimentional HPTLC analysis of the immunoprecipitate anti-caveolin-1 sample. First run in chlorophorm/methanol/aqueous 0.02% $CaCl_2$ by volume 55:45:10, second run: chlorophorm/methanol/water 55:20:3 by volume and analysed by digital autoradiography.

c-Src activity regulates cell motility

Since c-Src can act as a downstream effector of caveolin-1-mediated signalling [101], we tested the effect of Src kinase inhibition on the motility of A2780 cells. The in vitro motility of A2780 cells was strongly reduced in the presence of a selective Src inhibitor (Fig. 13). c-Src is enriched together with sphingolipids and caveolin-1 in the DRM prepared from A2780 cells expressing high level of GM3 synthase and characterized by a reduced cell motility. Thus we comparatively tested the levels of the total, active (Src-PY416) and inactive (Src-PY527) forms of Src in the total cell lysates and DRM fractions from A2780, A2780/HPR and A2780 SAT-I cells (Fig.14.).The total and DRM levels of c-Src and Src-PY416 were similar in the cell lines, while the low motility and high GM3 synthase expressing cells were characterized by a higher level of Src-PY527, the inactive form of Src, that resulted concentrated in the DRM fraction.

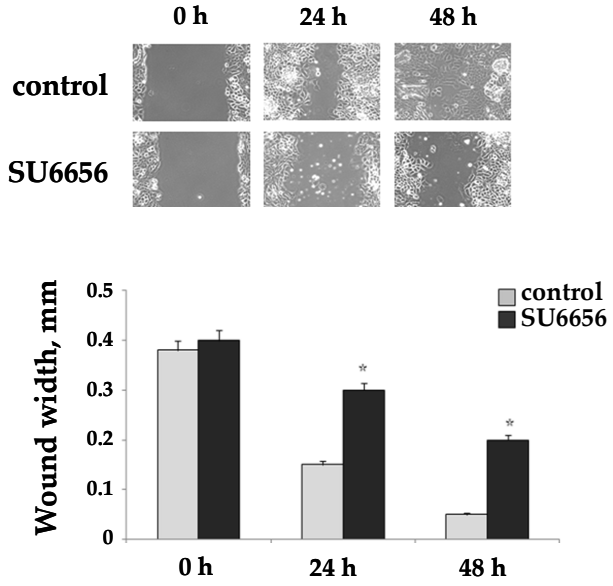

Figure 13. Effect of Src inhibition on motility of A2780 cells. A2780 cells were incubated in 10 % FBS-containing medium in absence (control) or presence of 3 μM SU6656 Src inhibitor. Cell monolayers were wounded and wound widths were measured at 0, 24 and 48 hours, phase contrast microscopy images of the wounds, representative images shown in the upper panel. The graph shows the data expressed as mm and are the means ± SD of three different experiments. * $P < 0.01$ *vs.* time-matched control.

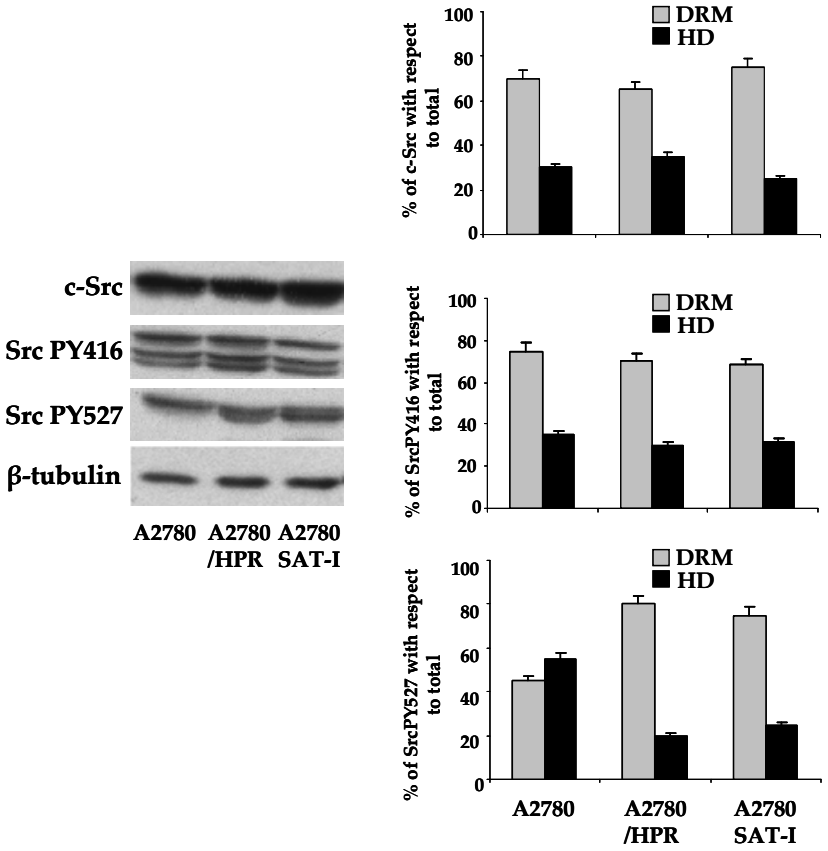

Figure 14. Total content and density gradient distribution of c-Src and its phosphorylated forms in A2780, A2780/HPR and SAT-I cells. Left Panel: total cell lysates were analysed by western blotting using specific antibodies against c-Src, Src PY416 and Src PY527, β-tubulin was simultaneously detected as loading control. The graphs show the distributions of c-Src (upper), Src PY416 (middle) and Src PY527 (lower) along the density gradient fractions from A2780, A2780/HPR and SAT-I cells. Cells were subjected to lysis and sucrose gradient centrifugation as described in Material and Methods section. Equal volumes of each gradient fraction were analysed by SDS-PAGE followed by western blotting detection using specific antibodies. The relative quantities of each protein in pooled DRM (fraction 5 and 6, grey) and HD (fractions 9-11, black) fractions were calculated by densitometry and wereexpressed as percentage of total signal associated with each antigen in the histograms. Data are the means values ± SD of three different experiments.

GM3 and caveolin-1 cross-linking study in living GM3 synthase overexpressing cells

A cross-linking assay on living A2780 SAT-I overexpressing cells was performed using a photoactivable radioactive derivative of GM3. After a pre-incubation with the [^{3}H]GM3N$_{3}$, the cells were irradiated with UV light to induce the cross-linking of GM3. Then cells were lysed and DRM fractions were prepared by sucrose gradient centrifugation.

Total cell lysates of mock and SAT-I cells were separated by SDS-PAGE and caveolin-1 expression was analysed by western blotting. The proteins cross-linked with photoactivable [^{3}H]GM3 were detected by digital autoradiography (Fig. 15 panel A). Overlapping the two images caveolin-1 can be recognized in the pattern of proteins cross-linked by [^{3}H]GM3N$_3$.

The gradient analysis show the distribution of [^{3}H]GM3N$_3$ and of caveolin-1 within the gradient fractions. The DRM fractions are enriched in both the molecules, in particular 30 % of the radioactivity was associated to DRM fraction, the radioactivity associated to the heavy gradient fractions as mainly due to the portion of ganglioside not stably inserted in the lipid bilayer (Fig.15 panel B).

Caveolin-1 was immunoprecipitated from this DRM and the immunoprecipitate was analysed by western, using a specific antibody anti-caveolin-1, and by autoradiography analysis (Fig. 15 panel C); the caveolin-1 present in DRM fraction was cross-linked by [^{3}H]GM3N$_3$.

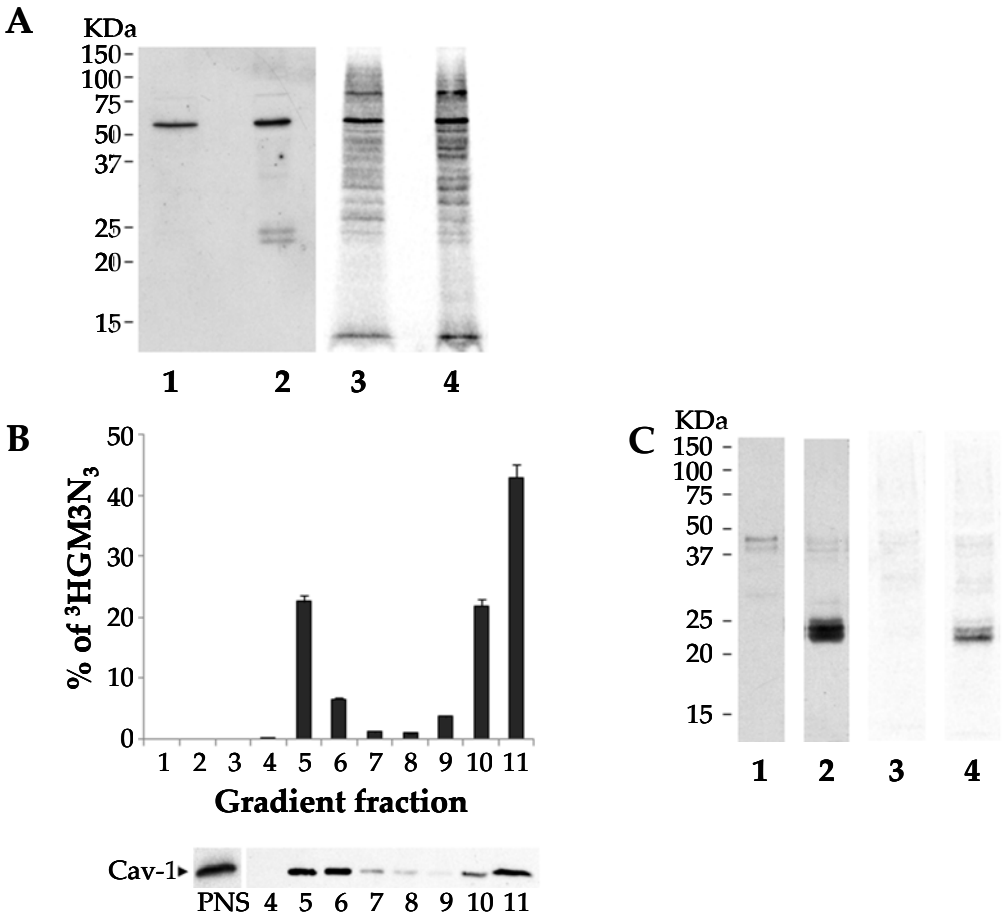

Figure 15. Photolabelling experiment and analysis of GM3-caveolin-1 complexes in SAT-I transfected A2780 cells. Cross-linking assay performed

on A2780 mock (lane 1, 3) and SAT-I transfected cells (lane 2, 4) by the use of photoactivable ^{3}H-labeled GM3. After cross-linking DRM fraction was prepared from SAT-I transfected A2780 cells in the presence of Triton X-100. Panel **A**: total cell lysate of mock (lane 1, 3) and SAT-I (lane 2, 4) separated by SDS-Page. In lane 1 and 2 caveolin-1 and β-tubulin were detected by western blot using specific antibodies. Lane 3 and 4 show the proteins cross-linked with photoactivable ^{3}H-GM3 detected by digital autoradiography (acquisition time 120 h; lane 3 and 4). Panel B: ^{3}H-GM3N$_3$ and caveolin-1 distribution within the gradient fractions. Panel **C**: immunoprecipitation of caveolin-1 from DRM fraction of SAT-I transfected cells, performed as described in Material and Methods section. Lane 1 and 2 are the results of SDS-page separation followed by western blot analysis with anti-caveolin-1 antibody; lanes 3 and 4 are the same PVDF membrane analysed by digital autoradiography, detecting the ^{3}H-GM3N$_3$ – caveolin-1 complexes.

Caveolin-1 transient silencing

As shown above, the caveolin-1 content is different in A2780 cells and the cells that have higher expression level of GM3 synthase, both A2780/HPR cells and SAT-1 clones. To further study the correlation between gangliosides and caveolin-1 and their effects on cell motility in our cell model, we tried to knock-down the expression levels of caveolin-1 in the A2780/HPR cells and SAT-1transfected cells using the system of small interference RNA (siRNA) that permits a transient silencing of the target gene, and as transfection control cells were treated with scrambled siRNA sequences. The silencing efficacy was evaluated through western blot analysis and immunofluorescence with the use of a specific antibody, data are shown in Figure 16 panel A. The administration for 72 hours of siRNA for caveolin-1 gene to A2780/HPR and SAT-1 cells induce a reduction of about 60 % and 90 %, respectively, of the caveolin-1 protein content respect to control scramble treated cells.

Caveolin-1 and PY14-caveolin-1 membrane expression in siRNA transfected A2780/HPR cells

To verify if the reduction in the total expression of Cav-1 is accompanied by a reduced expression of this protein at the plasma membrane level, an immunofluorescence analysis was performed with specific antibodies anti-cav-1 and anti-PY14-caveolin-1 in scrambled and siRNA transfected A2780/HPR cells. The cells were plated on glass coverslips and a first transient transfection with scrambled or Cav-1 siRNA was performed after 24 hours and repeated after 48 hours to obtain the greater possible reduction of Cav-1 expression. After 48 hours the cells were fixed, permeabilized and incubation with primary anti-Cav-1 and anti-PY14-Cav-1 antibodies was

performed, followed by incubation with FITC-conjugated secondary antibodies. The membrane expression of Cav-1 in scrambled A2780/HPR cells is clearly visible allowing the determination of cell boundaries (Fig. 16 Panel B), while in the Cav-1 siRNA transfected cells the cell membranes are not visible indicating that the caveolin-1 silencing causes a strong reduction in Cav-1 membrane localization. The PY14-Cav-1 membrane distribution results to be different from that of Cav-1: since Cav-1 is phosphorylated in active regions of the cell membrane, such as focal adhesions, its presence is not spread to the entire membrane but limited to few clusters. For this reason the immunofluorescence of scrambled A2780/HPR cells with a PY14-Cav-1 specific antibody makes visible just a few spots of cell membrane. In the siRNA transfected A2780/HPR cells these PY14-Cav-1 clusters on the cell membrane are no longer visible and this result is in agreement with the reduction of PY14-Cav-1 expression analysed by western blot. These data suggest that the Cav-1 silencing is not only able to reduce the total expression of Cav-1, but also to reduce the protein localization on the cell membrane and its activation consequent to PY14 phosphorylation .

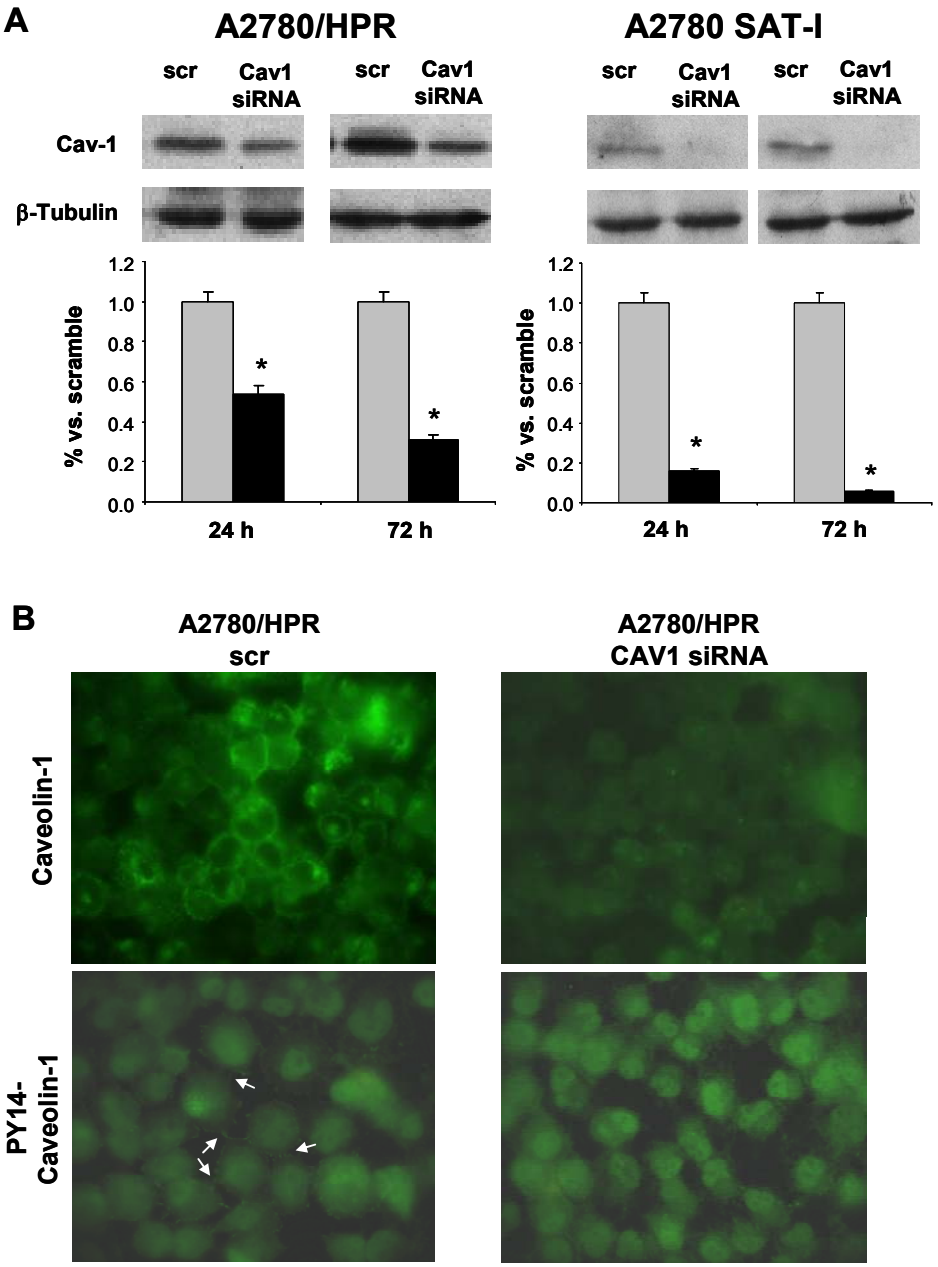

Figure 16. Caveolin-1 silencing in A2780/HPR and A2780 SAT-I cells. Panel A: Western blot analysis and quantification of caveolin-1 expression in A2780/HPR and A2780 SAT-I overexpressing cells treated with siRNA for CAV-1 gene or with scrambled siRNA as transfection control, after 24 and 72 hours treatment. beta-tubulin was detected as loading control. In graphs data of caveolin-1 expression are expressed as percentage vs. the respective cell type treated with scramble siRNA. Panel B: Immunofluorescence analysis of caveolin-1 and PY14-Cav-1 expression in A2780/HPR cells treated with siRNA for CAV-1 gene or with scrambled siRNA.

Cell motility analysis in caveolin-1 silenced cells

After assessing that the caveolin-1 siRNA silencing is effective, the first interest was to investigate if the caveolin-1 reduced expression level in cells with high GM3 synthase could have effects on cell motility. Caveolin-1 was silenced by siRNA administration, as described before, and after 24 hours the wound healing assay was started and followed for other 48 hours, at the end the cells were lysed for protein and lipid analysis. The results of wound healing assay show that cells silenced for caveolin-1 can reduce the wound widths, after 48 hours it is about 50 % respect to the time 0 h and are able to completely close the wound after 72 hours as shown in Figure 17 while the control scramble treated cells cannot close the wounds.

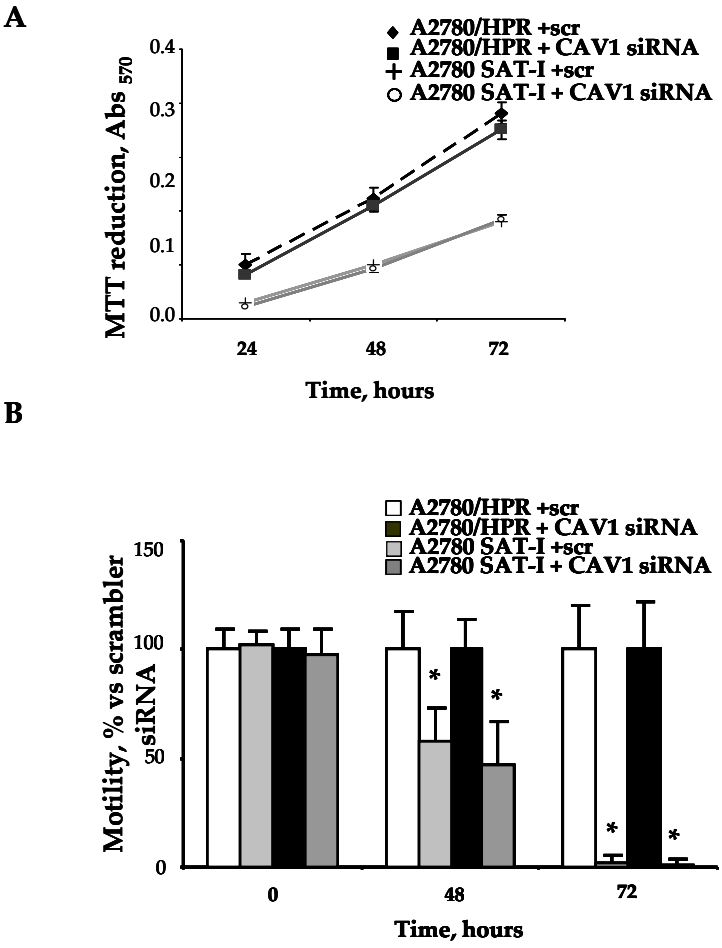

Figure 17. Effect on cell viability and cell motility of caveolin-1 silencing in A2780/HPR and A2780 SAT-I cells. Panel A: cell viability of A2780/HPR and A2780 SAT-I overexpressing cells treated with siRNA for CAV-1 gene or with scrambled siRNA was analysed by MTT reduction assay measured after 24, 48 and 72 hours plated cells. Panel B: wound healing assay was performed on the cited cells, as described in Material and Methods section.

Phase-contrast images of the wounds were recorded at different times and the wound widths were measured. Data are expressed in percentage respect to cells treated with scrambled cells and are the means ± SD of three different experiments. * $P < 0.001$ vs. respective scramble treated cells.

The endogenous lipid pattern were analysed after total lipid extraction from these same samples. The analysis of the organic phase, containing neutral and more hydrophobic lipids, were separated on TLC and analysed after reaction with orcinol spray, no significant differences in the lipid pattern were detected, as also the TLC analysis of the aqueous phase didn't show differences in ganglioside content after caveolin-1 transient silencing (Fig. 18).

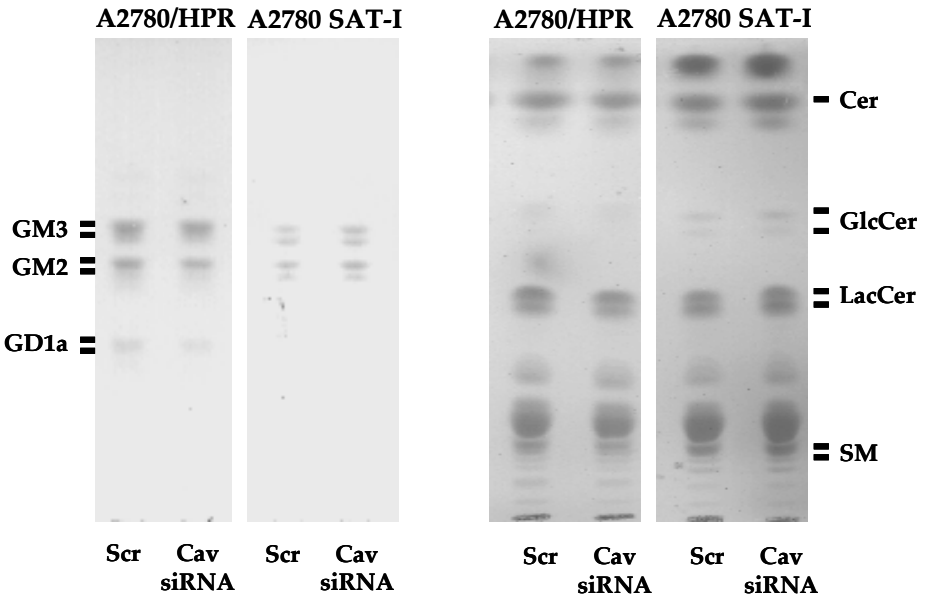

Figure 18. Lipid analysis of A2780/HPR and SAT-I cells silenced for caveolin-1. After a 72 hours treatment with siRNA for Cav-1 or scrambled siRNAs A2780/HPR and SAT-I clone were lysed in cold water and lipids were extracted, partitioned, as described in Material and Methods section, and analysed. Left Panel: aqueous phase analysis, on each lane the correspective to 500 μg, run in solvent system chloroform/methanol/0.2% aqueous $CaCl_2$ 50:42:11 by volume and detected with Erlich spray reagent. Right Panel: organic phase analysis, the correspective to 250 μg proteins were loaded on each lane, run in chloroform/methanol/water 55:20:3 by volume and detected with orcinol spray reagent.

Effect on HPR resistance

A further interest was to verify if the increased GM3 synthase activity, the higher ganglioside production and the consequent higher ceramide consumption could lead to a higher resistance to

the cytotoxic effect induced by HPR. HPR was administered to A2780 SAT-I clones, mock and A2780/HPR cells at different concentrations (0, 1, 5, 10 and 25 μM) and at different times mitochondrial metabolic activity was measured by MTT reduction assay. In the Figure 19 the effect of 5 μM HPR on the cells in time up to 144 hours has been measured, evaluating the cell growth as percentage *vs.* 24 hours time. All the SAT-I clones show a progressive decreasing in MTT reduction capability, while A2780/HPR cells are not showing variations during the time. This result suggests that in the A2780 cells the only overexpression of the enzyme GM3 synthase is not enough for establishing the resistance to the drug HPR.

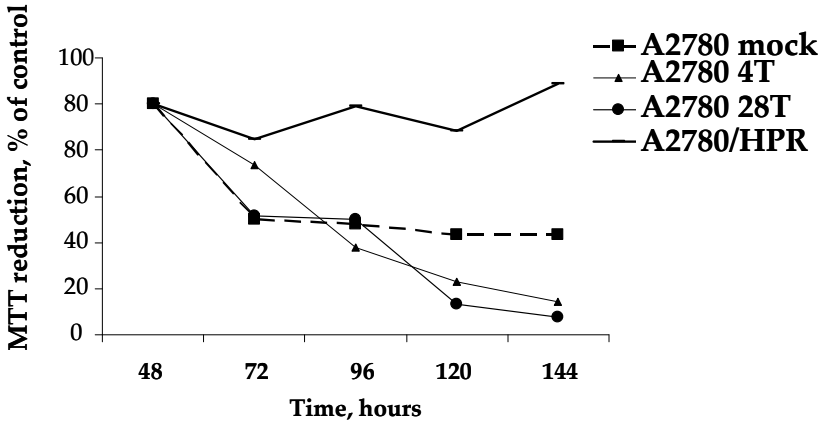

Figure 19. HPR-resistance test. To A2780 mock transfected, SAT-I overexpressing and A2780/HPR cells 5 μM HPR was administered. After the indicated times of colture cell's metabolic activity was measured by MTT assay. Data are expressed as % respect to the 24 h value and are the means of three different experiment perfomed in triple.

Mechanism of HPR resistance

Determination of growth kinetics

The growth rate of A2780 and A2780/HPR cells was measured by MTT reduction assay (Fig. 20 left panel), and the cell number was determined by counting cells with Bürker chamber (Figure 20 right panel), as described in Materials and Methods section. Both the measured parameters indicate that the A2780/HPR cell line is characterized by a significantly higher proliferation rate than the A2780 cell line.

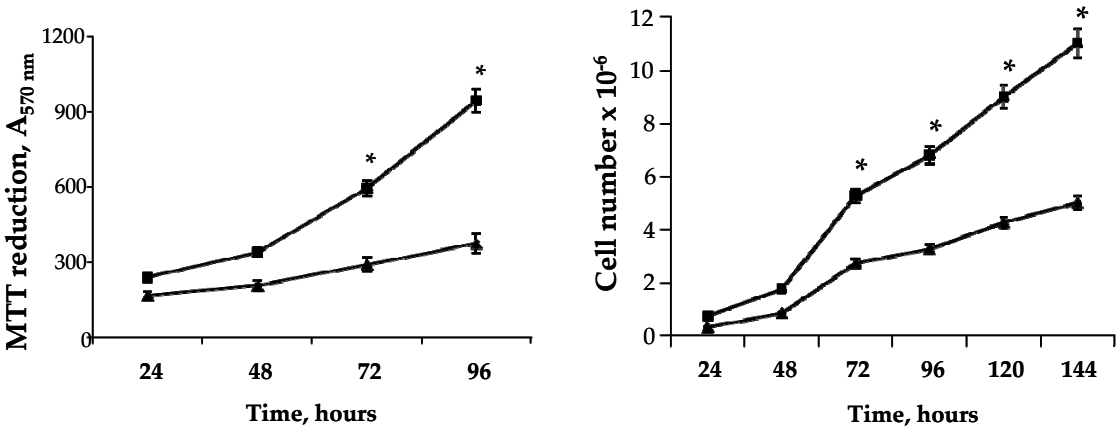

Figure 20. Determination of the proliferation rate in A2780 and A2780/HPR cells. Left panel: A2780 and A2780/HPR cells kept in culture for 24, 48, 72 and 96 hours, underwent a MTT reduction assay. The graphic shows the absorbance values at 570 nm measured at the different times indicated. Right Panel: the cells, kept in culture for 24, 48, 72, 96, 120 and 144 hours, were detached and counted. The graphic shows the number of cells counted at the different times. The data represent the average ± S.D. of three different experiments. * P<0.001 *vs.* A2780 cells.

HPR sensitivity

The sensitivity evaluation of A2780 and A2780/HPR cells to fenretinide was assessed by drug administration at increasing concentrations (0, 1, 5 and 10 μM). After 96 hours incubation the cell mitochondrial metabolic activity of control and treated cells was evaluated by MTT reduction assay. The data (Fig. 21) indicate that A2780/HPR cells are less sensitive to the cytotoxic effect of the drug than the parental A2780 cells. After 96 hours treatment with 5 μM HPR the mitochondrial oxidative capability of A2780 cells was reduced by 80% compared to the vehicle treated cells, while in A2780/HPR cells it is reduced only by 10% compared to control cells. In presence of 10 μM HPR the viability of A2780 cells is totally absent, while it is reduced by 50 % in A2780/HPR cells compared to the control cells.

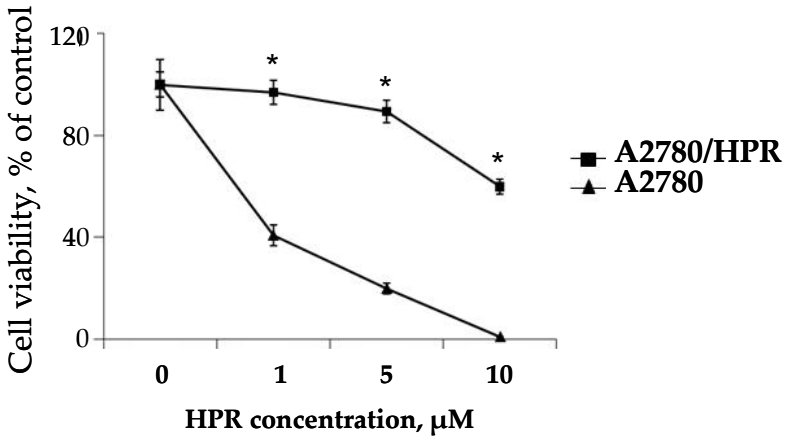

Figure 21. Determination of HPR sensitivity in A2780 and A2780/HPR cell lines. Quantitative determination of cell viability of A2780 and A2780/HPR cell lines with MTT reduction assay after treatment with different HPR concentration (0, 1, 5 and 10 μM) for 96 hours. Data are expressed as percentage in respect to the controls (cells treated with vehicle DMSO). Data represent the average ± S.D. of three different experiments. * P<0.001 *vs.* A2780 cells treated with the same HPR concentration.

Sphingolipid analysis in A2780 and A2780/HPR cells

The difference in the lipid expression pattern between A2780 and A2780/HPR cells was evaluated through metabolic labelling of the cell sphingolipids with [1-^{3}H]sphingosine. The cells were incubated in presence of [1-^{3}H]sphingosine for a short *pulse,* 45 minutes. With the used experimental conditions the two cell lines incorporated similar amounts of radioactivity (23.8 nCi/mg of proteins in A2780 cells and 21 nCi/mg of proteins in A2780/HPR cells). The cell lipids were extracted with organic solvents then separated and analysed by high performance TLC with n-butanol/acetic acid/water 3:1:1 (by volume) as solvent system (Fig. 22), as described in the Materials and Methods section. The radioactivity associated to every band was quantified through the appropriate software (Biospace). This analysis provided data about a different S1P production in the two cell lines: in A2780 cells the percentage of radioactivity associated to the S1P was 0.71% (0.17 ± 0.01 nCi/mg of proteins) compared to the total radioactivity, while in A2780/HPR cells it was 1.33% (0.28 ± 0.02 nCi/mg of proteins). Therefore experiments of metabolic labelling by short *pulse* with radioactive sphingosine demonstrated that the S1P production is significantly higher in A2780/HPR cells than in A2780 cells.

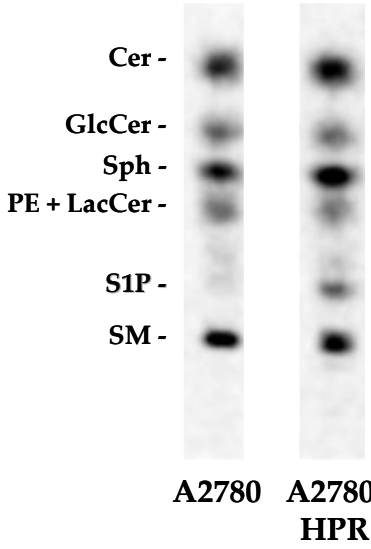

Figure 22. Sphingolipid expression pattern in A2780 and A2780/HPR cells. A2780 and A2780/HPR cells were incubated with [1-^{3}H]sphingosine for a 45 minute *pulse*, the lipids were extracted and the aqueous phase was obtained through phase separation in alkaline conditions. The lipids were separated through HPTLC with n-butanol/acetic acid/water 3:1:1 (v/v/v) and analyzed through digital autoradiography.

Sphingosine kinase analysis in A2780 and A2780/HPR cells

Previous data of our lab suggest that the sphingosine degradation pathway is altered in A2780/HPR cells, in particular more active than in A2780 cells [184]. The sphingosine degradation requires its conversion to S1P, reaction catalyzed by the enzyme sphingosine kinase, which exists in two isoforms (SK1 and SK2). The total SK in vitro activity and the expression of the two isoforms of SK were analyzed to verify the involvement of SK in the metabolism modofications.

Determination of the sphingosine kinase activity

To assess if the observed changes in S1P levels in A2780 and A2780/HPR cells correlates with a different enzyme activity, an assay was developed to measure the in vitro activity of sphingosine kinase using as substrate *D*-erythro-sphingosine and ^{32}P labelled ATP, evaluating its conversion to [^{32}P]S1P, as previously described in the Materials and Method section. The Figure 23 shows that the in vitro activity of sphingosine kinase is about 5 times higher in A2780/HPR cells compared to A2780 cells. This data is in agreement with the higher production of S1P that was observed in these cells, as previously described.

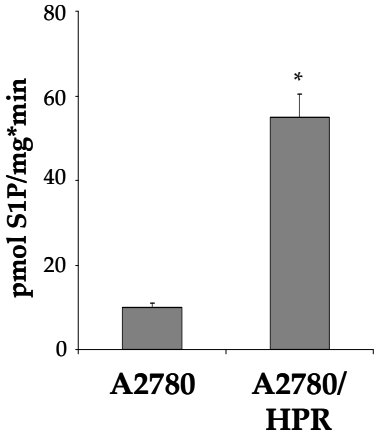

Figure 23. In vitro sphingosine kinase in A2780 and A2780/HPR cells. A2780 and A2780/HPR cells were lysed and the cell extracts were used to assess the sphingosine kinase activity through a specific in vitro assay using *D*-erythro-sphingosine as substrate. Data are expressed in pmol/min*mg of proteins. Data represent the means ± SD of two independent experiments. * $P < 0.05$ respect to A2780.

mRNA and protein expression analysis of sphingosine kinase isoforms

To evaluate if the increased activity of sphingosine kinase in A2780/HPR cells was due either to a transcriptional regulation or to a post-translational modification of one or both sphingosine kinase isoforms, the expression of SK1 and SK2 mRNA was assessed through quantitative Real Time PCR. The data in Figure 24 show that A2780/HPR cells are characterized by a higher production (almost the double) of SK1 mRNA compared to A2780 cells, while the levels of SK2 mRNA are similar.

The protein expression of the two isoforms of SK was analysed by Western Blot using specific antibodies for the two isoforms (Fig. 25). The data show that the amount of SK1 is about 4 times higher in A2780/HPR cells compared to A2780 cells, while the SK2 isoform has a similar expression in the two cell lines, confirming the results obtained by RT-PCR analysis.

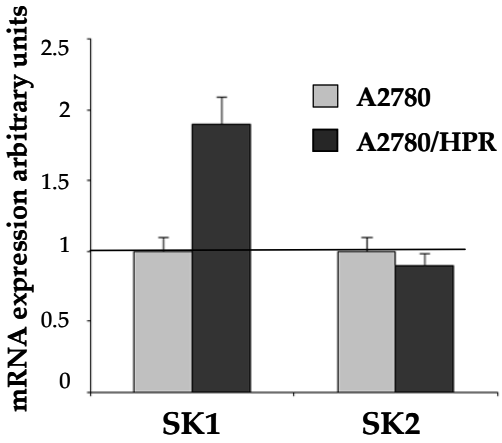

Figure 24. mRNA expression of the sphingosine kinase isoforms in A2780 and A2780/HPR cells. Semi-quantitative PCR analysis on the expression levels of SK1 and SK2 isoforms performed in A2780 and A2780/HPR cells by the simultaneous amplification of the housekeeping gene β-actin. Data are normalized *vs.* β-actin expression and using individual SK isoforms of the A2780 speciment set as 1. Data are the mean ± SD of three independent experiments performed in triplicate.

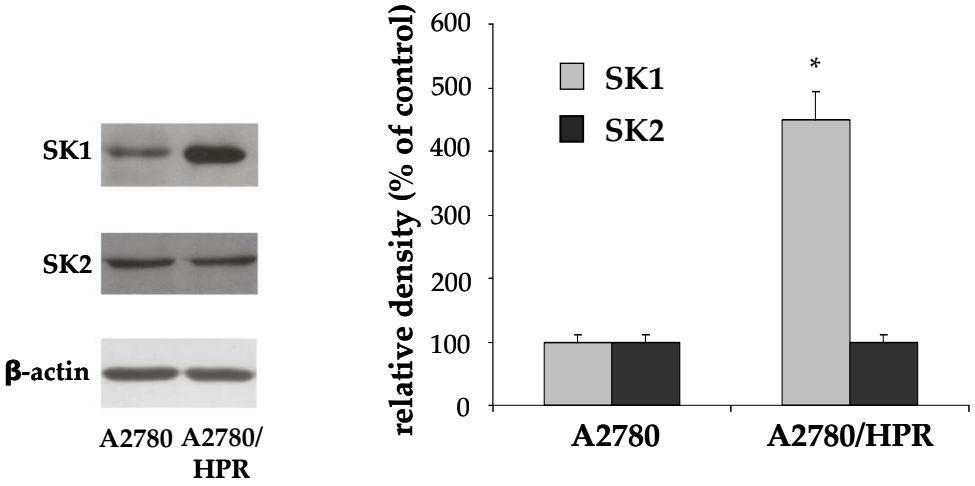

Figure 25. Protein expression of the sphingosine kinase isoforms in A2780 and A2780/HPR cells. Analysis of cell lysates of A2780 and A2780/HPR cells by Western Blot with specific anti-SK1 and anti-SK2 antibodies. Left Panel: representative image of Western Blot of three different experiments. Right Panel: histogram representing the densitometric quantification of SK1 and SK2 isoforms compared and normalized with β-actin, data expressed as percentage *vs.* A2780. * $P<0.05$ *vs.* A2780 cells.

Pharmacological inhibition of SK in A2780 and A2780/HPR cells

To investigate the involvement of SK in the modulation of cell proliferation and HPR sensitivity of A2780 and A2780/HPR cells, a potent and highly selective inhibitor, 2-(*p*-hydroxyanilino)-4-(*p*-

chlorophenyl)thiazole, was used to inhibit its activity. The consequences on S1P production, cell proliferation and HPR sensitivity were analysed as follows.

S1P production in SK inhibited A2780/HPR cells

A2780/HPR cells were pre-treated with the SK inhibitor for 24 hours then labelled with [1-^{3}H]sphingosine as previously described: after a short pulse of 45 minutes with [1-^{3}H]sphingosine, the lipids were extracted with organic solvents and the S1P was recovered through phase separation in alkaline conditions. Lipids were separated on HPTLC with n-butanol/acetic acid/water 3:1:1 (v/v/v) and analyzed by digital autoradiography. The SK inhibitor treatment did not affect the total lipid labelling. As shown in Figure 26 left panel, the treatment with SK inhibitor effectively reduced the production of S1P: in A2780/HPR cells radioactivity associated with S1P changed from 0.28 nCi/mg of proteins in control cells, to 0.06 nCi/mg of proteins in the cells treated with the inhibitor.

Effect of SK inhibition on the proliferation rate

The proliferation rate of A2780 and A2780/HPR cells, in basal conditions or in presence of the SK inhibitor, was assessed measuring the cell viability by MTT reduction assay (Figure 26 right panel). The proliferation rate was reduced of about 3 times, after 96 hours, in the inhibitor treated cells compared to the control cells, in both A2780 and A2780/HPR cell lines. These data suggest that the SK activity is essential for proliferation in both cell lines, even if the expression and the activity levels of the enzyme are different in the two cells, as reported above.

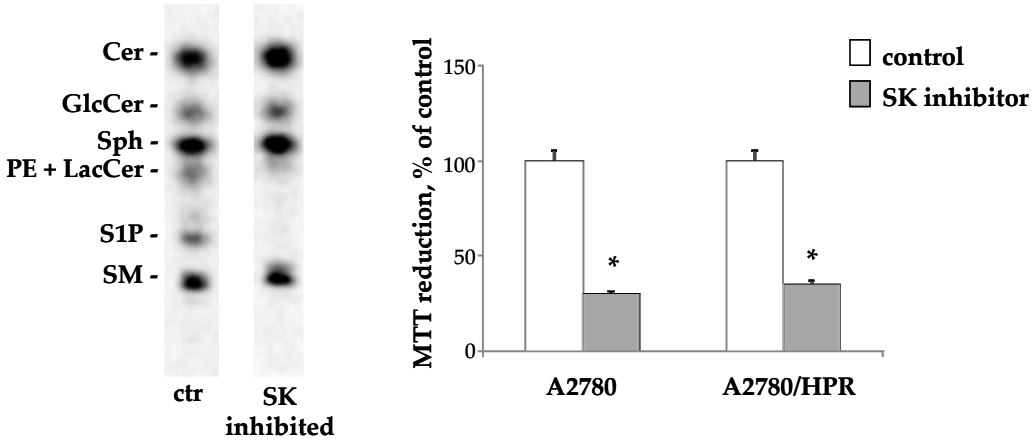

Figure 26. Effects of SK pharmacological inhibition on S1P production and proliferation rate in A2780 and A2780/HPR cells. Left Panel: A2780/HPR cells were treated with the SK inhibitor and then metabolically labelled with [1-^{3}H]sphingosine. Lipids were extracted and the aqueous phase was

obtained through phase separation in alkaline conditions. The lipids were separated by HPTLC with n-butanol/acetic acid/water 3:1:1 (v/v/v) solvent system and analyzed through digital autoradiography. Right Panel: A2780 and A2780/HPR cells were treated with the SK inhibitor and, after 96 hours, the proliferation was assessed by MTT reduction assay. The data represent the average ± SD of three different experiments. * P<0.001 *vs.* controls.

Study of correlations between SK activity and fenretinide cytotoxic effect

Effects of SK inhibition on the A2780/HPR cells

HPR was administered at different concentrations, 0, 5 and 10 μM, to A2780/HPR in the presence or not (control) of the SK inhibitor. The results, shown in Figure 27 left panel, indicate a strong viability reduction in cells treated contemporarily with the SK1 inhibitor and HPR at 5 or 10 μM compared to the control cells. Further the cell number, evaluated by count with Bürker chamber, is minor after SK inhibition, in presence or absence of HPR. These data suggest that the SK1 activity, and therefore the S1P production, is important not only for the cell proliferation, but also for the HPR-dependent alteration on the proliferation rate in A2780/HPR cells.

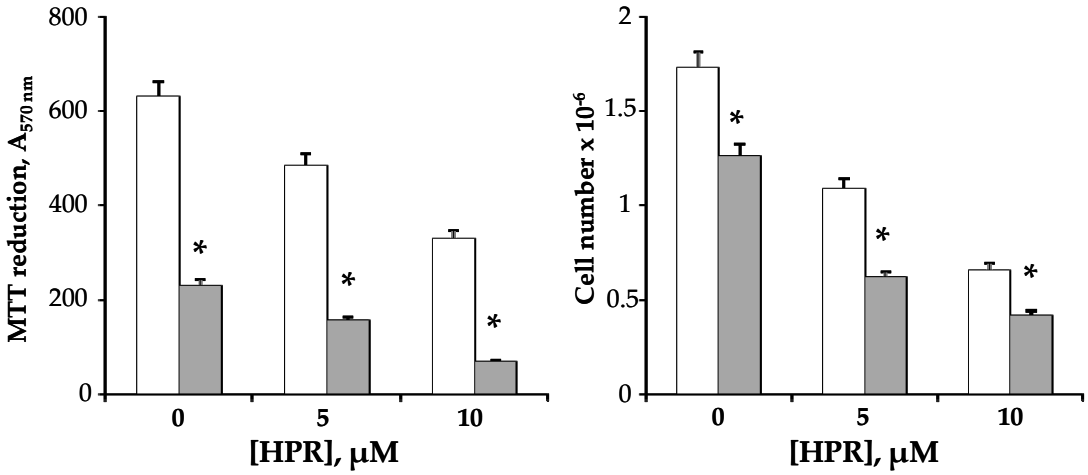

Figure 27. Effect of the SK inhibition on A2780/HPR cell proliferation. Left Panel: the cells were treated with the SK inhibitor and with different HPR concentrations (0, 5 and 10 μM), after 96 hours the mitochondrial metabolic activity was measured through MTT reduction assay. Right Panel: the cell number was measured through count with Bürker chamber. Data represent the average ± SD of three different experiments. * P<0.001 *vs.* controls.

Effect on HPR sensitivity

To verify the effect of the SK inhibitor on the HPR sensitivity, the A2780/HPR cells were treated with or without the inhibitor in presence of different HPR concentrations (0, 5 and 10 μM) and cell death was analysed. Cells were counted with the Bürker chamber and the number of dead cells was determined by counting the Trypan Blue permeable cells. As can be seen in the Figure 28 upper panel, in presence of 10 μM HPR the treatment with the SK inhibitor induces a significant increase in the dead cell number (+61%) compared to the control. Furthermore to verify the presence of apoptosis the total genomic DNA and the chromatin fragmentation were analysed. The total genomic DNA cell content is decreased after SK inhibition and accentuated by the HPR increasing concentrations (Fig. 28 lower panel). Moreover the cells treated contemporarily treated with SK inhibitor and with 10 μM HPR are characterized by the appearance of fragmented chromatin, absent in the other samples.

All together these results suggests that SK inhibition sensitizes the A2780/HPR cells to the fenretinide induced apoptosis.

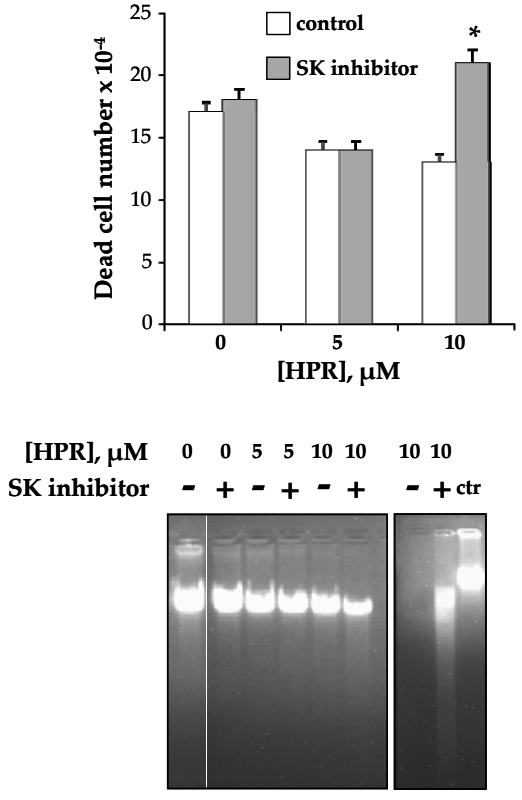

Figure 28. Effect of the SK inhibition on HPR sensitivity in A2780/HPR cells. Upper panel: dead cell number evaluated by Trypan Blue exclusion assay of A2780/HPR cells treated or not with SK inhibitor and in presence of

0, 5, 10 μM HPR. Lower panel: genomic DNA analysis by chromatin precipitation and chromatin fragmentation analysis by agarose gel electrophoresis. Data represent the average ± S.D. of three different experiments. * P<0.001 *vs.* controls (untreated cells).

Expression and effects of agonists and antagonists of S1PRs on proliferation and HPR resistance in A2780 and A2780/HPR cells

To obtain further information on the mechanism by which altered S1P formation mediates the onset of resistance to HPR in A2780 cells, the expression pattern of S1P receptors (S1PRs), that largely account for S1P multiple biological activities, was examined in both HPR-sensitive and –resistant cells, by quantitative real-time PCR analysis. Data presented in Figure 29 panel A show strict differences in S1PR expressions between the two cell lines, in particular normalizing individual S1PR mRNA content of resistant cells onto that of sensitive ones, a clearly tremendous increase in $S1P_1$ accompanied by a robust rise in $S1P_3$ mRNA content in HPR-resistant cells appears, whereas the other S1PR subtypes slightly reduced.

These data were corroborated by western blot analysis, the protein band corresponding to $S1P_1$ receptor is clearly detectable in A2780/HPR cells and not detectable in the sensible cells; moreover the $S1P_3$ protein content was sensibly augmented in HPR-resistant cells (Fig. 29 inset).

However analyzing the proliferation and cell viability of A2780 and A2780/HPR cells by MTT reduction assay, it resulted not affected by the treatment with different antagonists of S1PRs (Fig. 29 panel B): for $S1P_1$ (VPC23019 and W146), $S1P_2$ (JTE013) and for $S1P_3$ (VPC23019 and CAY10444).

Further we checked if the HPR-resistance could be regulated by the modulation of S1PR activity, treating A2780/HPR cells in the presence of 10 μM HPR and antagonists of the receptors or stimulating S1PRs activity by the use of agonists, S1P, SEW2871 for $S1P_1$ and VPC24191 for $S1P_1$ and $S1P_3$ in A2780 cells in the presence of 1 μM HPR. The results shown in Figure 29 panel C do not indicate an effect of these treatments, suggesting that the role of SK in the HPR-resistance in these cells is not mediated by the S1PRs.

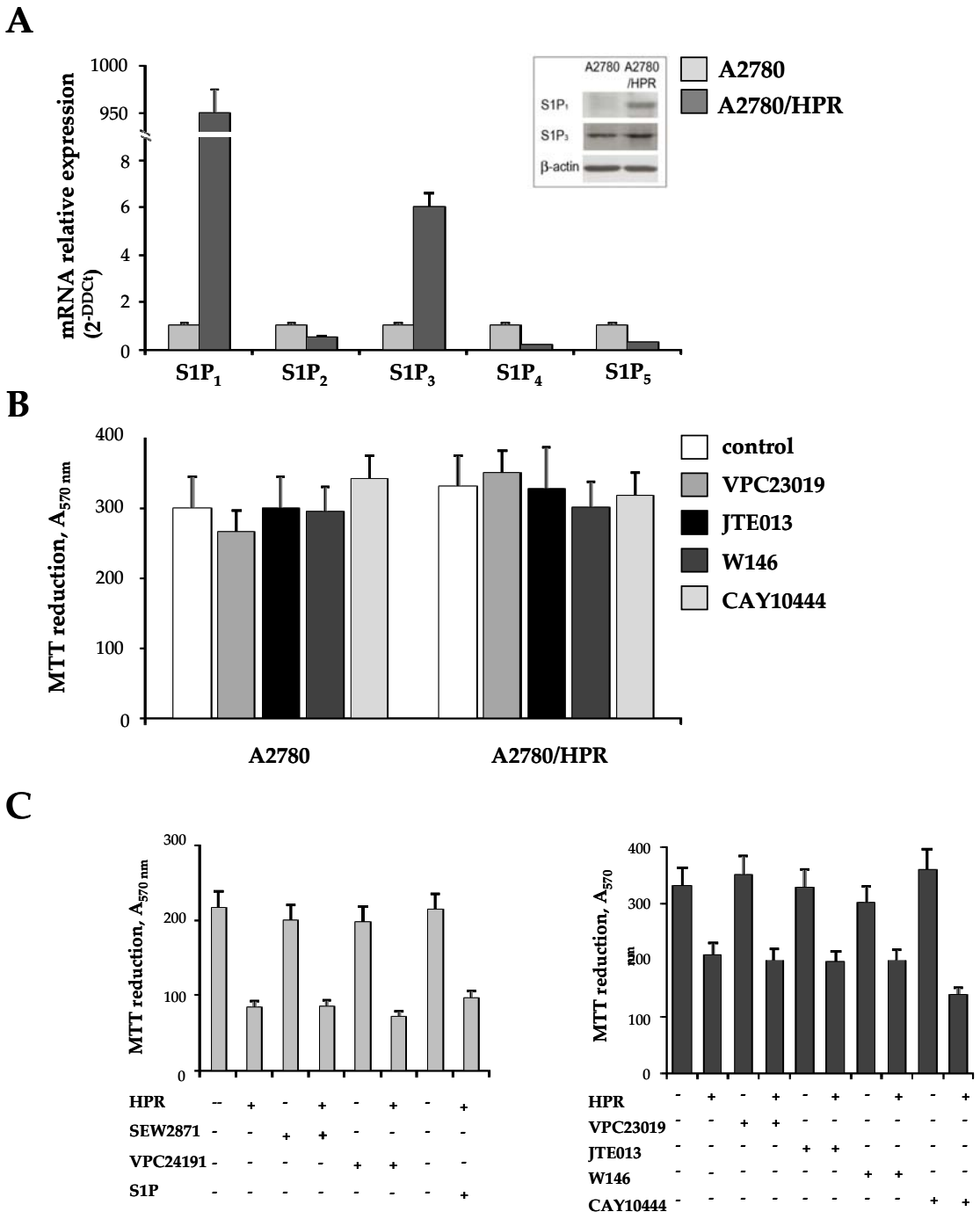

Figure 29.Expression and effects of agonists and antagonists of S1PRs on proliferation and HPR-resistance in A2780 and A2780/HPE cells. Panel A: quantitative Real-Time PCR analysis on A2780 and A2780/HPR cells by simultaneously amplification of the target genes: $S1P_1$, $S1P_2$, $S1P_3$, $S1P_4$ and $S1P_5$ together with 18S rRNA. The mRNA quantization was based on $2^{-\Delta\Delta Ct}$ method, utilizing for each receptor its expression in A2780 cells as calibrator. Data are the means ± SD of three independent experiments performed in triplicate. Inset: western blot analysis using anti-$S1P_1$ or anti-$S1P_3$ antibodies. Anti-β-actin as loading control. Panel B: twelve hours after seeding, A2780 and A2780/HPR cells were treated with different antagonists of sphingosine-

1-phosphate receptors, cell proliferation was evaluated after 96 hours as mitochondrial metabolic activity measured by the MTT reduction assay. Data are the means ± S.D. of three different experiments. Panel C: twelve hours after seeding, A2780 cells were treated with different agonists of S1PRs alone or in the presence of 1 μM HPR (left panel) and A2780/HPR cells were treated with different antagonists of S1PRs alone or in the presence of 10 μM HPR (right panel); after 96 hours, the mitochondrial metabolic activity was measured by the MTT reduction assay. Data are the means ± S.D. of three different experiments.

Ceramide and PE level analysis

A so far known the anti-proliferative and cytotoxic effect of HPR on A2780 cells is due by the increased levels of intracellular ceramide [184]. The higher activity of SK1 in A2780/HPR cells could be responsible for the increased sphingosine and consequently ceramide scavenging, by moving the rheostat to the S1P formation, and therefore increasing the resistance to HPR cytotoxicity. To confirm this hypothesis, the ceramide production in cells, treated with SK inhibitor and 10 μM HPR, was measured. Metabolic labelling of cell sphingolipids at the steady-state was performed through the incubation of A2780/HPR cells with [1-^{3}H]sphingosine for a 2 hour *pulse*, followed by a 48 hours *chase*. This approach allows the determination of changes in the intracellular ceramide in a sensible and quantitative way; in addition it is possible to measure the formation of radioactive PE, resulting from the recycling of the radioactive ethanolamine produced during the sphingosine or complex sphingolipid degradation. The sphingolipid analysis shows that the single treatment with HPR 10 μM induce a slight increase (+ 15 %) in the ceramide production compared to control, the treatment with the SK inhibitor significantly increased the ceramide level (+ 57 %) with a contemporary reduction of radioactive PE, indicating a reduced S1P formation and degradation (Fig. 30). Interestingly the contemporary cell treatment with 10 μM HPR and SK inhibitor caused a 2-fold increase of ceramide production. These data suggest that the SK inhibition enhances the sensitivity A2780/HPR cells the drug reducing the S1P formation and leading to a higher Ceramide/S1P ratio.

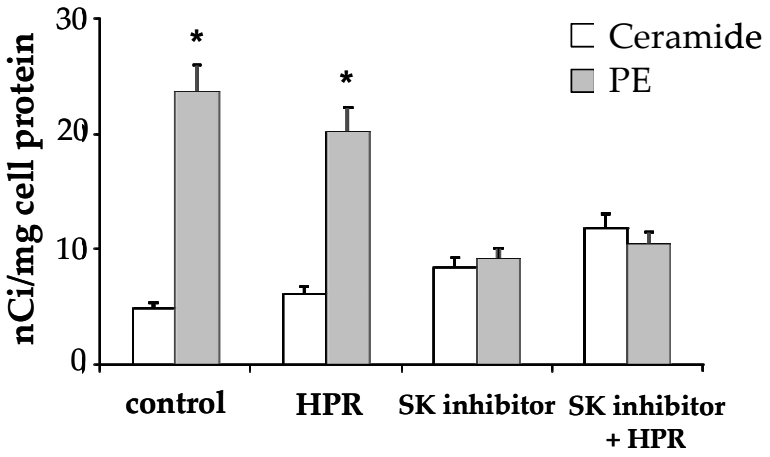

Figure 30. Effect of the SK inhibition on ceramide and PE production in A2780/HPR cells. The lipids of A2780/HPR cells were labelled at the steady-state with [1-^{3}H]sphingosine. After cell treatments with SK inhibitor and/or HPR 10 μM the lipid extracts were partitioned and the aqueous and organic phases were separated on HPTLC. The radioactivity associated to each lipid was assessed with the specific software. The radioactivity incorporation in ceramide and PE is expressed as nCi/mg of proteins. The data represent the average ± S.D. of three different experiments. * $P < 0.001$ *vs.* control cells.

SK1 overexpression in A2780 cells

Previous data suggest that an increased expression of sphingosine kinase could be important for drug resistance in A2780/HPR cells. To verify this hypothesis we overexpressed the enzyme SK1 in the cells characterized by low level of this enzyme expression, the A2780 cells. Cells were stably transfected with an expression vector coding for a tagged form of SK1 (pcDNA3-hSK^{wt}FLAG) and as transfection control with an insert-free plasmid (A2780 mock). The clones selection was performed with geneticine and after about30 days some colonies were subcloned and expanded.

To evaluate the effective SK1 overexpression in A2780 cells, a Western Blot analysis with an anti-FLAG M2 antibody was performed to verify the FLAG epitope expression in the selected clones. In Figure 31 upper panel, it is shown the result of 2 mock clones and 3 SK1 transfected clones. The FLAG expression is significantly present in the SK1 overexpressing clones, while it is absent in mock clones and in A2780 cells.

HPR sensitivity test of SK1 overexpressing cells

A2780 cells, 1 mock clone and 3 SK1 overexpressing clones were treated with 1 μM HPR. After 96 hours the total cell number was evaluated by counting with Bürker chamber and the dead cell number was determined with Trypan Blue exclusion assay. As shown in Figure 31lower panel, the

HPR treatment caused, as expected, a significant increased cell death in wild type cells and mock clones while the cell viability was not affected by HPR treatment in the SK1 clones, suggesting that this enzyme is sufficient to induce HPR resistance in these cells.

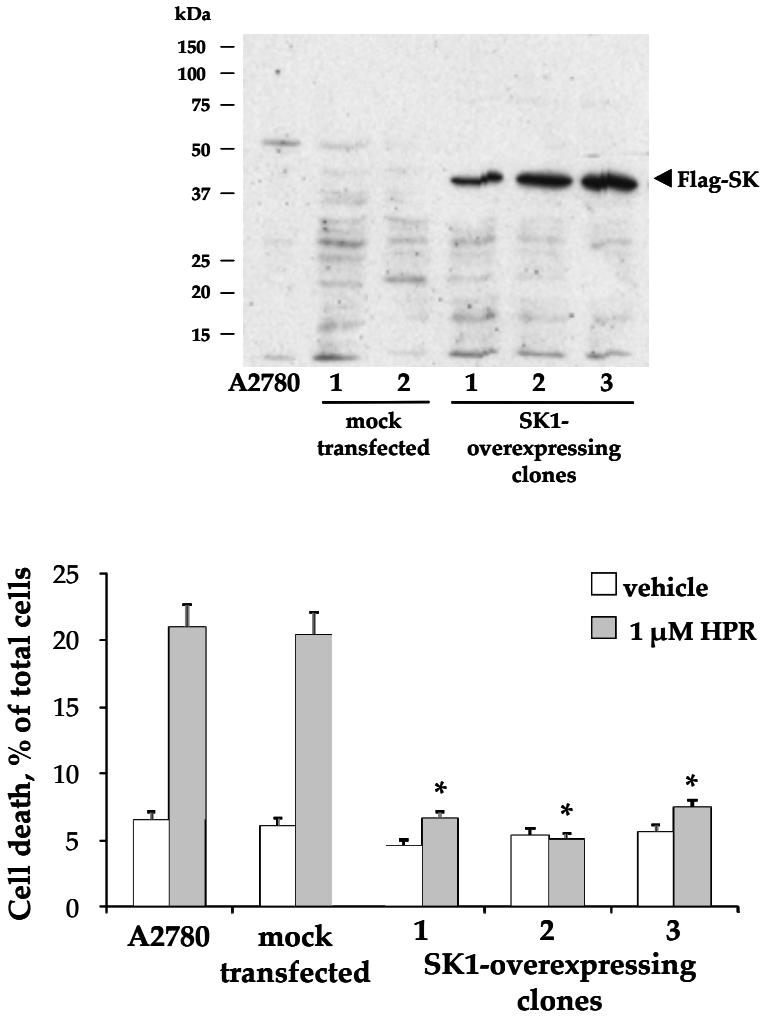

Figure 31. Effect of the SK1 overexpression on the HPR sensitivity of A2780 cells. Panel A: Western Blot analysis of the expression of FLAG M2 in transfected A2780 cells. The same amount of proteins were loaded on SDS-PAGE for wild type A2780 cells, mock clones and SK1 overexpressing clones. The FLAG M2 tagged SK1 was detected with an anti-FLAG M2 specific antibody. Panel B: A2780 cells, 1 mock and 3 overexpressing clones (1, 2 and 3) were treated with 1 μM HPR. After 48 hours the cells were counted in a Bürker chamber and the dead cell number was assessed through the Trypan Blue exclusion assay. The data represent the average ± SD of three different experiments. * $P < 0.001$ *vs.* vehicle treated cells.

Ceramide and dihydroceramide level mass spectrometry analysis

Ceramide and dihydroceramide cell content were analysed by mass spectrometry to deepen in the HPR mechanism and its relations with SK1 activity. This analysis has been performed on the following samples: A2780/HPR , A2780/HPR treated with 10 μM HPR, A2780/HPR treated with SK inhibitor, A2780/HPR treated with 10 μM HPR and SK inhibitor, SK1-transfected A2780 and SK1-transfected A2780 treated with HPR.

HPR treatment of SK1-transfected A2780 cells resulted in a significant rise in dihydroceramide levels, even if at a lesser extent that in A2780/HPR cells (Fig. 32). On the other hand treating SK1-transfected cells with HPR induces also a significant increase in ceramide levels, which are unchanged in the A2780/HPR cells with the same treatment.

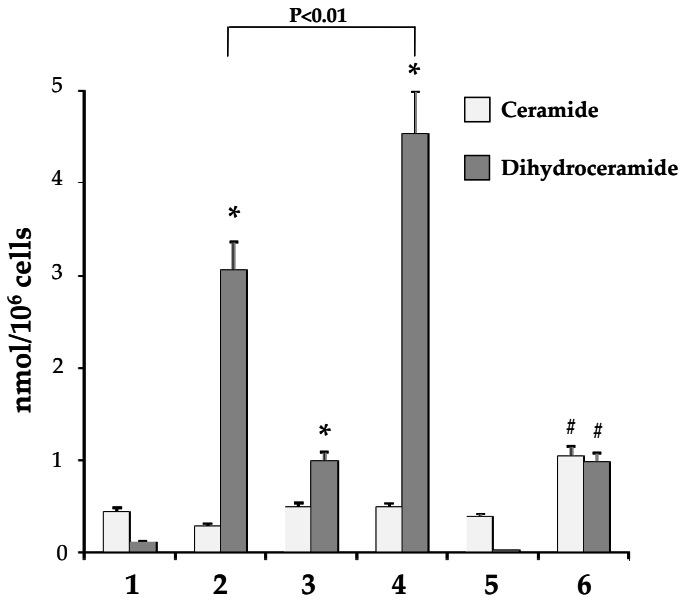

Figure 32. Mass spectrometry analysis of ceramide and dihydroceramide production in A2780/HPR and SK1-transfected cells. Ceramide and dihydroceramide content are expressed as nmol/10^6 cells in: A2780/HPR control (1), A2780/HPR treated with 10 μM HPR (2), A2780/HPR treated with SK inhibitor (3), A2780/HPR treated with 10 μM HPR and SK inhibitor (4), SK1-transfected A2780 (5) and SK1-transfected A2780 treated with HPR (6). Data are the means ± SD of three different experiments. * $P < 0.01$ *vs.* control cells. # $P < 0.025$ *vs*. SK1-transfected cells.

DISCUSSION

Sphingolipids, and in particular glycosphingolipids (GSL), are complex lipids enriched at the plasma membrane, the cell surface that mediate several interactions between the cell and its extracellular environment or other cells. Biological processes as cell proliferation, survival, differentiation and transformation are correlated with alterations in glicosphingolipid composition, and the consequent cell surface alterations. For example, the altered glycolipid sialylation plays important roles in regulating the processes of cell growth, survival, motility and invasiveness. Some studies demonstrate that main enzymes of the glicosphingolipid metabolism (as sialidase Neu3 and GM3 synthase) are differently expressed, and present a different activity, in tumor tissues (of colon, adenocarcinomas and other types) respect to non non-tumor tissues, introducing the possibility to make these enzymes becoming potential new biomarkers for tumor classification. Targeting the glycosphingolipid metabolic enzymes expression, by gene transfer or silencing, might further represent a novel therapeutic opportunity at least in some cancer types. However, several pieces of knowledge for the glicosphingolipid-based therapeutic modalities in cancer are still missing, in particular the exact role of different metabolic pathways and enzymes in determining the different ganglioside expression in tumor of different origin is not fully understood and furthermore the molecular mechanisms that can be affected by gangliosides appear very heterogeneous and likely very specific for a certain cellular context.

In the first part of this work ,glycosphingolipid metabolism and the effects of glycosphingolipid alterations on cell motility have been studied on variants of a human ovarian cancer cell line, A2780 cells. The A2780 cells are characterized by a low SAT-I expression, low GM3 synthase activity and a poor gangliosides content, and a high in vitro motility. On the other hand A2780/HPR cells, resistant to the fenretinide, and naturally expressing high level of the enzyme and of gangliosides, are characterized by a lower in vitro motility respect to wild type A2780 cells. This correlation between high expression of gangliosides, particularly of GM3 and GM2, and the reduced cell motility has been confirmed by exogenous ganglioside administrations and brefeldin-A treatment, which effectively increase the ganglioside cell content and reduce the in vitro cell motility of A2780 cells.. Furthermore the gene overexpression, by stable transfection of SAT-I in A2780 cells, confirmed the negative effect of high ganglioside content on the cell motility..

During the characterization of these A2780 cell variants an other important and marked difference has been noticed: the expression of caveolin-1, a very important membrane adapter protein, originally described as structural component of membrane invaginations called *caveolae*, but absent in our cell lines. Caveolin-1 is more expressed in the cells characterized by high GM3 synthase,

A2780/HPR and SAT-I transfected cells. It is known that cellular functions are more closely related to caveolins than to *caveolae*, and that a few cell regulation events can be surely ascribed to caveolins rather than to *caveolae* [219, 220]. Caveolin-1 is supposed to concentrate signalling molecules within cholesterol– and sphingolipid- rich membrane domains, its effects on tumors and on cell motility seem to be very heterogeneous and strongly dependent on the molecular partners interacting with this protein. Although caveolin-1 is excluded from the ganglioside/integrin/tetraspannin complex (the *glycosynapse type 3* described by Hakomori)that regulates the motility in colocarcinoma cells, it has been shown that a downstream signal of EGFR receptor, CD82-dependent, can be modulated by caveolin-1 [221], and on the other hand caveolin-1 has an important role in organizing the transduction of the integrin-signalling [101]. Caveolin-1 is particularly enriched in detergent resistant membrane domains, as well as gangliosides that segregate in these membrane regions, thus our studies have been focused on these particular domains. The interactions between caveolin-1 and the ganglioside GM3 have been studied through the *in vivo* cell labelling using a photoactivable and radioactive derivative of GM3, which after UV irradiation cross-linked all the interacting molecules, under these also caveolin-1 has been recognized and co-immunoprecipitated with GM3, confirming not only the co-localization but also the effective interaction of these two elements in our cell model. Moreover the DRM domains have been obtained by sucrose gradient ultracentrifugation of cell lysates from of A2780/HPR and SAT-I transfected cells. After the lipid and protein characterization of the DRM fractions the caveolin-1 has been immunoprecipitated in non-disruptive conditions, to permit the conservation of the complexes. These experiments describe a membrane complex composed of GM3, caveolin-1, integrin subunits α5 and β1 and the c-Src kinase present in the low motile cells.

It has been described that in the caveolin-1-mediated integrin signalling [101] c-Src can act as a downstream effector for the regulation on cell motility, so we tested the effect of a Src kinase selective inhibitor on the motility of A2780 cells. The *in vitro* motility of A2780 cells was strongly reduced in the presence of the Src inhibitor, confirming the role of the Src kinase in the motility regulation, also in our cell model. Furthermore, the analysis of the two phosphorylated forms of c-Src, revealed that the active form is equally expressed and distributed in the DRM fractions of all the cell variants, while the inactive c-Src is more expressed in the less motile A2780/HPR and SAT-I cells, and the consistent part of it is in the DRM. The interaction of Src with caveolin-1 is well established and has important consequences: Src induces the phosphorylation of caveolin-1 on the Tyr14 [222, 223] that induce a rearrangement of caveolin-1 in the cell. On the other hand this

caveolin phosphorylation creates a docking site for CSK, the kinase that inhibits Src, phosphorylating it at the Tyr527. These data permits to hypothesize that multimolecular membrane complex composed of GM3, caveolin-1, integrin subunits α5 and β1 that can regulate the cell motility through the c-Src kinase activity.

To deepen the study of caveolin-1, glycosphingolipids and cell motility the caveolin-1 expression has been modulated by transient silencing in A2780/HPR and SAT-I transfected cells. The knocked down caveolin-1 cell expression, and reduced membrane localization evidenced by immunofluorescence analysis, induce a marked reduction in the cell motility capability of both cell variants. The cell glycolipid composition has not been affected by the caveolin-1 modulated expression, in fact the endogenous content of all the lipids is unchanged in the cells silenced for caveolin-1 respect to the controls. These experiments permit to confirm the role of caveolin-1 in the regulation of cell motility of our cell model.

The second part of this work examines the other important phenotypic difference between A2780 and A2780/HPR cells: the sensibility to the drug fenretinide. A2780/HPR are ten times more resistant to the cytotoxic effect of HPR. The mechanism of action of this drug is so far not well known, however the effects of many antitumor drugs are at least in part a consequence of the drug-elicited increase in the ceramide cellular levels, a potent mediator of apoptosis and inhibitor of proliferation of a variety of tumor cell lines, and this is also the case of HPR. The antiproliferative effect of HPR in neuroblastoma, leukemia, breast, ovarian, prostate and colon carcinoma cell lines has been associated with the induction of apoptosis accompanied by increases in ceramide. The most relevant mechanism for the ceramide generation induced by HPR might be the *de novo* biosynthesis: HPR indeed induces the activation of serine palmitoyl-transferase and dihydroceramide synthase, while in a recent paper has been shown an inhibitory effect on the desaturase. This mechanism could also explain the dihydroceramide, rather than ceramide, accumulation in tumor cells treated with HPR, and this is the case of also A2780 cells, as shown in the mass spectrometry analysis [224]. In addition a recent study suggests that HPR cytotoxicity could be due, at least in part to the elevation in sphinganine levels [225].

This work is aimed to elucidate the aspects of the acquisition of resistance to the chemotherapeutic drugs, independently from the mechanisms underlying its cytotoxicity,. Alterations in the sphingolipid metabolism could lead to a reduced dihydroceramide formation or an increased clearance of dihydroceramide. For example in the case of multidrug-resistance, as many previous study have convincingly documented, the increased ceramide glycosilation permits to thwart the

drug-induced dihydroceramide accumulation preventing the cell death. But conversion of ceramide into glucosylceramide is not the only alteration in the sphingolipid metabolism occurring in tumor cell upon acquisition of drug-resistance. Dihydroceramide is the pivot of a very complex metabolic network, many different pathways can potentially contribute to the regulation of cellular ceramide levels and could be involved in the increased ability of cells to scavange ceramide and develop drug-resistance.

A2780/HPR is a cell line resistant to HPR, obtained from the parental A2780 cells after drug selection (with administrations of sublethal doses). In this cell line sphingolipid metabolism alterations and increased catabolic turnover of ceramide have been observed [11]. The increased GM3 synthase expression could be one of the pathways that permits to reduce the intracellular level of ceramide increasing the synthesis of complex glicosphingolipids. In this work the HPR-resistance of the SAT-I clones has been tested, but our results suggest that in the A2780 cells the overexpression of the enzyme GM3 synthase is not enough for the establishing of resistance to the drug HPR (Fig. 19).

From the observation of the two cell lines A2780 and A2780/HPR, emerges how these are characterized by a different proliferation (Fig. 20), in particular in the resistant cells the proliferation rate is about the double respect to the sensible ones. It is well established that sphingosine-1-phosphate (S1P) is characterized by opposite properties to those displayed by ceramide, and possibly by dihydroceramide, characteristics that generated the concept of a caramide/S1P rheostat, in which the ratio of the two lipids, and not the absolute content of each, are determinant for different cell fates. In this mechanism the enzymes that catalyzes the reactions between these sphingolipids play key roles and are able to regulate the rheostat. In agreement with this notion this study show that the altered sphingolipid metabolism displayed by the A2780/HPR is also characterized by enhanced S1P production (Fig. 22), resulting from the marked increase in the sphingosine kinase (SK) activity, due to the SK1 up-regulation, compared to A2780 cells. The pharmacological inhibition of SK, by the use of a selective and highly specific inhibitor, pulls down S1P formation and is able to markedly reduce the cell proliferation, and in A2780/HPR resistant cells the simultaneously administration of HPR, at the IC_{50} concentration, and the inhibitor of SK induces an increase in cell death, respect to the single administrations. The further way of SK activity manipulation has been the stable overexpression of the SK1 gene in the A2780 cells. The SK1 overexpressing cells results less sensible, or more resistant, to the cytotoxic effect of HPR: in the presence of HPR the SK1 clones don't show cell death as the control A2780 and mock transfected

do, this is most probably due to the higher production of the pro-growth and cell survival lipid S1P and the lower cellular levels of ceramide, detected by [1-^{3}H]sphingosine cell labelling. The overexpression of SK1 catalyzes the transformation of sphingosine into S1P, increasing the ceramide catabolism and finally establishing a different S1P/ceramide ratio that results in increased drug resistance to HPR.

In this work the S1P receptors involvement in the regulation of proliferation and HPR-resistance has been analysed in our cell models, by the use of specific agonists and antagonists of the different S1PR subtypes. The obtained results don't show significant differences of the agonists and antagonists, disengaging the receptors of S1P from the regulation of proliferation and HPR-resistance which were modulated by the SK activity in our cell model. It is intriguing that the S1PRs profile present big differences between A2780 and A2780/HPR cells, particularly S1P1 and S1P3 result higher expressed in resistant and higher proliferating cells, same situation verified in prostate cancer cells resistant to chemotherapy, in which these receptors regulate cell proliferation.

The findings of this work clearly demonstrate the role of SK1 in the regulation of HPR-resistance, through the modulation of the S1P/ceramide ratio, not excluding the participation of S1P as intracellular mediator, capable of addressing directly or indirectly elements of the anti-apoptotic machinery.

REFERENCES

1. Hakomori, S., Glycosynapses: microdomains controlling carbohydrate-dependent cell adhesion and signaling. An Acad Bras Cienc., 2004. 76(3): p. 553-572.
2. Kolesnick, R. and D.W. Golde, The sphingomyelin pathway in tumor necrosis factor and interleukin-1 signaling. Cell, 1994. 77(3): p. 325-8.
3. Liu, Y.Y., et al., Ceramide glycosylation potentiates cellular multidrug resistance. Faseb J, 2001. 15(3): p. 719-30.
4. Liu, Y.Y., et al., Expression of glucosylceramide synthase, converting ceramide to glucosylceramide, confers adriamycin resistance in human breast cancer cells. J Biol Chem, 1999. 274(2): p. 1140-6.
5. Gouaze, V., et al., Overexpression of glucosylceramide synthase and P-glycoprotein in cancer cells selected for resistance to natural product chemotherapy. Mol Cancer Ther, 2004. 3(5): p. 633-9.
6. Liu, Y.Y., et al., Oligonucleotides blocking glucosylceramide synthase expression selectively reverse drug resistance in cancer cells. J Lipid Res, 2004. 45(5): p. 933-40.
7. Pchejetski, D., et al., Chemosensitizing effects of sphingosine kinase-1 inhibition in prostate cancer cell and animal models. Mol Cancer Ther, 2008. 7(7): p. 1836-45.
8. Akao, Y., et al., High expression of sphingosine kinase 1 and S1P receptors in chemotherapy-resistant prostate cancer PC3 cells and their camptothecin-induced up-regulation. Biochem Biophys Res Commun, 2006. 342(4): p. 1284-90.
9. Nemoto, S., et al., Sphingosine kinase isoforms regulate oxaliplatin sensitivity of human colon cancer cells through ceramide accumulation and Akt activation. J Biol Chem, 2009. 284(16): p. 10422-32.
10. Guillermet-Guibert, J., et al., Targeting the sphingolipid metabolism to defeat pancreatic cancer cell resistance to the chemotherapeutic gemcitabine drug. Mol Cancer Ther, 2009. 8(4): p. 809-20.
11. Prinetti, A., et al., Altered Sphingolipid Metabolism in N-(4-Hydroxyphenyl)- retinamide-resistant A2780 Human Ovarian Carcinoma Cells. J. Biol. Chem., 2003. 278(8): p. 5574-5583.
12. Wymann, M.P. and R. Schneiter, Lipid signalling in disease. Nat Rev Mol Cell Biol, 2008. 9(2): p. 162-76.
13. Holthuis, J.C., et al., The organizing potential of sphingolipids in intracellular membrane transport. Physiol Rev, 2001. 81(4): p. 1689-723.
14. Obeid, L.M., et al., Programmed cell death induced by ceramide. Science, 1993. 259(5102): p. 1769-71.
15. Smith, E.R., et al., Effects of sphingosine and other sphingolipids on protein kinase C. Methods Enzymol, 2000. 312: p. 361-73.
16. Pettus, B.J., et al., Ceramide kinase mediates cytokine- and calcium ionophore-induced arachidonic acid release. J Biol Chem, 2003. 278(40): p. 38206-13.
17. Pettus, B.J., et al., Ceramide 1-phosphate is a direct activator of cytosolic phospholipase A2. J Biol Chem, 2004. 279(12): p. 11320-6.
18. Gomez-Munoz, A., et al., Ceramide-1-phosphate blocks apoptosis through inhibition of acid sphingomyelinase in macrophages. J Lipid Res, 2004. 45(1): p. 99-105.
19. Gomez-Munoz, A., et al., Ceramide-1-phosphate promotes cell survival through activation of the phosphatidylinositol 3-kinase/protein kinase B pathway. FEBS Lett, 2005. 579(17): p. 3744-50.
20. Mitra, P., et al., Ceramide kinase regulates growth and survival of A549 human lung adenocarcinoma cells. FEBS Lett, 2007. 581(4): p. 735-40.
21. Gangoiti, P., et al., Ceramide 1-phosphate stimulates macrophage proliferation through activation of the PI3-kinase/PKB, JNK and ERK1/2 pathways. Cell Signal, 2008. 20(4): p. 726-36.
22. Gouaze-Andersson, V. and M.C. Cabot, Glycosphingolipids and drug resistance. Biochim Biophys Acta, 2006. 1758(12): p. 2096-103.
23. Kolesnick, R.N., Sphingomyelin and derivatives as cellular signals. Prog Lipid Res, 1991. 30(1): p. 1-38.
24. Svennerholm, L., The Gangliosides. J Lipid Res, 1964. 5: p. 145-55.
25. Welti, R. and M. Glaser, Lipid domains in model and biological membranes. Chem Phys Lipids, 1994. 73(1-2): p. 121-37.

26. Prinetti, A., et al., Modulation of cell functions by glycosphingolipid metabolic remodeling in the plasma membrane. J Neurochem, 2007. 103 Suppl 1: p. 113-25.
27. Pyne, S. and N.J. Pyne, Sphingosine 1-phosphate signalling and termination at lipid phosphate receptors. Biochim Biophys Acta, 2002. 1582(1-3): p. 121-31.
28. Kolter, T., et al., Recent advances in the biochemistry of glycosphingolipid metabolism. Biochem Soc Trans, 1999. 27(4): p. 409-15.
29. Stoffel, W., Studies on the biosynthesis and degradation of sphingosine bases. Chem Phys Lipids, 1970. 5(1): p. 139-58.
30. Merrill, A.H., Jr., Characterization of serine palmitoyltransferase activity in Chinese hamster ovary cells. Biochim Biophys Acta, 1983. 754(3): p. 284-91.
31. Merrill, A.H., Jr. and E. Wang, Biosynthesis of long-chain (sphingoid) bases from serine by LM cells. Evidence for introduction of the 4-trans-double bond after de novo biosynthesis of N-acylsphinganine(s). J Biol Chem, 1986. 261(8): p. 3764-9.
32. Mandon, E.C., et al., Sphingolipid biosynthesis in cultured neurons. Down-regulation of serine palmitoyltransferase by sphingoid bases. Eur J Biochem, 1991. 198(3): p. 667-74.
33. Stoffel, W., D. LeKim, and G. Sticht, Metabolism of sphingosine bases. 8. Distribution, isolation and properties of D-3-oxosphinganine reductase. Stereospecificity of the NADPH-dependent reaction of 3-oxodihydrospingosine (2-amino-1-hydroxyoctadecane-3-one). Hoppe Seylers Z Physiol Chem, 1968. 349(12): p. 1637-44.
34. Sribney, M., Enzymatic synthesis of ceramide. Biochim Biophys Acta, 1966. 125(3): p. 542-7.
35. Mandon, E.C., et al., Subcellular localization and membrane topology of serine palmitoyltransferase, 3-dehydrosphinganine reductase, and sphinganine N-acyltransferase in mouse liver. J Biol Chem, 1992. 267(16): p. 11144-8.
36. Hirschberg, K., J. Rodger, and A.H. Futerman, The long-chain sphingoid base of sphingolipids is acylated at the cytosolic surface of the endoplasmic reticulum in rat liver. Biochem J, 1993. 290 (Pt 3): p. 751-7.
37. Rother, J., et al., Biosynthesis of sphingolipids: dihydroceramide and not sphinganine is desaturated by cultured cells. Biochem Biophys Res Commun, 1992. 189(1): p. 14-20.
38. Hannun, Y.A., Functions of ceramide in coordinating cellular responses to stress. Science, 1996. 274(5294): p. 1855-9.
39. Mathias, S., L.A. Pena, and R.N. Kolesnick, Signal transduction of stress via ceramide. Biochem J, 1998. 335 (Pt 3): p. 465-80.
40. Perry, D.K. and Y.A. Hannun, The role of ceramide in cell signaling. Biochim Biophys Acta, 1998. 1436(1-2): p. 233-43.
41. Bajjalieh, S.M., T.F. Martin, and E. Floor, Synaptic vesicle ceramide kinase. A calcium-stimulated lipid kinase that co-purifies with brain synaptic vesicles. J Biol Chem, 1989. 264(24): p. 14354-60.
42. Dressler, K.A. and R.N. Kolesnick, Ceramide 1-phosphate, a novel phospholipid in human leukemia (HL-60) cells. Synthesis via ceramide from sphingomyelin. J Biol Chem, 1990. 265(25): p. 14917-21.
43. Kolesnick, R.N. and M.R. Hemer, Characterization of a ceramide kinase activity from human leukemia (HL-60) cells. Separation from diacylglycerol kinase activity. J Biol Chem, 1990. 265(31): p. 18803-8.
44. Boudker, O. and A.H. Futerman, Detection and characterization of ceramide-1-phosphate phosphatase activity in rat liver plasma membrane. J Biol Chem, 1993. 268(29): p. 22150-5.
45. Dressler, K.A., S. Mathias, and R.N. Kolesnick, Tumor necrosis factor-alpha activates the sphingomyelin signal transduction pathway in a cell-free system. Science, 1992. 255(5052): p. 1715-8.
46. Trinchera, M., M. Fabbri, and R. Ghidoni, Topography of glycosyltransferases involved in the initial glycosylations of gangliosides. J Biol Chem, 1991. 266(31): p. 20907-12.
47. Futerman, A.H. and R.E. Pagano, Determination of the intracellular sites and topology of glucosylceramide synthesis in rat liver. Biochem J, 1991. 280 (Pt 2): p. 295-302.
48. Futerman, A.H., et al., Sphingomyelin synthesis in rat liver occurs predominantly at the cis and medial cisternae of the Golgi apparatus. J Biol Chem, 1990. 265(15): p. 8650-7.

49. Hanada, K., et al., Molecular machinery for non-vesicular trafficking of ceramide. Nature, 2003. 426(6968): p. 803-9.
50. van Echten, G. and K. Sandhoff, Ganglioside metabolism. Enzymology, Topology, and regulation. J Biol Chem, 1993. 268(8): p. 5341-4.
51. Merrill, A.H., Jr. and D.D. Jones, An update of the enzymology and regulation of sphingomyelin metabolism. Biochim Biophys Acta, 1990. 1044(1): p. 1-12.
52. Ito, M. and T. Yamagata, A novel glycosphingolipid-degrading enzyme cleaves the linkage between the oligosaccharide and ceramide of neutral and acidic glycosphingolipids. J Biol Chem, 1986. 261(30): p. 14278-82.
53. Zhou, B., et al., Isolation and characterization of ceramide glycanase from the leech, Macrobdella decora. J Biol Chem, 1989. 264(21): p. 12272-7.
54. Ito, M. and T. Yamagata, Purification and characterization of glycosphingolipid-specific endoglycosidases (endoglycoceramidases) from a mutant strain of Rhodococcus sp. Evidence for three molecular species of endoglycoceramidase with different specificities. J Biol Chem, 1989. 264(16): p. 9510-9.
55. Ito, M., Y. Ikegami, and T. Yamagata, Activator proteins for glycosphingolipid hydrolysis by endoglycoceramidases. Elucidation of biological functions of cell-surface glycosphingolipids in situ by endoglycoceramidases made possible using these activator proteins. J Biol Chem, 1991. 266(12): p. 7919-26.
56. Spence, M.W., Sphingomyelinases. Adv Lipid Res, 1993. 26: p. 3-23.
57. Riboni, L., et al., Formation of free sphingosine and ceramide from exogenous ganglioside GM1 by cerebellar granule cells in culture. FEBS Lett, 1992. 300(2): p. 188-92.
58. Riboni, L. and G. Tettamanti, Rapid internalization and intracellular metabolic processing of exogenous ganglioside by cerebellar granule cells differentiated in culture. J Neurochem, 1991. 57(6): p. 1931-9.
59. Tettamanti, G., et al., Salvage pathways in glycosphingolipid metabolism. Biochimie, 2003. 85(3-4): p. 423-37.
60. Brindley, D.N., Lipid phosphate phosphatases and related proteins: signaling functions in development, cell division, and cancer. J Cell Biochem, 2004. 92(5): p. 900-12.
61. Satoh, M., et al., Enhanced GM3 expression, associated with decreased invasiveness, is induced by brefeldin A in bladder cancer cells. Int. J. Oncol., 2001. 19(4): p. 723-731.
62. Kawamura, S., et al., Glycolipid composition in bladder tumor: A crucial role of GM3 ganglioside in tumor invasion. International Journal of Cancer, 2001. 94(3): p. 343-347.
63. Nojiri, H., et al., Glycotherapy for cancer: remodeling of ganglioside pattern as an effective approach for cancer therapy. Cancer Detec. Preven., 2002. 26(2): p. 114-120.
64. Watanabe, R., et al., Ganglioside G(M3) overexpression induces apoptosis and reduces malignant potential in murine bladder cancer. Cancer Res, 2002. 62(13): p. 3850-4.
65. Ono, M., et al., Motility Inhibition and Apoptosis Are Induced by Metastasis-suppressing Gene Product CD82 and Its Analogue CD9, with Concurrent Glycosylation. Cancer Res, 1999. 59(10): p. 2335-2339.
66. Ono, M., et al., GM3 Ganglioside Inhibits CD9-Facilitated Haptotactic Cell Motility: Coexpression of GM3 and CD9 Is Essential in the Downregulation of Tumor Cell Motility and Malignancy. Biochemistry, 2001. 40(21): p. 6414-6421.
67. Maecker, H.T., S.C. Todd, and S. Levy, The tetraspanin superfamily: molecular facilitators. Faseb J, 1997. 11(6): p. 428-42.
68. Hemler, M.E., Tetraspanin proteins mediate cellular penetration, invasion, and fusion events and define a novel type of membrane microdomain. Annu Rev Cell Dev Biol, 2003. 19: p. 397-422.
69. Hakomori, S. and K. Handa, Glycosphingolipid-dependent cross-talk between glycosynapses interfacing tumor cells with their host cells: essential basis to define tumor malignancy. FEBS Letters, 2002. 531(1): p. 88-92.

70. Bremer, E.G., J. Schlessinger, and S. Hakomori, Ganglioside-mediated modulation of cell growth. Specific effects of GM3 on tyrosine phosphorylation of the epidermal growth factor receptor. J Biol Chem, 1986. 261(5): p. 2434-40.
71. Toledo, M.S., et al., Cell growth regulation through GM3-enriched microdomain (glycosynapse) in human lung embryonal fibroblast WI38 and its oncogenic transformant VA13. J Biol Chem, 2004. 279(33): p. 34655-64.
72. Toledo, M.S., et al., Effect of ganglioside and tetraspanins in microdomains on interaction of integrins with fibroblast growth factor receptor. J Biol Chem, 2005. 280(16): p. 16227-34.
73. Nojiri, H., M. Stroud, and S. Hakomori, A specific type of ganglioside as a modulator of insulin-dependent cell growth and insulin receptor tyrosine kinase activity. Possible association of ganglioside-induced inhibition of insulin receptor function and monocytic differentiation induction in HL-60 cells. J Biol Chem, 1991. 266(7): p. 4531-7.
74. Iwabuchi, K., K. Handa, and S. Hakomori, Separation of "glycosphingolipid signaling domain" from caveolin-containing membrane fraction in mouse melanoma B16 cells and its role in cell adhesion coupled with signaling. J Biol Chem, 1998. 273(50): p. 33766-73.
75. Kawakami, Y., et al., Tetraspanin CD9 is a "proteolipid," and its interaction with alpha 3 integrin in microdomain is promoted by GM3 ganglioside, leading to inhibition of laminin-5-dependent cell motility. J Biol Chem, 2002. 277(37): p. 34349-58.
76. Mitsuzuka, K., et al., A specific microdomain ("glycosynapse 3") controls phenotypic conversion and reversion of bladder cancer cells through GM3-mediated interaction of alpha3beta1 integrin with CD9. J Biol Chem, 2005. 280(42): p. 35545-53.
77. Palade, G.E. and R.R. Bruns, Structural modulations of plasmalemmal vesicles. J Cell Biol, 1968. 37(3): p. 633-49.
78. Okamoto, T., et al., Caveolins, a family of scaffolding proteins for organizing "preassembled signaling complexes" at the plasma membrane. J Biol Chem, 1998. 273(10): p. 5419-22.
79. Scherer, P.E., et al., Caveolin isoforms differ in their N-terminal protein sequence and subcellular distribution. Identification and epitope mapping of an isoform-specific monoclonal antibody probe. J Biol Chem, 1995. 270(27): p. 16395-401.
80. Couet, J., M. Sargiacomo, and M.P. Lisanti, Interaction of a receptor tyrosine kinase, EGF-R, with caveolins. Caveolin binding negatively regulates tyrosine and serine/threonine kinase activities. J Biol Chem, 1997. 272(48): p. 30429-38.
81. Engelman, J.A., et al., Reciprocal regulation of neu tyrosine kinase activity and caveolin-1 protein expression in vitro and in vivo. Implications for human breast cancer. J Biol Chem, 1998. 273(32): p. 20448-55.
82. Razani, B., S.E. Woodman, and M.P. Lisanti, Caveolae: from cell biology to animal physiology. Pharmacol Rev, 2002. 54(3): p. 431-67.
83. Lisanti, M.P., et al., Caveolae, caveolin and caveolin-rich membrane domains: a signalling hypothesis. Trends Cell Biol, 1994. 4(7): p. 231-5.
84. Song, K.S., et al., Co-purification and direct interaction of Ras with caveolin, an integral membrane protein of caveolae microdomains. Detergent-free purification of caveolae microdomains. J Biol Chem, 1996. 271(16): p. 9690-7.
85. Shenoy-Scaria, A.M., et al., Cysteine3 of Src family protein tyrosine kinase determines palmitoylation and localization in caveolae. J Cell Biol, 1994. 126(2): p. 353-63.
86. Robbins, S.M., N.A. Quintrell, and J.M. Bishop, Myristoylation and differential palmitoylation of the HCK protein-tyrosine kinases govern their attachment to membranes and association with caveolae. Mol Cell Biol, 1995. 15(7): p. 3507-15.
87. Labrecque, L., et al., Regulation of vascular endothelial growth factor receptor-2 activity by caveolin-1 and plasma membrane cholesterol. Mol Biol Cell, 2003. 14(1): p. 334-47.
88. Fielding, P.E., et al., Mechanism of platelet-derived growth factor-dependent caveolin-1 phosphorylation: relationship to sterol binding and the role of serine-80. Biochemistry, 2004. 43(9): p. 2578-86.

89. Radel, C. and V. Rizzo, Integrin mechanotransduction stimulates caveolin-1 phosphorylation and recruitment of Csk to mediate actin reorganization. Am J Physiol Heart Circ Physiol, 2005. 288(2): p. H936-45.
90. Li, S., R. Seitz, and M.P. Lisanti, Phosphorylation of caveolin by src tyrosine kinases. The alpha-isoform of caveolin is selectively phosphorylated by v-Src in vivo. J Biol Chem, 1996. 271(7): p. 3863-8.
91. Lee, H., et al., Constitutive and growth factor-regulated phosphorylation of caveolin-1 occurs at the same site (Tyr-14) in vivo: identification of a c-Src/Cav-1/Grb7 signaling cassette. Mol Endocrinol, 2000. 14(11): p. 1750-75.
92. Han, D.C., T.L. Shen, and J.L. Guan, Role of Grb7 targeting to focal contacts and its phosphorylation by focal adhesion kinase in regulation of cell migration. J Biol Chem, 2000. 275(37): p. 28911-7.
93. Sanguinetti, A.R., H. Cao, and C. Corley Mastick, Fyn is required for oxidative- and hyperosmotic-stress-induced tyrosine phosphorylation of caveolin-1. Biochem J, 2003. 376(Pt 1): p. 159-68.
94. Wary, K.K., et al., A requirement for caveolin-1 and associated kinase Fyn in integrin signaling and anchorage-dependent cell growth. Cell, 1998. 94(5): p. 625-34.
95. Wiechen, K., et al., Caveolin-1 Is Down-Regulated in Human Ovarian Carcinoma and Acts as a Candidate Tumor Suppressor Gene. Am J Pathol, 2001. 159(5): p. 1635-1643.
96. Zheng, W., et al., Ceramides and other bioactive sphingolipid backbones in health and disease: lipidomic analysis, metabolism and roles in membrane structure, dynamics, signaling and autophagy. Biochim Biophys Acta, 2006. 1758(12): p. 1864-84.
97. Wiechen, K., et al., Caveolin-1 is down-regulated in human ovarian carcinoma and acts as a candidate tumor suppressor gene. Am J Pathol, 2001. 159(5): p. 1635-43.
98. Lee, S.W., et al., Tumor cell growth inhibition by caveolin re-expression in human breast cancer cells. Oncogene, 1998. 16(11): p. 1391-7.
99. Bender, F.C., et al., Caveolin-1 levels are down-regulated in human colon tumors, and ectopic expression of caveolin-1 in colon carcinoma cell lines reduces cell tumorigenicity. Cancer Res, 2000. 60(20): p. 5870-8.
100. Miotti, S., et al., Simultaneous expression of caveolin-1 and E-cadherin in ovarian carcinoma cells stabilizes adherens junctions through inhibition of src-related kinases. Am J Pathol, 2005. 167(5): p. 1411-27.
101. Wary, K.K., et al., A Requirement for Caveolin-1 and Associated Kinase Fyn in Integrin Signaling and Anchorage-Dependent Cell Growth. Cell, 1998. 94(5): p. 625-634.
102. Engelman, J.A., et al., p42/44 MAP kinase-dependent and -independent signaling pathways regulate caveolin-1 gene expression. Activation of Ras-MAP kinase and protein kinase a signaling cascades transcriptionally down-regulates caveolin-1 promoter activity. J Biol Chem, 1999. 274(45): p. 32333-41.
103. Williams, T.M. and M.P. Lisanti, The caveolin proteins. Genome Biol, 2004. 5(3): p. 214.
104. Ho, C.C., et al., Up-regulated caveolin-1 accentuates the metastasis capability of lung adenocarcinoma by inducing filopodia formation. Am J Pathol, 2002. 161(5): p. 1647-56.
105. Lauffenburger, D.A. and A.F. Horwitz, Cell migration: a physically integrated molecular process. Cell, 1996. 84(3): p. 359-69.
106. Sheetz, M.P., et al., Cell migration as a five-step cycle. Biochem Soc Symp, 1999. 65: p. 233-43.
107. Hynes, R.O., Integrins: versatility, modulation, and signaling in cell adhesion. Cell, 1992. 69(1): p. 11-25.
108. Sastry, S.K. and A.F. Horwitz, Integrin cytoplasmic domains: mediators of cytoskeletal linkages and extra- and intracellular initiated transmembrane signaling. Curr Opin Cell Biol, 1993. 5(5): p. 819-31.
109. Schwartz, M.A., M.D. Schaller, and M.H. Ginsberg, Integrins: emerging paradigms of signal transduction. Annu Rev Cell Dev Biol, 1995. 11: p. 549-99.
110. Giancotti, F.G. and E. Ruoslahti, Integrin signaling. Science, 1999. 285(5430): p. 1028-32.
111. Hynes, R.O., Integrins: bidirectional, allosteric signaling machines. Cell, 2002. 110(6): p. 673-87.
112. Bagrodia, S., et al., Cdc42 and PAK-mediated signaling leads to Jun kinase and p38 mitogen-activated protein kinase activation. J Biol Chem, 1995. 270(47): p. 27995-8.

113. Oktay, M., et al., Integrin-mediated activation of focal adhesion kinase is required for signaling to Jun NH2-terminal kinase and progression through the G1 phase of the cell cycle. J Cell Biol, 1999. 145(7): p. 1461-9.
114. Klekotka, P.A., et al., Specific residues within the alpha 2 integrin subunit cytoplasmic domain regulate migration and cell cycle progression via distinct MAPK pathways. J Biol Chem, 2001. 276(34): p. 32353-61.
115. Hedges, J.C., et al., A role for p38(MAPK)/HSP27 pathway in smooth muscle cell migration. J Biol Chem, 1999. 274(34): p. 24211-9.
116. Gu, J., et al., Shc and FAK differentially regulate cell motility and directionality modulated by PTEN. J Cell Biol, 1999. 146(2): p. 389-403.
117. Aoki, S., et al., Sphingosine 1-phosphate-related metabolism in the blood vessel. J Biochem, 2005. 138(1): p. 47-55.
118. Yatomi, Y., et al., Sphingosine 1-phosphate: synthesis and release. Prostaglandins, 2001. 64(1-4): p. 107-122.
119. Yang, L., et al., Metabolism and functional effects of sphingolipids in blood cells. Br J Haematol, 1999. 107(2): p. 282-93.
120. Van Veldhoven, P.P. and G.P. Mannaerts, Subcellular localization and membrane topology of sphingosine-1-phosphate lyase in rat liver. J Biol Chem, 1991. 266(19): p. 12502-7.
121. Yatomi, Y., et al., Sphingosine-1-phosphate: a platelet-activating sphingolipid released from agonist-stimulated human platelets. Blood, 1995. 86(1): p. 193-202.
122. Kihara, A., et al., Sphingosine-1-phosphate lyase is involved in the differentiation of F9 embryonal carcinoma cells to primitive endoderm. J Biol Chem, 2003. 278(16): p. 14578-85.
123. Herr, D.R., et al., Sply regulation of sphingolipid signaling molecules is essential for Drosophila development. Development, 2003. 130(11): p. 2443-53.
124. Brindley, D.N., et al., Lipid phosphate phosphatases regulate signal transduction through glycerolipids and sphingolipids. Biochim Biophys Acta, 2002. 1582(1-3): p. 33-44.
125. Spiegel, S. and A.H. Merrill, Jr., Sphingolipid metabolism and cell growth regulation. Faseb J, 1996. 10(12): p. 1388-97.
126. Merrill, A.H., Jr., et al., Sphingolipids--the enigmatic lipid class: biochemistry, physiology, and pathophysiology. Toxicol Appl Pharmacol, 1997. 142(1): p. 208-25.
127. Mattie, M., G. Brooker, and S. Spiegel, Sphingosine-1-phosphate, a putative second messenger, mobilizes calcium from internal stores via an inositol trisphosphate-independent pathway. J Biol Chem, 1994. 269(5): p. 3181-8.
128. Spiegel, S. and S. Milstien, Sphingosine-1-phosphate: an enigmatic signalling lipid. Nat Rev Mol Cell Biol, 2003. 4(5): p. 397-407.
129. Donati, C. and P. Bruni, Sphingosine 1-phosphate regulates cytoskeleton dynamics: implications in its biological response. Biochim Biophys Acta, 2006. 1758(12): p. 2037-48.
130. Seitz, G., et al., The role of sphingosine 1-phosphate receptors in the trafficking of hematopoietic progenitor cells. Ann N Y Acad Sci, 2005. 1044: p. 84-9.
131. Cyster, J.G., Chemokines, sphingosine-1-phosphate, and cell migration in secondary lymphoid organs. Annu Rev Immunol, 2005. 23: p. 127-59.
132. McVerry, B.J. and J.G. Garcia, In vitro and in vivo modulation of vascular barrier integrity by sphingosine 1-phosphate: mechanistic insights. Cell Signal, 2005. 17(2): p. 131-9.
133. Waeber, C., N. Blondeau, and S. Salomone, Vascular sphingosine-1-phosphate S1P1 and S1P3 receptors. Drug News Perspect, 2004. 17(6): p. 365-82.
134. Nagata, Y., et al., Entry of muscle satellite cells into the cell cycle requires sphingolipid signaling. J Cell Biol, 2006. 174(2): p. 245-53.
135. Mitra, P., et al., Role of ABCC1 in export of sphingosine-1-phosphate from mast cells. Proc Natl Acad Sci U S A, 2006. 103(44): p. 16394-9.
136. Ancellin, N., et al., Extracellular export of sphingosine kinase-1 enzyme. Sphingosine 1-phosphate generation and the induction of angiogenic vascular maturation. J Biol Chem, 2002. 277(8): p. 6667-75.

137. Taha, T.A., K.M. Argraves, and L.M. Obeid, Sphingosine-1-phosphate receptors: receptor specificity versus functional redundancy. Biochim Biophys Acta, 2004. 1682(1-3): p. 48-55.
138. Morales-Ruiz, M., et al., Sphingosine 1-phosphate activates Akt, nitric oxide production, and chemotaxis through a Gi protein/phosphoinositide 3-kinase pathway in endothelial cells. J Biol Chem, 2001. 276(22): p. 19672-7.
139. Igarashi, J. and T. Michel, Sphingosine 1-phosphate and isoform-specific activation of phosphoinositide 3-kinase beta. Evidence for divergence and convergence of receptor-regulated endothelial nitric-oxide synthase signaling pathways. J Biol Chem, 2001. 276(39): p. 36281-8.
140. Taha, T.A., Y.A. Hannun, and L.M. Obeid, Sphingosine kinase: biochemical and cellular regulation and role in disease. J Biochem Mol Biol, 2006. 39(2): p. 113-31.
141. Graler, M.H. and E.J. Goetzl, Lysophospholipids and their G protein-coupled receptors in inflammation and immunity. Biochim Biophys Acta, 2002. 1582(1-3): p. 168-74.
142. Alderton, F., et al., Tethering of the platelet-derived growth factor beta receptor to G-protein-coupled receptors. A novel platform for integrative signaling by these receptor classes in mammalian cells. J Biol Chem, 2001. 276(30): p. 28578-85.
143. Liu, H., et al., Sphingosine kinases: a novel family of lipid kinases. Prog Nucleic Acid Res Mol Biol, 2002. 71: p. 493-511.
144. Wattenberg, B.W., S.M. Pitson, and D.M. Raben, The sphingosine and diacylglycerol kinase superfamily of signaling kinases: localization as a key to signaling function. J Lipid Res, 2006. 47(6): p. 1128-39.
145. Olivera, A., et al., Sphingosine kinase expression increases intracellular sphingosine-1-phosphate and promotes cell growth and survival. J Cell Biol, 1999. 147(3): p. 545-58.
146. Xia, P., et al., An oncogenic role of sphingosine kinase. Curr Biol, 2000. 10(23): p. 1527-30.
147. Igarashi, N., et al., Sphingosine kinase 2 is a nuclear protein and inhibits DNA synthesis. J Biol Chem, 2003. 278(47): p. 46832-9.
148. Liu, H., et al., Sphingosine kinase type 2 is a putative BH3-only protein that induces apoptosis. J Biol Chem, 2003. 278(41): p. 40330-6.
149. Maceyka, M., et al., SphK1 and SphK2, sphingosine kinase isoenzymes with opposing functions in sphingolipid metabolism. J Biol Chem, 2005. 280(44): p. 37118-29.
150. Billich, A., et al., Phosphorylation of the immunomodulatory drug FTY720 by sphingosine kinases. J Biol Chem, 2003. 278(48): p. 47408-15.
151. Sugiura, M., et al., Ceramide kinase, a novel lipid kinase. Molecular cloning and functional characterization. J Biol Chem, 2002. 277(26): p. 23294-300.
152. Pitson, S.M., et al., The nucleotide-binding site of human sphingosine kinase 1. J Biol Chem, 2002. 277(51): p. 49545-53.
153. Yokota, S., et al., Asp177 in C4 domain of mouse sphingosine kinase 1a is important for the sphingosine recognition. FEBS Lett, 2004. 578(1-2): p. 106-10.
154. Maceyka, M., et al., Sphingosine kinase, sphingosine-1-phosphate, and apoptosis. Biochim Biophys Acta, 2002. 1585(2-3): p. 193-201.
155. Alvarez, S.E., S. Milstien, and S. Spiegel, Autocrine and paracrine roles of sphingosine-1-phosphate. Trends Endocrinol Metab, 2007. 18(8): p. 300-7.
156. Olivera, A., J. Rosenthal, and S. Spiegel, Effect of acidic phospholipids on sphingosine kinase. J Cell Biochem, 1996. 60(4): p. 529-37.
157. Granata, R., et al., Dual effects of IGFBP-3 on endothelial cell apoptosis and survival: involvement of the sphingolipid signaling pathways. Faseb J, 2004. 18(12): p. 1456-8.
158. Delon, C., et al., Sphingosine kinase 1 is an intracellular effector of phosphatidic acid. J Biol Chem, 2004. 279(43): p. 44763-74.
159. Young, K.W., et al., Ca2+/calmodulin-dependent translocation of sphingosine kinase: role in plasma membrane relocation but not activation. Cell Calcium, 2003. 33(2): p. 119-28.
160. Hannun, Y.A. and C. Luberto, Ceramide in the eukaryotic stress response. Trends Cell Biol, 2000. 10(2): p. 73-80.

161. Levade, T. and J.P. Jaffrezou, Signalling sphingomyelinases: which, where, how and why? Biochim Biophys Acta, 1999. 1438(1): p. 1-17.
162. Kolesnick, R. and Y.A. Hannun, Ceramide and apoptosis. Trends Biochem Sci, 1999. 24(6): p. 224-5; author reply 227.
163. Morita, Y., et al., Oocyte apoptosis is suppressed by disruption of the acid sphingomyelinase gene or by sphingosine-1-phosphate therapy. Nat Med, 2000. 6(10): p. 1109-14.
164. Bose, R., et al., Ceramide synthase mediates daunorubicin-induced apoptosis: an alternative mechanism for generating death signals. Cell, 1995. 82(3): p. 405-14.
165. Hannun, Y.A., et al., Sphingosine inhibition of protein kinase C activity and of phorbol dibutyrate binding in vitro and in human platelets. J Biol Chem, 1986. 261(27): p. 12604-9.
166. Cuvillier, O., L. Edsall, and S. Spiegel, Involvement of sphingosine in mitochondria-dependent Fas-induced apoptosis of type II Jurkat T cells. J Biol Chem, 2000. 275(21): p. 15691-700.
167. Hung, W.C., H.C. Chang, and L.Y. Chuang, Activation of caspase-3-like proteases in apoptosis induced by sphingosine and other long-chain bases in Hep3B hepatoma cells. Biochem J, 1999. 338 (Pt 1): p. 161-6.
168. Pyne, S. and N.J. Pyne, Sphingosine 1-phosphate signalling in mammalian cells. Biochem J, 2000. 349(Pt 2): p. 385-402.
169. Spiegel, S. and S. Milstien, Sphingosine-1-phosphate: signaling inside and out. FEBS Lett, 2000. 476(1-2): p. 55-7.
170. Illuzzi, G., et al., Sphingosine kinase mediates resistance to the synthetic retinoid N-(4-hydroxyphenyl)retinamide in human ovarian cancer cells. J Biol Chem, 2010. 285(24): p. 18594-602.
171. Reed, J.C., Bcl-2 and the regulation of programmed cell death. J Cell Biol, 1994. 124(1-2): p. 1-6.
172. Mathias, S., K.A. Dressler, and R.N. Kolesnick, Characterization of a ceramide-activated protein kinase: stimulation by tumor necrosis factor alpha. Proc Natl Acad Sci U S A, 1991. 88(22): p. 10009-13.
173. Bosch, I. and J. Croop, P-glycoprotein multidrug resistance and cancer. Biochim Biophys Acta, 1996. 1288(2): p. F37-54.
174. Gottesman, M.M. and I. Pastan, Biochemistry of multidrug resistance mediated by the multidrug transporter. Annu Rev Biochem, 1993. 62: p. 385-427.
175. Hannun, Y.A. and C.M. Linardic, Sphingolipid breakdown products: anti-proliferative and tumor-suppressor lipids. Biochim Biophys Acta, 1993. 1154(3-4): p. 223-36.
176. Friche, E., et al., Decreased DNA topoisomerase II in daunorubicin-resistant Ehrlich ascites tumor cells. Cancer Res, 1991. 51(16): p. 4213-8.
177. Sietsma, H., R.J. Veldman, and J.W. Kok, The involvement of sphingolipids in multidrug resistance. J Membr Biol, 2001. 181(3): p. 153-62.
178. Merrill, A.H., Jr., et al., Role of dietary sphingolipids and inhibitors of sphingolipid metabolism in cancer and other diseases. J Nutr, 1995. 125(6 Suppl): p. 1677S-1682S.
179. Okazaki, T., R.M. Bell, and Y.A. Hannun, Sphingomyelin turnover induced by vitamin D3 in HL-60 cells. Role in cell differentiation. J Biol Chem, 1989. 264(32): p. 19076-80.
180. Malisan, F. and R. Testi, Lipid signaling in CD95-mediated apoptosis. FEBS Lett, 1999. 452(1-2): p. 100-3.
181. Liu, J., et al., Renaturation and tumor necrosis factor-alpha stimulation of a 97-kDa ceramide-activated protein kinase. J Biol Chem, 1994. 269(4): p. 3047-52.
182. Lavie, Y., et al., Accumulation of glucosylceramides in multidrug-resistant cancer cells. J Biol Chem, 1996. 271(32): p. 19530-6.
183. Lucci, A., et al., Glucosylceramide: a marker for multiple-drug resistant cancers. Anticancer Res, 1998. 18(1B): p. 475-80.
184. Prinetti, A., et al., Altered sphingolipid metabolism in N-(4-hydroxyphenyl)-retinamide-resistant A2780 human ovarian carcinoma cells. J Biol Chem, 2003. 278(8): p. 5574-83.
185. Baran, Y., et al., Alterations of ceramide/sphingosine 1-phosphate rheostat involved in the regulation of resistance to imatinib-induced apoptosis in K562 human chronic myeloid leukemia cells. J Biol Chem, 2007. 282(15): p. 10922-34.

186. Schnitzer, S.E., et al., Hypoxia enhances sphingosine kinase 2 activity and provokes sphingosine-1-phosphate-mediated chemoresistance in A549 lung cancer cells. Mol Cancer Res, 2009. 7(3): p. 393-401.
187. Acquotti, D., et al., Geometrical and conformational properties of ganglioside GalNAc-GD1a, IV4GalNAcIV3Neu5AcII3Neu5AcGgOse4Cer. Eur J Biochem, 1994. 225(1): p. 271-88.
188. Ghidoni, R., et al., On the structure of two new gangliosides from beef brain. J Neurochem, 1976. 27(2): p. 511-5.
189. Mauri, L., et al., A procedure for the preparation of GM3 ganglioside from GM1-lactone. Glycoconj J, 1999. 16(3): p. 197-203.
190. Mauri, L., et al., Synthesis of radioactive and photoactivable ganglioside derivatives for the study of ganglioside-protein interactions. Glycoconj J, 2004. 20(1): p. 11-23.
191. Appierto, V., et al., Decrease in drug accumulation and in tumour aggressiveness marker expression in a fenretinide-induced resistant ovarian tumour cell line. Br J Cancer, 2001. 84(11): p. 1528-34.
192. Berselli, P., et al., Human GM3 synthase: a new mRNA variant encodes an NH2-terminal extended form of the protein. Biochim Biophys Acta, 2006. 1759(7): p. 348-58.
193. Pitson, S.M., et al., Expression of a catalytically inactive sphingosine kinase mutant blocks agonist-induced sphingosine kinase activation. A dominant-negative sphingosine kinase. J Biol Chem, 2000. 275(43): p. 33945-50.
194. Mehlen, P., et al., The DCC gene product induces apoptosis by a mechanism requiring receptor proteolysis. Nature, 1998. 395(6704): p. 801-4.
195. Donati, C., et al., Tumor necrosis factor-alpha exerts pro-myogenic action in C2C12 myoblasts via sphingosine kinase/S1P2 signaling. FEBS Lett, 2007. 581(23): p. 4384-8.
196. Livak, K.J. and T.D. Schmittgen, Analysis of relative gene expression data using real-time quantitative PCR and the 2(-Delta Delta C(T)) Method. Methods, 2001. 25(4): p. 402-8.
197. Scandroglio, F., et al., Thin layer chromatography of gangliosides. Glycoconj J, 2008.
198. Riboni, L., P. Viani, and G. Tettamanti, Estimating sphingolipid metabolism and trafficking in cultured cells using radiolabeled compounds. Methods Enzymol, 2000. 311: p. 656-82.
199. Bartlett, G.R., Phosphorus assay in column chromatography. J Biol Chem, 1959. 234(3): p. 466-8.
200. Svennerholm, L., Quantitative estimation of sialic acids. II. A colorimetric resorcinol-hydrochloric acid method. Biochim Biophys Acta, 1957. 24(3): p. 604-11.
201. Boyle, P.J., et al., Apoptosis of human breast carcinoma cells in the presence of cis-platin and L-/D-PPMP: IV. Modulation of replication complexes and glycolipid: Glycosyltransferases. Glycoconj J, 2006. 23(3-4): p. 175-87.
202. Valaperta, R., et al., Plasma membrane production of ceramide from ganglioside GM3 in human fibroblasts. Faseb J, 2006. 20(8): p. 1227-9.
203. Chigorno, V., et al., A radiometric assay for ganglioside sialidase applied to the determination of the enzyme subcellular location in cultured human fibroblasts. Anal Biochem, 1986. 153(2): p. 283-94.
204. Zetter, B.R., Assay of capillary endothelial cell migration. Methods Enzymol, 1987. 147: p. 135-44.
205. Saqr, H.E., D.K. Pearl, and A.J. Yates, A review and predictive models of ganglioside uptake by biological membranes. J Neurochem, 1993. 61(2): p. 395-411.
206. Chigorno, V., et al., Association of gangliosides to fibroblasts in culture: A study performed with GM1 [14C]-labelled at the sialic acid acetyl group. Glycoconjugate Journal, 1985. V2(3): p. 279-291.
207. Sonnino, S., et al., Specific ganglioside-cell protein interactions: a study performed with GM1 ganglioside derivative containing photoactivable azide and rat cerebellar granule cells in culture. Neurochem Int, 1992. 20(3): p. 315-21.
208. Prinetti, A., et al., Sphingolipid-enriched membrane domains from rat cerebellar granule cells differentiated in culture. A compositional study. J Biol Chem, 2000. 275(16): p. 11658-65.
209. Murate, T., et al., Cell type-specific localization of sphingosine kinase 1a in human tissues. J Histochem Cytochem, 2001. 49(7): p. 845-55.
210. Sonnino, S., et al., A photoreactive derivative of radiolabeled GM1 ganglioside: preparation and use to establish the involvement of specific proteins in GM1 uptake by human fibroblasts in culture. Biochemistry, 1989. 28(1): p. 77-84.

211. Chigorno, V., et al., Formation of a cytosolic ganglioside-protein complex following administration of photoreactive ganglioside GM1 to human fibroblasts in culture. FEBS Lett, 1990. 263(2): p. 329-31.
212. Prinetti, A., et al., Association of Src-family protein tyrosine kinases with sphingolipids in rat cerebellar granule cells differentiated in culture. Glycoconj J, 2000. 17(3 -4): p. 223-32.
213. Loberto, N., et al., The membrane environment of endogenous cellular prion protein in primary rat cerebellar neurons. J Neurochem, 2005. 95(3): p. 771-83.
214. Olivera, A., J. Rosenthal, and S. Spiegel, Sphingosine kinase from Swiss 3T3 fibroblasts: a convenient assay for the measurement of intracellular levels of free sphingoid bases. Anal Biochem, 1994. 223(2): p. 306-12.
215. Valsecchi, M., et al., Ceramide and sphingomyelin species of fibroblasts and neurons in culture 10.1194/jlr.M600344-JLR200. J. Lipid Res., 2007. 48(2): p. 417-424.
216. Lowry, O.H., et al., Protein measurement with the folin phenol reagent. J. Biol. Chem., 1951. 193(1): p. 265-275.
217. Hinrichs, J.W., et al., ATP-binding cassette transporters are enriched in non-caveolar detergent-insoluble glycosphingolipid-enriched membrane domains (DIGs) in human multidrug-resistant cancer cells. J Biol Chem, 2004. 279(7): p. 5734-8.
218. Prinetti, A., K. Iwabuchi, and S. Hakomori, Glycosphingolipid-enriched signaling domain in mouse neuroblastoma Neuro2a cells. Mechanism of ganglioside-dependent neuritogenesis. J Biol Chem, 1999. 274(30): p. 20916-24.
219. Head, B.P. and P.A. Insel, Do caveolins regulate cells by actions outside of caveolae? Trends Cell Biol, 2007. 17(2): p. 51-7.
220. Sonnino, S. and A. Prinetti, Sphingolipids and membrane environments for caveolin. FEBS Lett, 2009. 583(4): p. 597-606.
221. Wang, X.Q., et al., Suppression of epidermal growth factor receptor signaling by protein kinase C-alpha activation requires CD82, caveolin-1, and ganglioside. Cancer Res, 2007. 67(20): p. 9986-95.
222. Mastick, C.C., M.J. Brady, and A.R. Saltiel, Insulin stimulates the tyrosine phosphorylation of caveolin. J Cell Biol, 1995. 129(6): p. 1523-31.
223. Aoki, T., R. Nomura, and T. Fujimoto, Tyrosine Phosphorylation of Caveolin-1 in the Endothelium. Experimental Cell Research, 1999. 253(2): p. 629-636.
224. Valsecchi, M., et al., Sphingolipidomics of A2780 human ovarian carcinoma cells treated with synthetic retinoids. J Lipid Res, 2010. 51(7): p. 1832-40.
225. Wang, H., et al., N-(4-Hydroxyphenyl)retinamide increases dihydroceramide and synergizes with dimethylsphingosine to enhance cancer cell killing. Mol Cancer Ther, 2008. 7(9): p. 2967-76.